THE UNIVERSITY OF ALBERTA

RADIOHALOGENATED PYRIMIDINE NUCLEOSIDES AS POTENTIAL NON-INVASIVE DIAGNOSTIC AGENTS FOR HERPES SIMPLEX ENCEPHALITIS

by

(C) JOHN SAMUEL

A THESIS

SUBMITTED TO THE FACULTY OF GRADUATE STUDIES AND RESEARCH

IN PARTIAL FULFILMENT OF THE REQUIREMENTS FOR THE DEGREE

OF DOCTOR OF PHILOSOPHY

IN

PHARMACEUTICAL SCIENCES

FACULTY OF PHARMACY AND PHARMACEUTICAL SCIENCES

EDMONTON, ALBERTA

FALL 1985

THE UNIVERSITY OF ALBERTA

RELEASE FORM

NAME OF AUTHOR JOHN SAMUEL

TITLE OF THESIS RADIOHALOGENATED PYRIMIDINE NUCLEOSIDES AS POTENTIAL NON-INVASIVE DIAGNOSTIC AGENTS FOR HERPES SIMPLEX ENCEPHALITIS

DEGREE FOR WHICH THESIS WAS PRESENTED DOCTOR OF PHILOSOPHY

YEAR THIS DEGREE GRANTED FALL 1985

Permission is hereby granted to THE UNIVERSITY OF ALBERTA LIBRARY to reproduce single copies of this thesis and to lend or sell such copies for private, scholarly or scientific research purposes only.

The author reserves other publication rights, and neither the thesis nor extensive extracts from it may be printed or otherwise reproduced without the author's written permission.

(SIGNED) John

PERMANENT ADDRESS:

KANNYEL THERRATHIL
THAMALLACKAL, KARUVATTA
HARIPAD, KERALA, INDIA

DATED Oct 9, 1985

THE UNIVERSITY OF ALBERTA

FACULTY OF GRADUATE STUDIES AND RESEARCH

The undersigned certify that they have read, and recommend to the Faculty of Graduate Studies and Research, for acceptance, a thesis entitled Radiohalogenated Pyrimidine Nucleosides as Potential Non-Invasive Diagnostic Agents for Herpes Simplex Encephalitis submitted by John Samuel in partial fulfilment of the requirements for the degree of Doctor of Philosophy in Pharmaceutical Sciences.

.....

Supervisor

.....

.....

.....

.....

.....

.....

External Examiner

Date Oct 8, 1985

DEDICATION

To

my parents

ABSTRACT

Herpes simplex encephalitis (HSE) is considered to be the most common fatal encephalitis in North America. At present brain biopsy is the only definitive means of diagnosing HSE. The aim of this study was to develop radiolabeled nucleoside analogs as biochemical probes for the non-invasive diagnosis of HSE.

[^{131}I, ^{125}I, and ^{123}I]-(*E*)-5-(2-Iodovinyl)-2'-deoxyuridine (IVdU) were synthesised by the reaction of (*E*)-5-(2-carboxyvinyl)-2'-deoxyuridine with radioactive iodide in the presence of chloramine-T. [^{131}I]-IVdU was also prepared using the cuprous ion catalysed halogen isotope exchange method. [^{82}Br]-(*E*)-5-(2-Bromovinyl)-2'-deoxyuridine (BVdU) was synthesised by the reaction of (*E*)-5-(2-carboxyvinyl)-2'-deoxyuridine with [^{82}Br]-NH_4Br in the presence chloramine-T and by direct neutron activation of BVdU containing natural abundance bromine.

In vitro uptake studies for [^{131}I]-IVdU demonstrated its selective uptake in a deoxythymidine kinase positive herpes simplex virus type 1 (HSV-1)-infected cells. The uptake was dependent upon the duration of exposure of cells to [^{131}I]-IVdU, the infecting dose of the virus, and the concentration of [^{131}I]-IVdU. *In vivo* tissue distribution studies on [^{125}I]-IVdU showed a 5.4 to 6.4 times higher uptake in a HSV-1-infected rabbit brain relative to an uninfected brain at 1 hour after an intravenous injection of [^{125}I]-IVdU. The brain to blood ratio of radioactivity in infected rabbits was about 0.5. *In vivo* pharmacokinetic and metabolic studies of [^{131}I]-IVdU in dogs showed its rapid metabolic degradation (biological half-life of about 3 minutes) to the corresponding base [^{131}I]-(*E*)-5-(2-iodovinyl)uracil and [^{131}I]-iodide. The renal excretion of radioactivity was extremely slow (8% of the total radioactivity injected was recovered from urine in 8 h). Diagnostic imaging in the planar and SPECT mode was performed using [^{131}I]-IVdU and [^{123}I]-IVdU respectively in a HSE rabbit model. Neither planar nor tomographic images differentiated the HSV-1-infected brain from an uninfected brain.

In vitro uptake studies of

[5-^{131}I]-1-(2-deoxy-2-fluoro-β-D-ribofuranosyl)-5-iodouracil,

[2-^{14}C]-1-(2-deoxy-2-fluoro-β-D-ribofuranosyl)-5-chlorouracil,

[2-^{14}C]-1-(2-deoxy-2-fluoro-β-D-ribofuranosyl)-5-fluorouracil, and

[5-^{131}I]-1-(2-deoxy-2-fluoro-β-D-arabinofuranosyl)-5-iodouracil have exhibited selective uptake in deoxythymidine kinase positive HSV-1-infected cells, suggesting that they deserve further biological evaluation as potential non-invasive diagnostic agents for HSE.

ACKNOWLEDGEMENTS

I express my sincere thanks to :

Prof. Leonard I. Wiebe, Prof. Edward E. Knaus, and Prof. D. Lorne Tyrrell, my supervisors for their excellent guidance and constant encouragement throughout the course of these investigations ,

Dr. M. John Gill and Dr. Dorothy R. Tovell for their enthusiastic participation in this collaborative project,

Prof. Brian C. Lentle for making available the facilities for diagnostic imaging and Mr. James Thornton for assistance with imaging procedures,

Dr. Paul Reese for drawing majority of the figures and Ms. Siew Tang for typing assistance,

Dr. Richard Flanagan, Mr. Peter Ford, Mr. Takashi Iwashina, Mr. Graeme Boniface, Dr. Hemant Misra, Dr. John Mercer, Dr. Doug Abrams, Dr. Yip Lee, and Ms. Diane Jette for their helping hand at various stages of this work, and

Alberta Heritage Foundation for Medical Research for financial support in the form of a studentship.

Table of Contents

Chapter — Page

I. INTRODUCTION 1

A. Radionuclide Brain Imaging 1

B. Herpes Simplex Encephalitis 5

C. Nucleoside Analogs as Selective anti-HSV Drugs 16

II. MATERIALS AND METHODS 28

A. General 28

Chemicals and solvents 28

Radioisotopes 28

Instrumental analysis 29

Chromatography 30

Radioactivity measurements 30

B. Chemical Synthesis 31

5-Chloromercuri-2'-deoxyuridine 31

(E)-5-(2-Carbethoxyvinyl)-2'-deoxyuridine 31

(E)-5-(2-Carboxyvinyl)-2'-deoxyuridine 32

(E)-5-(2-Iodovinyl)-2'-deoxyuridine 32

(E)-5-(2-Bromovinyl)-2'-deoxyuridine 33

(E)-5-(2-Carboxyvinyl)-2'-deoxyuridine-3',5'-diacetate 34

(E)-5-(2-Iodovinyl)-2'-deoxyuridine-3',5'-diacetate 35

5-Formyl uracil 35

(E)-5-(2-Carboxyvinyl)uracil 35

(E)-5-(2-Iodovinyl)uracil 36

C. Radiochemical Synthesis 36

[^{131}I, ^{125}I, ^{123}I]-(E)-5-(2-Iodovinyl)-2'-deoxyuridine 36

[^{131}I]-(E)-5-(2-Iodovinyl)-2'-deoxyuridine-3',5'-diacetate 37

[^{82}Br]-(E)-5-(2-Bromovinyl)-2'-deoxyuridine (BVdU) 38

D. Quantitative Uptake Studies of Radiolabeled Nucleosides in HSV-1-Infected Cells *In Vitro* 38

Cells 38

Viruses 39

Radiolabeled nucleosides 39

Quantitation of cellular uptake of radiolabeled nucleosides by primary rabbit kidney (PRK) cells 40

E. Tissue Distribution of [^{131}I]-IVdU in a Herpes Simplex Encephalitis Animal Model 40

Animal model 40

Quantitative tissue distribution of [^{125}I]-IVdU 41

F. Pharmacokinetics and Metabolism of [^{131}I]-IVdU in Dogs 41

Quantitative radio high-pressure liquid chromatography (r-HPLC) 41

Metabolism of [^{131}I]-IVdU in blood *in vitro*. 42

Metabolism of [^{131}I]-IVdU in blood *in vivo*. 42

G. Diagnostic Imaging 43

Planar imaging 43

SPECT 43

III. RESULTS AND DISCUSSION 44

A. The Problem and the Approach 44

B. Chemical Synthesis 46

C. Radiochemical Syntheses 53

D. Quantitative Uptake Studies of ^{131}I-Labeled (E)-5-(2-Iodovinyl)-2'-deoxyuridine in Herpes Simplex Virus-Infected Cells *In Vitro* 60

Time-response curve for cellular uptake of [^{131}I]-IVdU 61

Effect of increasing infecting dose of virus on [^{131}I]-IVdU uptake 65

Dose-response curve for [^{131}I]-IVdU uptake 66

E. Tissue Distribution of [^{125}I]-IVdU in a Herpes Simplex Encephalitis Animal Model 66

F. Pharmacokinetics and Metabolism of [^{131}I]-(E)-5-(2-Iodovinyl)-2'-deoxyuridine in Dogs 73

Metabolism of [^{131}I]-IVdU in blood *in vitro* 73

Metabolism of [^{131}I]-IVdU in dog *in vivo* 76

G. Diagnostic Imaging 84

H. Quantitative Uptake Studies of Radiolabeled Nucleosides in Herpes Simplex Virus-Infected Cells *In Vitro* 92

IV. SUMMARY AND CONCLUSIONS 104

REFERENCES 108

APPENDIX 125

A. Yield Calculation for the ^{81}Br(n,γ)^{82}Br Nuclear Reaction 125

List of Tables

Table		Page
.1	Human Herpesviruses	8
.2	Deoxythymidine Kinase Isoenzymes of Various Origins	10
.3	Assessment of Different Non-Invasive Diagnostic Tests for HSE	14
.4	*In Vitro* Anti-HSV Activities of Some Second Generation Nucleoside Analogs	18
.5	Inhibition Constants (K_i) of Some Antiviral Nucleosides for Deoxythymidine Kinases of Various Origins	20
.6	Inhibition Constants of Some Antiviral Nucleoside Triphosphates for DNA Polymerases of Various Origins	23
.7	Radiochemical Synthesis of IVdU	57
.8	Preparation of [^{77}Br]-BVdU	59
.9	Tissue Distribution of [^{125}I]-IVdU (Expressed As % Injected Dose Per Gram Tissue)in a Rabbit Model 1 Hour After i.v Injection of 0.74 MBq of [^{125}I]-IDdU (Mean of Two Animals with Range)	68
.10	Tissue Distribution of [^{125}I]-IVdU (Expressed as % Injected Dose per Gram Tissue) in a Rabbit Model 6 Hours After i.v Injection of 0.74 MBq of [^{125}I]-IVdU (Mean of Two Animals with Range)	69
.11	Tissue Distribution of [^{125}I]-IVdU(Expressed as Tissue to Blood Ratio)in a Rabbit Model 1 Hour After i.v Injection of 0.74 MBq of [^{125}I]-IVdU(Mean of Two Animals with Range)	70
.12	Tissue Distribution of [^{125}I]-IVdU(Expressed as Tissue to Blood Ratio)in a Rabbit Model 6 Hours After i.v Injection 0.74 MBq of [^{125}I]-IVdU (Mean of Two Animals with Range)	71
.13	Recovery of Radioactivity from Urine for Various Times After i.v Injection of [^{131}I]-IVdU(Mean of Two Experiment with Range)	80
.14	*In Vitro* Anti-HSV Activity of Some 5-Halogenated 1-(2-deoxy-2-fluoro-β-D-arabinofuranosyl)-uracils	96
.15	Percent Uptake of Radiolabeled Nucleoside Analogs in HSV-1 (TK^+)-Infected cells at 4 h and 24 h	102

List of Figures

Figure — Page

.1 Diagram of a Virion of Herpes Simplex Virus. 6

.2 Some Second Generation Nucleoside Analogs with Antiherpes Activity. 17

.3 Selective Metabolic Trapping of (*E*)-5-(2-Halovinyl)-2'-deoxyuridines in Herpes Simplex Virus-Infected Cells. 45

.4 Chemical Structure for (*E*)-5-(2-Halovinyl)-2'-deoxyuridines. 47

.5 General Synthetic Route for the Synthesis of IVdU and BVdU. 48

.6 Reaction Mechanism for Coupling of Dilithium Palladium Tetrachloride with 5-Chloromercuri Nucleosides. 49

.7 Synthesis of IVdU and BVdU using the Chloramine-T Method. 51

.8 Synthesis of IVdU-3',5'-diacetate. 52

.9 Synthesis of (*E*)-5-(2-iodovinyl)uracil. 54

.10 Synthesis of Radiohalogenated IVdU and BVdU. 56

.11 Time-Response Curve for [^{131}I]-IVdU Uptake in HSV-1 (TK$^+$) (n=3) and Mock-Infected (n=2) PRK cells. (Mean and Range). 62

.12 Effect of Increasing the Titer of the Infecting Dose on the Uptake of [^{131}I]-IVdU in HSV-1 (TK$^+$) (n=3)), HSV-1 (TK$^-$) (n=2), Mock-Infected Cells (n=3) (Mean and Range). 63

.13 Effect of Increasing Concentrations of [^{131}I]-IVdU on its Uptake in HSV-1 (TK$^+$) (n=3), HSV-1 (TK$^-$) (n=2), Mock-Infected Cells (n=2)) (Mean and Range). 64

.14 A Typical Radio High-Pressure Liquid Chromatogram of Plasma Sample Containing [^{131}I]-IVdU and its Metabolites. 74

.15 Metabolites of [^{131}I]-IVdU in Blood *In Vitro*. 76

.16 Metabolites of [^{131}I]-IVdU (specific activity, 1665 MBq /mmol) in Dogs *In Vivo* (n=2). 78

.17 Metabolites of [^{131}I]-IVdU (specific activity, 37 TBq /mmol) in Dog *In Vivo* (n=1). 79

.18 Schematic Presentation of the Metabolism of [^{131}I]-IVdU in Dogs *in vivo*. 82

.19 Planar Whole Body Image of an Uninfected Rabbit 1 h After an Intravenous Injection of [^{131}I]-IVdU. 85

Figure Page

.20 Planar Image (Head) of an HSV-1-infected Rabbit 1 h After an Intravenous Injection of [^{131}I]-IVdU. 86

.21 Chemical Structures for 1-(2-deoxy-2-fluoro-β-D-ribofuranosyl)-5-halouracils and 1-(2-deoxy-2-fluoro-β-D-arabinofuranosyl)-5-halouracils. 94

.22 *In Vitro* Uptake of [5-^{131}I]-FIRU in HSV-1 (TK$^+$) (n=5), HSV-1 (TK$^-$) (n=4), and Mock-Infected Cells (n=4) 98

.23 *In Vitro* Uptake of [2-^{14}C]-FCRU in HSV-1 (TK$^+$) (n=5) , HSV-1 (TK$^-$) (n=4), and Mock-Infected Cells (n=4) 99

.24 *In Vitro* Uptake of [2-^{14}C]-FFRU in HSV-1 (TK$^+$) (n=5), HSV-1 (TK$^-$) (n=4), and Mock-Infected Cells (n=4) 100

.25 *In Vitro* Uptake of [5-^{131}I]-FIAU in HSV-1 (TK$^+$) (n=5), HSV-1 (TK$^-$) (n=4), and Mock-Infected Cells (n=4) 101

List of Plates

Plate | Page

.1 SPECT Images of an Uninfected Rabbit 30 min after Intracarotid Injection of [^{123}I]-IVdU 89

.2 SPECT Images of an HSV-1-Infected Rabbit 30 min after Intracarotid Injection of [^{123}I]-IVdU 91

List of Abbreviations

ACG	9-(2-hydroxyethoxymethyl)guanine
ACG-MP	9-(2-hydroxyethoxymethyl)guanine-5'-monophosphate
ACG-TP	9-(2-hydroxyethoxymethyl)guanine-5'-triphosphate
ara-A	9-β-D-arabinofuranosyl adenine
ara-AMP	9-β-D-arabinofuranosyl adenine-5'-monophosphate
ATP	adenosine-5'-triphosphate
BBB	blood-brain barrier
BME	Basal Medium Eagle's
Bq	Becquerel(s)
BVdU	(*E*)-5-(2-bromovinyl)-2'-deoxyuridine
BVdU-DP	(*E*)-5-(2-bromovinyl)-2'-deoxyuridine-5'-diphosphate
BVdU-MP	(*E*)-5-(2-bromovinyl)-2'-deoxyuridine-5'-monophosphate
BVdU-TP	(*E*)-5-(2-bromovinyl)-2'-deoxyuridine-5'-diphosphate
BVU	(*E*)-5-(2-bromovinyl)uracil
C	cytosine
°C	degree Celsius
cm	centimeter(s)
CMV	cytomegalovirus
CNS	central nervous system
CPM	counts per minute
CSF	cerebrospinal fluid
CT	computed tomography
CTP	cytidine-5'-triphosphate
dATP	deoxyadenosine-5'-triphosphate
dC	deoxycytidine
dCMP	deoxycytidine-5'-monophosphate

dCTP	deoxycytidine-5'-triphosphate
dGDP	deoxyguanosine-5'-diphosphate
dGTP	deoxyguanosine-5'-triphosphate
DHPG	9-[(1,3-dihydroxy-2-propoxy)methyl]guanine
DMF	dimethyl formamide
DNA	deoxyribonucleic acid
dT	deoxythymidine
dTDP	deoxythymidine-5'-diphosphate
dTMP	deoxythymidine-5'-monophosphate
DTPA	diethylene triamine pentacetic acid
dTTP	deoxythymidine-5'-triphosphate
dU	deoxyuridine
dUTP	deoxyuridine-5'-triphosphate
EBV	Epstein-Barr virus
EEG	electroencephalography
ECT	emission computed tomography
FDG	2-deoxy-2-fluoro-D-glucose
FDG-6-P	2-deoxy-2-fluoro-D-glucose-6-phosphate
FBAU	1-(2-deoxy-2-fluoro-β-D-arabinofuranosyl)-5-bromouracil
FBRU	1-(2-deoxy-2-fluoro-β-D-ribofuranosyl)-5-bromouracil
FCAU	1-(2-deoxy-2-fluoro-β-D-arabinofuranosyl)-5-chlorouracil
FCRU	1-(2-deoxy-2-fluoro-β-D-ribofuranosyl)-5-chlorouracil
FFAU	1-(2-deoxy-2-fluoro-β-D-arabinofuranosyl)-5-fluorouracil
FFRU	1-(2-deoxy-2-fluoro-β-D-ribofuranosyl)-5-fluorouracil
FIAC	1-(2-deoxy-2-fluoro-β-D-arabinofuranosyl)-5-iodocytosine
FIAC-MP	1-(2-deoxy-2-fluoro-β-D-arabinofuranosyl)-5-iodocytosine-5'-monophosphate

FIAC-TP	1-(2-deoxy-2-fluoro-β-D-arabinofuranosyl)-5-iodocytosine-5'-triphosphate
FIAU	1-(2-deoxy-2-fluoro-β-D-arabinofuranosyl)-5-iodouracil
FIAU-MP	1-(2-deoxy-2-fluoro-β-D-arabinofuranosyl)-5-iodouracil-5'-monophosphate
FIRU	1-(2-deoxy-2-fluoro-β-D-ribofuranosyl)-5-iodouracil
FMAU	1-(2-deoxy-2-fluoro-β-D-arabinofuranosyl)-5-methyluracil
G	guanine
g	gram(s)
GBq	gigaBecquerel
GDP	guanosine-5'-diphosphate
GMP	guanosine-5'-monophosphate
GTP	guanosine-5'-triphosphate
h	hour(s)
^{1}H NMR	proton magnetic resonance spectra
HPLC	high-pressure liquid chromatography
hrms	high resolution mass spectra
HSE	herpes simplex encephalitis
HSV	herpes simplex virus
HSV-1	herpes simplex virus type 1
HSV-2	herpes simplex virus type 2
Hz	hertz
id	internal diameter
ID_{50}	inhibitory dose-50
IdU	5-iodo-2'-deoxyuridine
i.v	intravenous
IVdU	(*E*)-5-(2-iodovinyl)-2'-deoxyuridine

IVdU-DP	(*E*)-5-(2-iodovinyl)-2'-deoxyuridine-5'-diphosphate
IVdU-MP	(*E*)-5-(2-iodovinyl)-2'-deoxyuridine-5'-monophosphate
IVdU-TP	(*E*)-5-(2-iodovinyl)-2'-deoxyuridine-5'-triphosphate
IVU	(*E*)-5-(2-iodovinyl)uracil
KBq	kiloBecquerel
K*i*	inhibition constant
L	litre(s)
M	molar
MBq	megaBecquerel
MEM	Minimum Essential Medium
mg	milligram(s)
min	minute(s)
mL	millilitre(s)
mM	millimolar
μM	micromolar
mmol	millimole(s)
μmol	micromole(s)
mol	mole(s)
mp	melting point
MS	mass spectra
MW	molecular weight
N	normal
n	neutron(s)
n	number(s)
NBS	N-bromosuccinimide
NCA	no-carrier-added
NIS	N-iodosuccinimide

NIAID	National Institute of Allergy and Infectious Diseases
ng	nanogram(s)
nmol	nanomole(s)
NMR	nuclear magnetic resonance
nmol	nanomole(s)
P	partition coefficient (octanol : water)
PBS	phosphate buffered saline
PFU	plaque forming unit(s)
pI	isoelectric point
PET	positron emission tomography
PRK	primary rabbit kidney
RDP	ribonucleoside diphosphate
R_f	retardation factor
r-HPLC	radio high-pressure liquid chromatography
RIPA	radioimmune precipitation assay
s	second(s)
S	sedimentation coefficient
SPECT	single photon emission computed tomography
TBq	TeraBecquerel
TD_{50}	toxic dose-50
TK	deoxythymidine kinase
TK^+	deoxythymidine kinase positive
TK^-	deoxythymidine kinase negative
TLC	thin layer chromatography
TLRC	thin layer radio chromatography
TS	thymidylate synthetase
UV	ultraviolet spectra

UTP	uridine-5'-triphosphate
VZV	varicella-zoster virus

I. INTRODUCTION

A. Radionuclide Brain Imaging

The imaging of brain using radionuclides originated in 1948, when George Moore at the University of Minnesota reported the detection of brain tumors with [^{131}I]-diiodofluorescein using a Gieger-Muller counter (1). Advances in the subsequent years included the development of the rectilinear scanners , which preceeded the introduction of scinitillation camera (2-4). In 1958 Anger, at the University of California at Berkeley, introduced an imaging system with no moving parts (5). This was a major contribution to neuronuclear medicine since dynamic rapid-sequence flow studies of the brain could now be done. When $^{99}Tc^{m}$-labeled pertechnetate became available as a radiopharmaceutical for brain imaging in 1964 (6), radionuclide brain scans became widely used in the late 1960s and early 1970s. A variety of lesions involving breakdown of the blood-brain barrier (BBB) could be detected non-invasively by this method. However, these images suffered from poor spatial resolution and provided little anatomical or functional detail.

The concept of emission tomography (ECT) for three dimensional scans was introduced by Kuhl and Edward in 1963 (7). An idea ahead its time, this methodology had little immediate impact in the medical field, probably due to the lack of appropriate radiopharmaceuticals and inadequate instrumentation. However, the same principle of reconstruction tomography found an important application in X-ray transmission computed tomography (CT) in 1973 (8, 9). The brain images obtained by CT were superior to conventional radionuclide brain images with respect to spatial resolution. In the late 1970s, CT became the best method for evaluation of many neurological disorders, resulting in a dramatic decline in the number of radionuclide studies of brain. However, with recent developments in the design of radiopharmaceuticals for functional imaging of brain and advances in radiation detection systems, ECT has reemerged as an important brain imaging technique.

The physical principles of tomography have been reviewed (10, 11). Tomographic imaging requires the acquisition of a series of images at different angular orientations with respect to the target organ. These images are then processed using a filtered back-projection algorithm to obtain tomographic images showing the distribution of the radionuclide in the tissue section of interest (11). There are two types of ECT *viz* positron emission tomography (PET) and single photon emission computed tomography (SPECT). They differ with respect to the type of radionuclide used and the detection system required for imaging. PET imaging requires the use of positron emitting radionuclides such as ^{11}C, ^{13}N, ^{15}O and ^{18}F. This imaging technique detects annihilation radiation by coincidence counting. SPECT can be performed using γ-ray emitting nuclides such as $^{99}Tc^{m}$ and ^{123}I. The detection system operates in the single photon mode. The inherent advantages and disadvantages of PET and SPECT have been reviewed (12). The annihilation coincidence detection used in PET offers higher spatial resolution than that obtained by single photon detection used in SPECT. A PET unit requires, in most instances, facilities for on-site production of the radionuclides and preparation of the radiopharmaceuticals, since medically useful positron emitting nuclides have extremely short half-lives. PET programs require a large financial investment, thereby limiting their availability to medical research institutions. Since the cost factor for SPECT is more favourable than for PET, at present it is the most commonly used ECT in general hospitals.

Radiopharmaceuticals used in brain imaging may be classified into two major groups : non-specific agents used for the evaluation of vascularity of brain and metabolic analogs used for functional imaging. The non-specific agents include macromolecules such as $^{99}Tc^{m}$- or ^{131}I-labeled human serum albumin and small molecules such as [$^{99}Tc^{m}$]- diethylene triamine pentaacetic acid (DTPA) and [$^{99}Tc^{m}$]-glucoheptonate. These radiopharmaceuticals are used to detect brain lesions associated with increased regional vasularity and/or permeability using tomographic or planar brain imaging techniques. Radiopharmaceuticals for the evaluation of brain function are designed as probes for regional cerebral metabolism. They include probes for energy metabolism, neurotransmitters and their analogs, and centrally acting drugs. These

studies require imaging in the tomographic (PET or SPECT) mode.

Transport of molecules across the blood-brain barrier (BBB) is one of the important factors to be considered in the design of radiopharmaceuticals for brain imaging. The BBB, a unique microanatomic feature of brain, constitutes a barrier to the passage of compounds not required for brain metabolism and thus limits the movement of potentially toxic substances from blood to brain (13). Chemicals entering the brain cells do so either by carrier mediated transport (eg: glucose) or by passive diffusion across the lipid bilayer by virtue of their high lipid solubility (eg: oxygen). The rationale for the use of non-specific radiopharmaceuticals is based on their inability to cross the intact BBB. Several pathological conditions of the central nervous system (CNS) are associated with regional breakdown of the BBB. Radiopharmaceuticals used in the evaluation of the BBB will be useful to delineate such areas using a diagnostic brain scan.

The ability to cross the BBB is an essential requirement of radiopharmaceuticals designed as probes of brain metabolism. An excellent example of a radiopharmaceutical entering the brain by carrier mediated transport is [^{18}F]-2-deoxy-2-fluoro-D-glucose (FDG) (14). The hexose carrier in the BBB has stringent stereochemical requirements for all positions of the substrate except for C_2 (15, 16). 2-Deoxy-2-fluoro-D-glucose therefore satisfies the structural requirements for the transport across the BBB. The design of [^{18}F]-flouro analogs as radiopharmaceuticals, which retain the BBB transport characteristics of the natural substrates has also been successfully applied to aminoacid derivatives (eg: [^{18}F]-6-fluoro-L-dopa) (17, 18).

An alternate approach to facilitate the BBB transport of radiopharmaceuticals is to increase their lipophilicity. The brain capillary permeability of a compound is related to its octanol/water partition coefficient (P) and molecular weight (19). For compounds with molecular weight below 400, increasing lipophilicity will improve the brain capillary permeability. Dischino *et al* have reported a parabolic relationship between log P (partition coefficient for octanol/water) values and brain extractability for a group of ^{11}C-labeled

compounds and have suggested an optimal log P range of 0.9 to 2.5 for radiopharmaceuticals designed to cross the BBB by virtue of their lipid solubility (20).

The design of metabolic analogs as biochemical probes for cerebral function is one important approach to the development of radiopharmaceuticals for brain imaging. The biochemical rationale behind the development of [^{18}F]-FDG as a non-invasive probe for quantitation of regional cerebral glucose metabolism illustrates such an approach (21, 22). Brain meets its energy requirements exclusively from D-glucose. Hence, the rate of cerebral glucose metabolism could serve as an important index for neurological investigations. FDG is a good substrate for hexokinase (23) and therefore will be phosphorylated to the 6-phosphate (FDG-6-P). FDG-6-P is not subject to metabolism by the enzymes glucose-6-phosphate dehydrogenase and glucose phosphate isomerase, unlike glucose-6-phosphate (24, 25). There is very little glucose-6-phosphatase activity in the brain (26, 27). Hexose-6-phosphates exhibit very low permeability across the plasma membrane. Therefore FDG-6-P, once formed, is trapped in cerebral tissue. This metabolic trapping of [^{18}F]-FDG can be monitored non-invasively by PET and can be used as an index of regional cerebral glucose metabolism. Pharmacokinetic models of FDG utilization could be used for the tomographic quantitation of regional cerebral glucose metabolic rate (28). The clinical applications of [^{18}F]-FDG have been recently reviewed (14, 29).

A similar principle has been used to study dopamine metabolism in brain (17, 18). Dopamine does not cross the BBB and is produced in brain by decarboxylation of its immediate precursor L-dopa. This amino acid crosses the BBB by an active transport process. [6-^{18}F]-L-dopa possesses transport characteristics similar to dopa and is a substrate for a cerebral aromatic acid decarboxylase. PET studies using this compound in normal human subjects suggests its potential as a probe for quantitative regional cerebral metabolism of dopamine (18). Drugs acting on the CNS such as chlorpromazine and flunitrazepam labeled with ^{11}C have been used in PET studies for non-invasive mapping of specific receptors in brain (30, 31).

Besides ECT and CT another important tomographic mode of imaging - nuclear magnetic resonance (NMR) imaging - has recently become available as a non-invasive tool for neurological investigations (32, 33). The full potential of ECT and NMR in brain imaging remains to be explored. Therefore it is difficult to project the relative importance of these three imaging modalities for the future. The greatest strength of CT is its ability to show intracranial morphology with high resolution. It is quite likely that NMR imaging may provide this in the near future. One desirable feature of NMR imaging is that it does not use ionising radiation. ECT is advantageous since it provides information on regional brain biochemistry and therefore is of value in understanding the biochemical aspects of diseases and objective monitoring of therapy. The tracer technique used in ECT would seem to be superior to other imaging modalities with respect to flexibility of studying specific biochemical pathways by determining biochemical components that contribute to an observed disturbance. Since each of these imaging methods have different advantages, it is expected that the information derived would be complementary and would helpful in acquiring the overall pathophysiological picture of the CNS.

B. Herpes Simplex Encephalitis

Herpes simplex virus (HSV), the causative organism for herpes simplex encephalitis (HSE), belongs to the family of herpetoviridae, commonly known as the herpesvirus group (34). The core of the herpesviruses consists of a single molecule of double stranded DNA with a molecular weight (MW) of about 100×10^6, wrapped around an associated protein (Fig 1). This DNA-protein core is enclosed in a protein capsid shell with an icosahedral symmetry. The tegument surrounding the capsid consists of assymmetrically distributed globular material. A lipid bilayer membrane envelops the tegument and is studded with glycoprotein projections. There are two main immunological variants of HSV, type 1 and type 2. The common clinical manifestations of HSV-1 are herpes labialis (cold sore), gingivostomatitis, and keratoconjunctivitis. The most common site of HSV-2 infection is the genital organs and the

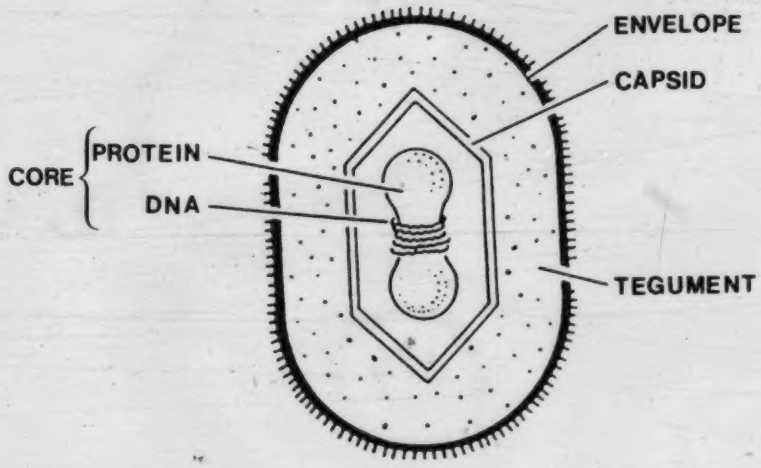

Fig. 1 Diagram of a Virion of Herpes Simplex Virus.

infection is usually transmitted venereally. In addition to HSV, the major human pathogens of herpesviruses are varicella-zoster virus (VZV), cytomegalovirus (CMV), and Epstein-Barr virus (EBV). Some characteristic of herpesviruses including the human diseases caused by them are shown in Table 1.

The pathogenesis of HSV infections has been extensively reviewed (35-39). Following a primary infection, both HSV-1 and HSV-2, establish latent infection in the neurons of the sensory ganglia innervating the site of primary infection. The infected ganglia becomes a reservoir of latent virus, which upon reactivation, may establish a recurrent infection. The details of the mechanisms for latency and recurrence have not been fully elucidated, and some aspects are still the subject of opposing views. The virus is believed to reach the ganglia by centripetal axonal migration (36, 40-42). However, some reports indicate that under certain circumstances the virus may reach the site of latency as a result of viremia (43, 44). During the latent state, the infectious virus cannot be isolated from cell-free ganglia homogenates. Ritchie and Timbury have discussed the possibility of insertion of the viral genome into the host DNA during latency (45). A variety of stimuli including sunlight, emotional stress, menstruation, and surgical procedures have been reported to be associated with the reactivation of the latent virus (38, 46). The mechanism(s) of reactivation by these stimuli is (are) not yet clear. Hill and Blyth have suggested that the reactivation process is mediated through an increased synthesis of prostaglandins (47-49). However, there is no definitive evidence supporting this theory.

HSV induces synthesis of many virus-specific proteins in the infected cells. Among these, the enzymes deoxythymidine kinase (TK) and DNA polymerase have received considerable attention as potential targets for the design of antiviral drugs. TK is a 'salvage pathway' enzyme that catalyzes the phosphorylation of deoxythymidine (dT) to the corresponding 5'-monophosphate (dTMP). TK isoenzymes of various origins have been extensively studied (50-53). Human cells contain two types of TK enzymes : deoxythymidine kinase F (TK-F) found primarily in the cytosol fraction and deoxythymidine kinase A (TK-A)

Table 1. Human Herpesviruses.

Virus	DNA		Site of	Human
	Molecular Weight (10^6) (Approximate)	G + C Content (%)	Latency	Disease(s)
HSV-1	100	70	Neurons	Herpes Labialis, Kerato-conjuntivitis, Herpes Encephalitis
HSV-2	100	69	Neurons	Genital herpes, Neonatal Herpes
VZV	80-100	46	Neurons	Chicken Pox, Shingles
CMV	130-150	58.5	Epithelial or White Blood Cells	Cytomegalic Inclusion Disease
EBV	110-115	57-59	Lymphocytes	Infectious Mononucleosis, Burkitt's Lymphoma, Nasopharangeal Carcinoma

G = Guanine
C = Cytosine

localized mainly in the mitochondrial matrix (50). TK-A does not play a significant role in the generation of dT phosphates for nuclear DNA synthesis. HSV-1- and HSV-2-encoded TK isoenzymes are distinctively different from human TKs. The HSV-1- and HSV-2-induced TK enzymes differ antigenically from the human enzymes. With respect to molecular weight (MW), isoelectric point (pI), phosphate donor specificities and substrate specificities, the virus-encoded enzymes differ from TK-F, but resemble TK-A (Table 2) (50, 53-58). However, HSV-induced TKs have larger sedimentation coefficients (S) than the mitochondrial enzyme. Unlike TK-A, the viral enzymes are not subject to feed back inhibition by deoxycytidine triphosphate (dCTP). The broad substrate specificities of HSV-encoded enzymes is of special interest for the design of selective antiviral agents (59-61).

The virus-induced TK enzymes play a very important role in the DNA replication of HSV. The dTMP produced by TK is a precursor of dTTP, which is one of the four deoxyribonucleoside triphosphates required for DNA synthesis. dTTP is also required as an allosteric effector for the reduction of guanosine diphosphate (GDP) to deoxyguanosine diphosphate (dGDP) by the host enzyme ribonucleoside diphosphate (RDP) reductase (62, 63). dGDP is the precursor of deoxyguanosine triphosphate (dGTP). The intracellular concentration of dGTP is usually significantly lower than that of the other three deoxyribonucleoside triphosphates dATP, dCTP, and dTTP and therefore is a critical factor controlling the rate of DNA synthesis. Kit *et al* have pointed out that the major role of TK enzymes in the rapid synthesis of DNA may in fact be its indirect stimulation of the biosynthesis of dGTP (50). An HSV-1-induced RDP reductase has been recently isolated (64, 65). This enzyme appear to be not subject to significant allosteric modulation and therefore unlikely to be influenced by TK activity. The virus-encoded TK is considered to be important in relation to the pathogenesis and latency of HSV-1 and HSV-2. TK-deficient (TK^-) mutants of HSV have been reported to be less pathogenic as compared to the TK-positive (TK^+) strains (66). The expression of the TK gene is also observed to be an essential requirement for the establishment of HSV infection in sensory ganglia and therefore the latent stage of infection

Table 2. Deoxythymidine Kinase Isoenzymes of Various Origins

Enzyme	Molecular Weight	Isoelectric Point (pI)	Sedimentation Coefficient (S)	Phosphate Donor	Feed back Inhibitors	Natural Substrates
Human Cytosolic (TK-F)	90,000	9.7	5.2	ATP	dTTP	dT,dU
Human Mitochondrial (TK-A)	70,000	5.6	4.5	ATP,UTP CTP,GTP	dTTP dCTP	dT,dU
HSV-1	70,000	6.0-6.5	5.2	ATP,UTP CTP,GTP	dTTP	dT,dU,dC
HSV-2	70,000	6.3	4.9	ATP,UTP CTP,GTP	dTTP	dT,dU,dC

(67, 68).

The enzyme responsible for the incorporation of nucleotides into the growing polynucleotide chain is DNA polymerase. This enzyme is essential for DNA replication. Mammalian cells contain three classes of DNA polymerases designated as α, β, and γ (69). HSV-induced DNA polymerases differ from these three host cell enzymes with respect to molecular weight, elution profile on ion-exchange columns, primer template preferences and effect of monovalent and divalent cations (69-73). The unique features of HSV-induced DNA polymerases include their requirement for high salt concentration for maximal activity (74) and sensitivity to low phosphonoacetate concentrations (75). The virus-induced DNA polymerase enzymes are essential for the replication of HSV (76). The viral DNA polymerase is considered to be the primary target of the antiviral action of several selective antiviral drugs (61).

Herpes simplex encephalitis (HSE) is a rare clinical manifestation of HSV. However, it is considered to be the most common sporadic encephalitis in North America (77). Whitley *et al* have reviewed the epidemiological aspects of HSE (78). In a series of 113 biopsy-proven cases examined, HSE occurred in all age groups, in both sexes and was non-seasonal. HSE in adults is usually a focal infection and over 95% of the adult HSE are caused by HSV-1 (79, 80). Neonatal HSE is usually caused by HSV-2 and may be disseminated or localized (81). Untreated HSE is reported to be associated with a high mortality rate (70%) and severe morbidity (82).

The pathogenesis of HSE is not yet clearly understood. In neonatal HSE, the virus is most often transmitted from an infected maternal genital tract during delivery. Other less frequent routes including transplacental transmission also exist (83). Adult HSE may be caused by a primary infection or by reactivation of a latent infection (84). Restriction endonuclease analysis of viral DNA has been used to investigate the possible existence of neurovirulent strains of HSV-1 (85, 86). HSV-1 isolates used in these studies appeared to be different at the molecular level and showed no common denominator suggestive of neurovirulence (86, 87). In view of the small proportion of the DNA examined in these studies, results should not be

considered as conclusive evidence for nonexistance of neurovirulent strains of HSV. Potential routes responsible for viral spread from the site of latency have been investigated (88-92). The most common site of latency for HSV-1 is believed to be the trigeminal ganglia. Davis and Johnson have postulated that viral spread occurs from the trigeminal ganglia to the brain through tentorial nerves, which innervate the fascia near the temporal and frontal lobes (88). A more direct route involving the spread of the virus from the olfactory bulb has been proposed by other investigators (90-92). The olfactory spread theory has been supported by demonstrated presence of HSV in the olfactory bulb and degeneration in the olfactory tract in some HSE patients (90-92). It is also possible that brain itself could have been the site of latency (90). The detection of HSV-1 genome in human brain tissue supports this postulate (93, 94).

In adults, HSE causes localized tissue necrosis of brain usually in the frontal and temporal regions (95, 96). However, rare patients with infection of parietal lobe, occipital lobe and brain stem have also been reported (97-99). Pathological changes, evident from light and electron microscopy studies include lymphocyte infiltration, neuronal and glial cell loss, and eosinophilic intracellular inclusion bodies usually containing viral particles (82, 100, 101).

Clinical presentations of HSE are non-specific. Whitley *et al* have reviewed the clinical symptoms of 110 cases of biopsy-proven HSE (78). Alteration of consciousness, fever, headache, seizures all were common, but not uniform, among patients with HSE. Such clinical features could also be observed with nearly equal frequency among the biopsy-negative patients initially suspected of HSE. From these studies Whitley *et al* have concluded that there is no unique group of symptoms that distinguishes patients with HSE from those having other illness affecting the CNS.

Non-invasive methods investigated for the diagnosis of HSE include electroencephalography (EEG) (102, 103), X-ray transmission computed tomography (CT) (104, 105), and radionuclide brain imaging using [$^{99}Tc^{m}$]-sodium pertechnetate or chelates (106, 107). Whitley *et al* assessed the diagnostic value of these tests in a number of

biopsy-positive and biopsy-negative patients, all initially suspected of having HSE (78). A comparison of the sensitivities and specificities of the various diagnostic tests evaluated for HSE (Table 3) indicated that EEG was the most sensitive of these tests, but suffered from unacceptably high false positive results. Radionuclide and CT imaging showed higher specificity, but had unacceptably low sensitivity. Two immunological methods have been investigated as diagnostic tests for HSE. A ratio of serum to cerebrospinal fluid (CSF) concentrations of HSV antibodies lower than 20 has been proposed as indicative of HSE (108). Another method involving detection of HSV antigens in CSF has also been proposed (109). The low sensitivities of these methods particularly early in desease make them unreliable tests for definitive diagnosis of HSE.

A definitive diagnosis of HSE is currently achieved by brain biopsy and then identification of the virus by *in vitro* culture techniques (110, 111). The presence of the virus in the biopsy tissue may be demonstrated more rapidly by electron microscopy or immunofluorescence (79, 112). Brain biopsy as a diagnostic test has a sensitivity of 95% (79). The invasive nature of this procedure has been the major objection to its use (113). In a consecutive series of 50 brain biopsy studies, Kaufman *et al* have noted a total morbidity and mortality rate of 13% (110), whereas Bazra *et al* estimated these risks to be in the range of 0.5 to 2% (114). In view of the risks involved in brain biopsy, Caplan has argued in favour of blind therapy using ara-A in patients with clinical picture and non-invasive tests suggestive of HSE (115). This view is likely to gain increasing support with the availability of less toxic antiviral agents such as acycloguanosine (ACG) for the treatment of HSE. Whitley *et al* have pointed out the special benefit of brain biopsy in that, as well as confirming the diagnosis in the HSE positive cases, it may also provide alternate diagnosis for other treatable diseases in a significant number of HSE-negative patients (116). The present controversy associated with the diagnosis of HSE clearly illustrates the urgent need for the development of a specific and sensitive non-invasive test for HSE.

Table 3. Assessment of Different 'Non-Invasive' Diagnostic Tests for HSE

Diagnostic Test	Sensitivity (%)	Specificity (%)
Electroencephalography	81	41
Radionuclide Brain Imaging	50	86
Computed Tomography	59	78
Serum to CSF Antibody Ratio	50	81
HSV Antigen in CSF	64	86

Ara-A is the only drug currently licensed for the treatment of HSE (82, 116). Treatment with ara-A is estimated to decrease the mortality rate of HSE from 70% to 40% (116). The level of consciousness at the time of initiation of therapy and the age of the patient are the major factors influencing the therapeutic outcome. Prognosis is usually much better in patients below 30 years of age at all levels of consciousness. Ara-A therapy is most successful favouring complete recovery in patients within this age group, provided they were only lethargic at the begining of therapy. Older patients, who are comatose at the time of treatment initiation are unlikely to benefit from ara-A. The toxic effects reported with use of this drug include nausea, vomiting, diarrhea, bone marrow supression, tremor and confusion (116, 117). Due to its poor water solubility, the intravenous administration of ara-A requires a large fluid load. This poses a problem in HSE patients with cerebral edema. The use of ara-AMP, a prodrug of ara-A, has been proposed to overcome this problem (118). However,the National Institute of Allergy and Infectious Diseases (NIAID) collaborative clinical trials indicated that the patients who recieved ara-AMP did not benefit from therapy (119). It has been pointed out that this may be due to unfavourable factors related to the patient such as age and level of consciousness at the time of therapy initiation. A selective and specific drug acycloguanosine (ACG) is currently being investigated as a therapeutic agent for HSE. A recent multicenter study from Sweden has compared the therapeutic efficacy of ACG versus ara-A in 53 confirmed cases of HSE (120). They reported a significantly lower mortality rate for ACG treated patients (19%) as compared to ara-A treated patients (50%). Six months after the acute illness, 56% of ACG treated patients returned to normal life as compared to 13% of ara-A treated patients. These results suggest the superiority of ACG for the treatment of HSE relative to ara-A. More recent antiherpes drugs such as (*E*)-5-(2-bromovinyl)-2'-deoxyuridine (BVdU), 1-(2-deoxy-2-fluoro-β-D-arabinofuranosyl)-5-iodocytosine (FIAC), and 9-[(1,3-dihydroxy-2-propoxy)methyl]guanine (DHPG) await clinical evaluation as therapeutic agents for HSE.

C. Nucleoside Analogs as Selective anti-HSV Drugs

Three nucleoside analogs that have been used as therapeutic agents for herpes simplex infections during the past two decades are 5-iodo-2'-deoxyuridine (IdU), 5-trifluoromethyl-2'-deoxyuridine (trifluorothymidine, TFT) and 9-β-D-arabinofuranosyl adenine (adenine arabinoside, ara-A). These compounds are often referred to as first generation antiherpes drugs. In recent years several new analogs have been developed, which are superior in selectivity and/or potency to the first generation drugs. There are two major factors that have contributed to the development of these second generation nucleoside analogs. First, recent advances in nucleoside chemistry has increased the possibility for molecular modification of nucleosides resulting in synthesis of numerous chemical analogs of naturally occurring nucleosides. Second, elucidation of the biochemical steps involved in HSV replication has revealed certain virus-specific enzymes which are potential targets for the design of antiviral drugs. The selective antiviral action of the nucleoside analogs has been reviewed recently. (61, 121, 122). The present discussion is focussed on the biochemical aspects of the selective antiherpes activity of the second generation nucleoside analogs and their metabolic degradation *in vivo*.

The most important selective nucleoside analogs which are active against HSV may be grouped into three categories :

1. acycloguanosine nucleosides,
2. (*E*)-5-(2-halovinyl)-2'-deoxyuridines and their analogs, and
3. 1-(2-deoxy-2-fluoro-β-D-arabinofuranosyl)pyrimidine analogs.

The chemical structures of these compounds are shown in Fig 2. These compounds have all been reported to be highly potent and selective in their action against HSV. The relative potencies of these compounds are listed in Table 4. While acycloguanosine nucleosides and 1-(2-deoxy-2-fluoro-β-D-arabinofuranosyl)pyrimidines are equally effective against HSV-1 and HSV-2 replication, (*E*)-5-(2-halovinyl)-2'-deoxyuridine analogs exhibit a 100-1000 fold greater potency against HSV-1 relative to HSV-2. The greatest selectivity index (TD_{50}/ID_{50})

Acycloguanosine Nucleosides

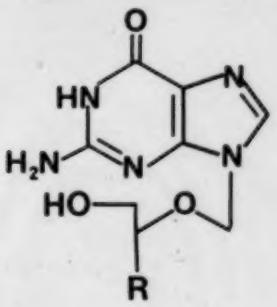

R	Compound
H	ACG
CH_2OH	DHPG

(*E*)-5-(2-Halovinyl)-2'-deoxyuridines and their Analogs

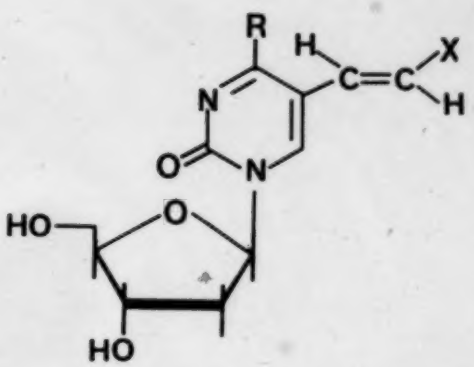

R	X	Compound
OH	Br	BVdU
OH	I	IVdU
NH_2	Br	BVdC

1-(2-Deoxy-2-fluoro-β-D-arabinofuranosyl)pyrimidine Nucleosides

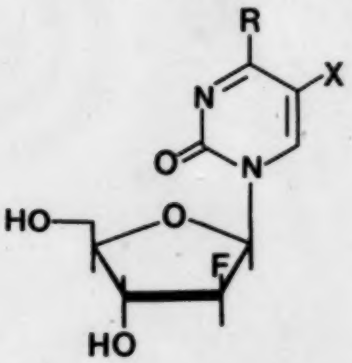

R	X	Compound
NH_2	I	FIAC
OH	I	FIAU
OH	CH_3	FMAU

Fig. 2 Some Second Generation Nucleoside Analogs with Antiherpes Activity.

Table 4. *In Vitro* Anti-HSV Activities of Some Second Generation Nucleoside Analogs

Compound	ID_{50} [1] (μM) HSV-1	HSV-2	TD_{50} [2] (μM)	References
ACV	0.1	0.1	15-300	123-129,129,133
DHPG	0.2	0.3	150	125-129
BVdU	0.003	1	200	128, 130-133
IVdU	0.012	2	200	128,130
BVdC	0.2	30	200	134
FIAC	0.01	0.01	10	128,131,135
FIAU	0.03	0.06	3	136
FMAU	0.01	0.01	1	136

[1] Concentration required to inhibit virus replication by 50%

[2] Concentration required to inhibit host cell growth or metabolism by 50%

was noted for (*E*)-5-(2-bromovinyl)-2'-deoxyuridine (BVdU) in its inhibitory effects against HSV-1. 9-(2-Hydroxyethoxymethyl)guanine (acycloguanosine, ACG, acyclovir) has been evaluated extensively in the clinic. BVdU and 1-(2-fluoro-2-deoxy-β-D-arabinofuranosyl)-5-iodocytosine (fluoroiodoarabinosylcytosine, FIAC) have been subjected to phase I clinical trials. A large number of placebo-controlled double-blind clinical studies have demonstrated the clinical efficacy of ACG for the treatment of a variety of HSV-1 and HSV-2 infections (137). ACG is effective for the topical treatment of herpes keratitis, and primary genital herpes (138, 139). ACG has been used successfully by the oral route for the treatment of primary and recurrent genital herpes (140), and intravenously for the treatment of mucocutaneous HSV infections in imunocompromised patients (141-144) and herpes simplex encephalitis (120). BVdU has been shown to be effective clinically for the topical treatment of HSV-1 herpes keratitis (145) and for the oral treatment of HSV-1 mucocutaneous infections (146). Clinical trials involving FIAC have been directed mainly at the systemic treatment of VZV infections in immunocompromised patients (147). The toxic effects (nausea and myelosupression) reported in this study suggest a narrow safety margin for FIAC.

Nucleosides are subject to a number of metabolic alterations in biological systems. Their preferential transformation by HSV-encoded enzymes provides the basis for their selective antiviral activity. They are also subject to several degradative enzymatic changes *in vivo*. Such biotransformations may limit their antiviral activity *in vivo*. An understanding of the different viral and host enzymes interacting with antiviral drugs would be of great value in the design of nucleoside analogs for use as therapeutic or diagnostic agents for HSV infections.

Some unique features of deoxythymidine kinase (TK) enzymes encoded by HSV-1 and HSV-2 have already been discussed in section B. These enzymes have a much broader substrate specificity than the human cytosolic TK. The inhibition constants (K*i*) for several nucleoside analogs for TKs of various origins are compared in Table 5. The nucleosides referred to all have greater affinity for HSV-1 and HSV-2 encoded TKs than host cytosolic enzymes. Therefore

Table 5. Inhibition Constants (K*i*) of Some Antiviral Nucleosides for Deoxythymidine Kinases of Various Origins

Compound	Mean K*i* (μM)			
	Human		HSV-1	HSV-2
	Cytosolic	Mitochondrial		
BVdU	>150	0.83	0.24	4.24
IVdU	>150	1.08	0.27	5.71
FIAC	>100	1.09	6.59	-
FIAU	26	100	0.68	1.54
FMAU	>100	>100	2.99	44.37

these compounds could serve as preferential substrates for the viral TKs and are selectively phosphorylated to their 5'-monophosphates in HSV-infected cells (127, 148-152). Table 5 suggests that mitochondrial TK have a high affinity for these nucleosides and therefore may phosphorylate them. However, such phosphorylation mediated by mitochondrial TK would be minimal, as this enzyme does not play an important role in generating nucleotides for nuclear DNA synthesis. Therefore, in the uninfected cells phosphorylation of the above nucleosides occurs only to a very limited level. The TK-mediated phosphorylation of nucleosides is very crucial to their selective inhibitory activity on HSV replication. Mutations of the viral genome within the TK locus often results in viral strains which are resistant to one or more nucleoside analogs (153-155). Such mutants may show a reduction or total loss in their ability to synthesise TK or express a TK with altered substrate specificity (156-160). HSV mutants which have completely lost their ability to synthesise TK (TK^- strains) are usually resistant to all nucleoside analogs shown in Fig. 2. The mutant strains with altered substrate specificity show resistance to some nucleosides while being sensitive to others (160).

It is the 5'-triphosphate derivative of the nucleosides that exerts the antiviral action. Therefore the nucleoside-5'-monophosphates formed in HSV-infected cells must undergo further phosphorylation to the 5'-diphosphates and subsequently to the 5-'triphosphates before they inhibit HSV replication. The TK encoded by HSV-1 has deoxythymidylate kinase activity and therefore phosphorylates some but not all nucleoside-5'monophosphates to the 5'-diphosphates (161, 162). (*E*)-5-(2-Halovinyl)-2'-deoxyuridine-5'-monophosphates (BVdU-MP, IVdU-MP) have been shown to be converted to the corresponding 5'-diphosphates by HSV-1-encoded TK (151, 161, 163). HSV-2-encoded TK has little or no deoxythymidylate kinase activity and therefore cannot phosphorylate BVdU-MP and IVdU-MP. This may explain in part the 100-1000 fold lower activity of BVdU and IVdU against HSV-2 as compared to HSV-1. Mutations of the TK gene resulting in loss of deoxythymidylate kinase activity of this multifunctional enzyme gives HSV strains which are resistant to BVdU (164). ACG-5'-monophosphate (ACG-MP) does not serve as a substrate

for TK induced by HSV. Instead ACG-MP is phosphorylated by host cell-encoded guanosine monophosphate (GMP) kinase (165). Conversion of the nucleoside diphosphates to the corresponding triphosphates is effected by one or more of the nonspecific host cell kinase enzymes (166).

The most important target enzyme for the antiviral action of the nucleosides is the virus-encoded DNA polymerase. The 5'-triphosphates of the nucleosides may interact with DNA polymerases at two levels. First, they act as inhibitors of viral DNA polymerase enzymes. For example, the triphosphates of ACG, BVdU, FIAC (ACG-TP, BVdU-TP, FIAC-TP) compete with the structurally similar natural substrates dGTP, dTTP and dCTP respectively, for the corresponding sites of DNA polymerse enzymes (167-170). Table 6 compares the K*i* values for ACG-TP, BVdU-TP and FIAC-TP for HSV-1 and cellular DNA polymerases. These triphosphate analogs have a greater affinity for the HSV-1-encoded DNA polymerases relative to human DNA polymerases and therefore can act as selective competitive inhibitors of the former. ACG-TP has been recently reported to be a suicide inhibitor of herpes simplex virus DNA polymerase (171). In general the inhibitory effects of these compounds on HSV-1 and HSV-2 DNA polymerases are nearly equal (172). The selective inhibitory effects of the nucleoside-5'-triphosphates on HSV-encoded DNA polymerases would partly explain their selective antiviral activity. In addition, the nucleoside triphosphates can also serve as substrates for DNA polymerases and thus be incorporated into DNA. ACG-TP, BVdU-TP, IVdU-TP and FIAC-TP all have been reported to be substrates for DNA polymerases and incorporated into DNA (167, 170-174). ACG-TP and FIAC-TP are better substrates for viral than cellular DNA polymerases (167, 170). BVdU-TP and IVdU-TP are very good substrates for both viral and cellular DNA polymerases (172-174). Since initial phosphorylation of the above nucleosides is limited to HSV-infected cells, the eventual incorporation into DNA will also be confined to DNA of such infected cells. BVdU, even in infected cells, when used in low concentraions is incorporated only into viral DNA (175). The incorporation of ACG into DNA causes chain termination, since ACG does not have a 3'-OH group for further chain elongation

Table 6. Inhibition Constants (K*i*) of Some Antiviral Nucleoside Triphosphates for DNA Polymerases of Various Origins

Nucleoside Triphosphate	Ki (μM) HSV-1	Human (α)	Human (β)
ACG-TP	0.03	0.15	11.9
BVdU-TP	0.25	3.6	16.4
FIAC-TP	0.26	2.7	7.9

(176). This results in accumulation of short DNA fragments in the infected cells. ACG-MP incorporated into DNA is not excised by the 3',5' exonuclease activity associated with HSV-encoded DNA polymerases (169). The incorporation of BVdU into viral DNA proceeds via an internucleotide linkage. The DNA thus formed has been shown to be more labile, which is evident from the dose-dependent increase in single strand breaks (175). Besides, the substitution of dT in DNA by BVdU impairs the template activity of DNA for transcription (177). FIAC and FMAU may be incorporated by the internucleotide linkage or at the 3' terminals of the DNA (61). Thus, the abnormal DNA formed by incorporation of the antiviral nucleoside is one important factor contributing to the inhibitory effect of these drugs on HSV replication.

The incorporation of any of the above nucleoside analogs into the host cell DNA would result in toxic side effects such as teratogenesis, carcinogenesis , induction of oncogenic viruses, and chromosomal damage. Such toxic effects have been reported for the first generation antiviral drug IdU (178). Since selective antiherpes drugs such as ACG and BVdU are not incorporated into host DNA to any significant degree, these drugs would be expected to be free from such toxic effects. Toxicity studies for ACG and BVdU indicates they are free from carcinogenic and teratogenic effects (61, 137). In contrast to IdU, ACG and BVdU do not induce the release of oncorna particles (179). They do not cause chromosomal damage except at very high concentrations (137, 180). In view of the higher safety margin observed for the second generation nucleoside analogs it is not surprising that new compounds such as ACG are replacing the more toxic first generation drugs in clinical use.

Mutations of the DNA polymerase gene of HSV would result in strains expressing altered DNA polymerase enzymes (153-155, 181). Such HSV mutants may be resistant to one or more antiviral nucleosides. Mutations in different regions of the DNA polymerase locus would result in induction of resistance to different nucleosides. ACG resistance is located within map units 40.2 - 41.8, whereas BVdU resistance is located within map units 41.0 - 42.8 (153, 181). Since the regions of the enzyme conferring resistance to different compounds vary,

resistance to one of them need not necessarily mean cross-resistance to other analogs (155).

The nucleoside analogs discussed are also subject to degradative changes *in vivo*. A major catabolic pathway for the 5-substituted analogs of deoxythymidine involves phosphorolytic cleavage of the N-glycosidic bond (182). In mammals two enzymes are known to catalyze this cleavage, namely deoxythymidine phosphorylase and uridine phosphorylase (182, 183). Thymidine phosphorylase is specific for 2'-deoxypyrimidines and is the main enzyme responsible for degradation of deoxythymidine in man (182). Blood platelets, liver and spleen are very rich sources of this enzyme (184,185). The 5-substituted deoxythymidine analogs are very good substrates for this enzyme (186). Thus, BVdU is rapidly metabolised *in vivo* to the corresponding base (*E*)-5-(2-bromovinyl)uracil (BVU) and 2-deoxyribose-1-phosphate (187). Unlike BVdU, BVU possesses very slow elimination characteristics and could be detected in blood over a period of 24 hours after the administration of BVdU. This rapid *in vivo* metabolism of BVdU limits its bioavailability and therefore the therapeutic efficacy. Two approaches to counteract the phosphorolysis of BVdU have been investigated in animal models. 6-Aminothymine, an inhibitor of deoxythymidine phosphorylase, has been shown to increase the biological half-life of BVdU significantly (188). However, this requires the use of large amounts of inhibitor and is unlikely to gain clinical acceptance. An alternate approach involves the regeneration of BVdU by reversal of phosphorolysis (187, 188). This may be achieved by the administration of a deoxyribosyl donor such as deoxythymidine or 5-substituted deoxythymidine analogs (5-XdU, X=CH_3, F, Cl, I). The general reaction is as follows:

$$\text{BVU} + \text{5-XdU} \rightleftharpoons \text{BVdU} + \text{5-XU},$$

where 5-XU is the 5-subtituted uracil. This suggests that other 2'-deoxyuridine analogs may be used *in vivo* to potentiate the therapeutic activity of BVdU.

The 5'-monophosphates of pyrimidine nucleosides may interact with deoxythymidylate synthetase (TS). This enzyme is responsible for the conversion of deoxyuridine-5'-monophosphate to deoxythymidine-5'-monophosphate (189). BVdU-MP is a

good substrate for TS (190). The *in vitro* studies on BVdU-MP have suggested TS-mediated conversion of the inert 5-bromovinyl group to a reactive allylic bromide group. If such a chemically reactive form of BVdU-MP is formed *in vivo*, it may interact with a number of nucleophiles present in the cells. Thus, the possibility of generating an alkylating agent derived from BVdU-MP cannot be excluded. The nature of intracellular metabolites produced by the action of TS on BVdU-MP and its implication to antiviral action is not yet clearly understood. The 5'-monophosphates of 5-iodo- and 5-bromopyrimidine nucleosides are known to undergo TS-mediated dehalogenations (191). Such a deiodination has been reported for FIAU-MP (192). However, TS does not deiodinate FIAC-MP (192).

Deoxycytidine analogs such as BVdC and FIAC and their 5'-monophosphates are subject to deamination by deoxycytidne deaminase and deoxycytidine monophosphate deaminase (193, 194). This results in formation of the corresponding deoxyuridine derivatives. Although the metabolic products arising from deamination of the above nucleosides are still active as antiviral agents, this transformation is considered to be undesirable. Deoxycytidine analogs offer certain advantages over the deoxyuridine compounds since they are not susceptible to phosphorolytic cleavage and their 5'-monophosphates are not substrates or inhibitors of TS. Deamination may be blocked by the administration of tetrahydrouridine or 2'-deoxytetrahydrouridine, which are potent inhibitors of the deaminase enzymes (193, 194). The use of these deaminase inhibitors in conjunction with antiviral drugs such as BVdC and FIAC is yet to be investigated.

Unlike the pyrimidine nucleosides discussed above ACG does not undergo extensive metabolic degradations *in vivo* (195). The only major metabolite is 9-carboxymethoxymethyl guanine, which accounts for up to 14% of the administered dose in humans. This biotransformation is mediated by alcohol dehydrogenase (195).

The previous discussion describing the biochemical aspects of nucleosides suggest certain general requirements for their selective antiviral activity. To exert a selective and potent inhibitory effect on HSV, the nucleoside analog should be able to selectively interact with viral

TK, viral and/or cellular deoxythymidylate kinase, and viral DNA polymerases, while avoiding enzymes such as cellular TKs, cellular DNA polymerases, nucleoside phosphorylases, dC(dCMP) deaminases and TS.

II. MATERIALS AND METHODS

A. General

Chemicals and solvents

All chemicals were of reagent grade quality. 2'-Deoxyuridine (dU), N-iodosuccinimide (NIS), and chloramine-T were purchased from Sigma Chemical Company, St. Louis, Missouri, USA. 5-(Hydroxymethyl)uracil was obtained from Aldrich Chemical Company, Inc., Milwaukee, Wisconsin, USA. N-Bromosuccinimide (NBS) was purchased from Fisher Scientific Company, Fair Lawn, New Jersey, USA. [^{81}Br]-Sodium bromide (97.8% enriched ^{81}Br) was obtained from Oakridge National Laboratories, Oakridge, USA. All solvents used for high-pressure liquid chromatography (HPLC) were of HPLC grade and were purchased from Fisher Scientific Company. Solvents used for chemical and radiochemical syntheses were dried by routine methods, fractionally distilled and stored over molecular sieves.

Basal Medium Eagle's (BME), Minimum Essential Medium (MEM) and foetal calf serum were purchased from Flow Laboratories, Virginia, USA. All bottles of serum were heat inactivated at 56° C for 30 min and maintained at 4° C until use. Trypsin (1:250) was purchased from Difco Laboratories, Detroit, Michigan, USA. Penicillin was obtained from Ayerst Laboratories, Montreal, Canada. Streptomycin was obtained from Glaxo Laboratories, Toronto, Canada. Modified radioimmune precipitation assay (RIPA) buffer was prepared by making an aqueous solution of 0.15 M sodium chloride, 1% sodium deoxycholate, 1% Triton X-100, 1% sodium dodecyl sulphate and 0.01 M Tris HCl buffer. All tissue culture flasks and plates were purchased from Beckton-Dickson, Oxnard, California, USA.

Radioisotopes

All radioactive iodide samples (^{131}I, ^{125}I and ^{123}I) were of radioiodination grade. ^{131}I and ^{125}I samples were supplied as a 'no-carrier-added' (NCA) solution of sodium iodide by

Edmonton Radiopharmacy Centre, Edmonton, Canada. ^{123}I samples obtained from Edmonton Radiopharmacy Centre were supplied as an NCA solution of sodium iodide containing ammonium hydroxide by Atomic Energy Commission Ltd., Vancouver, Canada. [^{82}Br]-Bromide samples required for radiobrominations were prepared from [^{81}Br]-NaBr by the following method. Amberlite CG-120 (Na^+) was converted to Amberlite CG-120 (NH_4^+) by treating with excess NH_4Cl aqueous solution and washing with deionised water several times. [^{81}Br]-NaBr (10 mg) in deionised water (0.5 mL) was added to a column (1 cm id X 50 cm length) containing Amberlite CG-120 (NH_4^+) and eluted with deionised water. The eluant was evaporated *in vacuo* and the residue [^{81}Br]-NH_4Br was collected (5 mg, 52.5% yield). [^{82}Br]-NH_4Br was prepared from the above sample of [^{81}Br]-NH_4Br by the $^{81}Br(n,\gamma)^{82}Br$ nuclear reaction at the University of Alberta SLOWPOKE Reactor Facility at a neutron flux of 1×10^{12} n cm^{-2} s^{-1}. A typical yield was 2.3 MBq mg^{-1} of [^{82}Br]-NH_4Br for a 4 h irradiation. The theoretical yield calculated was 2.6 MBq mg^{-1} (Appendix).

Instrumental analysis

Melting points (mp) were determined on a Buchi capillary apparatus and are uncorrected. Proton magnetic resonance spectra (^1H NMR) were recorded on a Bruker WH-200 (200 MHz) or a Bruker AM-300 (300 MHz) NMR spectrometer using deuterated dimethyl sulfoxide (DMSO-d_6) or deuterated methanol (CH_3OH-d_4) as solvent and tetramethylsilane as an internal standard. Ultravoilet spectra (UV) were recorded on a Unicam SP 800 spectrometer using methanol as the solvent. High resolution mass spectra (hrms) for exact mass measurement were obtained on an AEI MS-50 mass spectrometer. HPLC purifications and analysis were performed on a Tracor system (Tracor 950 Chromtographic Pump, Tracor 970 A Variable Wavelengh Detector) or Waters system (Model 860 Automated Gradient Controller, Model 510 and M-45 Solvent Pumps, Model U6K Injector and Model 480 LC Ultraviolet Detector).

Chromatography

Thin layer chromatography (TLC) separations were carried out on Whatman MK 6F microslides (Whatman Inc., New Jersey, USA) using one of the following solvents:

1. chloroform : methanol (85:15 by volume)
2. chloroform : methanol (95:5 by volume)
3. ethyl acetate : acetic acid : methanol (7:1:1 by volume)
4. n-propanol : water : ethyl acetate (1:2:4 by volume)

Thin layer radiochromatography (TLRC) was performed on a Berthold LB 2832 Automatic TLC Linear Analyzer equipped with a Berthold LB 281 Proportional Counter and a Canberra Series 40 Multichannel Analyzer. Column chromatographic separations, unless otherwise specified, were performed using silica gel 60 (70-230 mesh) using a glass column (2 cm id X 40 cm length). Preparative HPLC separations were carried out using a Whatman Partisil-10 CCS/C_1 reverse phase M-9 preparative column (9.4 mm id X 25 cm length) using methanol : water (40 : 60 by volume) as eluant at a flow rate of 2 mL min^{-1}. Analytical HPLC were done using reverse phase C_{18} radial pak cartridge (8 mm id X 12 cm length, 10 μ particle size), which were obtained from Waters Associates, Mississagua, Ontario, Canada. Unless otherwise stated the mobile phase and flow rates were the same as those used for preparative HPLC. An ultraviolet absorption (at 298 nm or 296 nm) detection system was used for detection of non-radioactive eluants. An ultraviolet absorption (at 298 nm or 296 nm) detection system and a γ-ray detection system were used in conjunction for the detection of radioactive eluants.

Radioactivity measurements

Radioactivities for γ-emitting radionuclide samples with high total activity (37 KBq or more) were estimated using a Picker Dose Calibrator. Samples with low total activity ^{125}I were counted on a Beckman 8000 gamma counter by the double photopeak method (program # 9). Samples with low total activity of ^{131}I were counted on a Beckman 8000 (program # 6) or a Tracor 2200 (window : 300 to 420 Kev), or a Tracor 2200 gamma counter. Low activity ^{82}Br

samples and all ^{14}C-labeled samples were counted on a Beckman LS 9000 liquid scintillation counter (program # 10 and 3 respectively) using Aquasol II (New England Nuclear) as the fluor.

B. Chemical Synthesis

5-Chloromercuri-2'-deoxyuridine

Mercuric acetate (4.18 g, 1.31 mmol) in water (12 mL) was added to a solution of 2'-deoxyuridine (2.84 g, 1.24 mmol) in water (18 mL). To this an additional quantity of water (10 mL) was added and the mixture was stirred for 2.5 h at 50° C. This resulted in formation of a thick white suspension. The reaction mixture was cooled to 40° C and to this, a solution of sodium chloride (1.8 g, 3 mmol) in water (6 mL) was added. The reaction mixture was cooled to room temperature and stirred for another 2 h. The fine white precipitate was filtered, washed in succession with 0.1 N aqueous sodium chloride solution (24 mL), water (16 mL), ethanol (8 mL) and diethyl ether (12 mL). The air dried precipitate was stored in a vacuum dessicator over phosphorous pentoxide overnight. The dried product (4.85 g, 84.2% yield) was used for subsequent reactions without further purification; mp 210-212° C (dec) [Lit (196) 210.5-211° C (dec)].

(E)-5-(2-Carbethoxyvinyl)-2'-deoxyuridine

5-Chloromercuri-2'-deoxyuridine (3.47 g, 7.5 mmol), ethyl acrylate (8.9 mL, 82 mmol) and a 0.1 M methanolic solution of Li_2PdCl_4 (79 mL, 7.9 mmol) were stirred under nitrogen for 10 h. The mixture was filtered, the precipitate collected, warmed in methanol (120 mL), and refiltered. The combined filtrate was treated with hydrogen sulfide gas until precipitation was complete. The solution was filtered and the solvent was removed *in vacuo*. The residue was dissolved in water (10 mL) and left overnight at 0-4° C for crystallization. The product was collected and dried *in vacuo* to give the title product (1.25 g, 46% yield); R*f* 0.5

(solvent 1), mp 186-188° C.

^{1}H NMR (DMSO-d_6) δ : 1.23 (3H, t, J=6 Hz, CH_2 $C\underline{H}_3$), 2.17 (2H, m, C_2'-H_2), 3.62 (2H, m, C_3'-H_2), 4.15 (2H, q, J=6 Hz, $C\underline{H}_2$ CH_3), 3.80 (1H, m, C_3'-H), 4.26 (1H, m, C_4'-H), 6.14 ((1H, dd, J=6 Hz, C_1'-H), 6.85 (1H, d, J=15 Hz, vinylic $C_{(1)}$-H), 7.37 ((1H, d, J=15 Hz, vinylic $C_{(2)}$-H), 8.43 (1H, s, C_6-H), 11.6 (1H, s, N_3-H).

(E)-5-(2-Carboxyvinyl)-2'-deoxyuridine

A mixture of (*E*)-5-(2-carbethoxyvinyl)-2'-deoxyuridine (1.5 g, 4.6 mmol) and 0.5 N aqueous potassium hydroxide (4 mL) were stirred at room temperature for 1 h. The reaction mixture was neutralized with Dowex 50X 8-200-[H^+] ion exchange resin and then the ion exchange resin was removed by filtration. The filtrate was evaporated to dryness *in vacuo*. The residue was crystallized from aqueous ethanol to yield the title compound (1.01 g, 73.7% yield); R*f* 0.47 (solvent 3), mp 220-230° C.

^{1}H NMR (CH_3OH-d_4) δ : 2.15 (2H, m, C_2'-H_2), 3.68 (2H, m, C_3'-H_2), 3.75 (1H, m, C_4'-H), 4.40 (1H, m, C_3'-H), 6.18 (1H, dd, J=6 Hz, C_1'-H), 6.7 (1H, d, J=15 Hz, vinylic $C_{(1)}$-H), 6.95 (1H, d, J=15 Hz, vinylic $C_{(2)}$-H), 8.25 (1H, s, C_6-H).

(E)-5-(2-Iodovinyl)-2'-deoxyuridine

(a) N-Iodosuccinimide (NIS) method

(*E*)-5-(2-Carboxyvinyl)-2'-deoxyuridine (40 mg, 13 μmol) was dissolved in dry dimethyl formamide (DMF) (2.5 mL). To this, potassium acetate (30 mg, 34 μmol) and N-iodosuccinimide (34 mg, 15 μmol) were added and the mixture was stirred at room temperature for 24 h. The solvent was evaporated *in vacuo* and the residue was purified by column chromatography [solvent ; chloroform : methanol (85:15 by volume)] to give the title compound which failed to crystallize (15 mg, 30.4% yield); R*f* 0.42 (solvent 1).

^{1}H NMR (CH_3OH-d_4) δ : 2.15 (2H, m, C_2'-H_2), 3.62 (2H, m, C_3'-H_2), 3.81 (1H, m, C_4'-H), 4.28 (1H, m, C_3'-H), 6.16 (1H, dd, J=6 Hz, C_1'-H), 7.15 (1H, d, J=15 Hz,

vinylic $C_{(1')}$-H), 7.25 (1H, d, J = 15 Hz, vinylic $C_{(2')}$-H), 8.10 (1H, s, C_6-H)
UV (CH_3OH) : λ_{max} 252 nm and 298 nm, λ_{min} 275 nm. The ^1H NMR and UV data were in agreement to those reported in the literature (197).

(b) Chloramine-T method

(*E*)-5-(2-Carboxyvinyl)-2'-deoxyuridine (10 mg, 30 μmol) was dissolved in dry dimethyl formamide (DMF) (1 mL). To this, solutions of potassium acetate (5 mg, 60 μmol) in ethanol (100 μL), sodium iodide (5 mg, 30 μmol) in ethanol (100 μL) and chloramine-T (10 mg, 44 μmol) were added and the mixture was stirred at room temperature for 1 h. The reaction product was purified as described under method (a) to give the title compound (3 mg, 26.3% yield). The product was shown to be identical to the product obtained by the NIS method with respect to R*f* value, UV and ^1H NMR characterisitcs. It also co-chromatographed (analytical HPLC : UV detection at 298 nm, retention time 12.8 min ; preparative HPLC : retention time 21.3 min) with the above product obtained using method (a).

(E)-5-(2-Bromovinyl)-2'-deoxyuridine

(a) N-Bromosuccinimide (NBS) method

(*E*)-5-(2-Carboxyvinyl)-2'-deoxyuridine (75 mg, 25 μmol) was dissolved in water (4 mL) by heating with potassium acetate (50 mg, 5 μmol). While still hot, N-bromosuccinimide (45 mg, 25 μmol) was added in small portions to the clear mixture. The mixture was stirred at room temperature for 2 h at which time the reaction was complete as indicated by TLC. The solution was then left overnight at 0-4° C for crystallization of the product. The crystals were collected (25 mg) and the mother liquor was evaporated to dryness *in vacuo*. The residue was fractionated by column chromatography [solvent ; chloroform : methanol (90:10 by volume)] to give an additional quantity of the title product (10 mg, 42% total yield); R*f* 0.45 (solvent 1), mp 164-165° C.

^{1}H NMR (CH_3OH-d_4) : 2.28 (2H, m, C_2'-H_2), 3.78 (2H, m, C_5'-H_2), 3.93 (1H, m, C_4'-H), 4.40 (1H, m, C_3'-H), 6.25 (1H, dd, J=6 Hz, C_1'-H), 6.80 (1H, d, J=15 Hz, vinylic $C_{(1)}$-H), 7.38 (1H, d, J=15 Hz, vinylic $C_{(2)}$-H), 8.14 (1H, s, C_6-H).

UV (CH_3OH) : λ_{max} 252 nm and 296 nm, λ_{min} 271 nm. The UV and ^{1}H NMR data were in agreement with those reported in the literature (197).

(b) Chloramine-T method

(*E*)-5-(2-Carboxyvinyl)-2'-deoxyuridine (10 mg, 34 μmol) was dissolved in dry dimethyl formamide (DMF) (1 mL). To this a solution of potassium acetate (5 mg, 60 μmol) in ethanol (100 μL), sodium bromide (3.5 mg, 34 μmol) in ethanol (100 μL) and chloramine-T (10 mg, 44 μmol) were added and the mixture stirred at room temperature for 15 min. The reaction product was purified by preparative HPLC (uv detection at 296 nm, retention time : 18.6 min) to give the title compound (2 mg, 18% yield). This product was identical to the product obtained by NBS method with respect to R*f* value, UV and ^{1}H NMR characteristics and co-chromatography (preparative HPLC).

(E)-5-(2-Carboxyvinyl)-2'-deoxyuridine-3',5'-diacetate

(*E*)-5-(2-Carboxyvinyl)-2'-deoxyuridine (100 mg, 336 μmol) in pyridine (1 mL) was stirred with acetic anhydride (1 mL) at room temperature overnight. The solvent was evaporated *in vacuo*. The residue was crystallized from ethanol (95%) to give the title product (71 mg, 55.4% yield); R*f* 0.72 (solvent 3), mp 190-195° C (dec).

^{1}H NMR (CH_3OH-d_4) δ : 2.15 (6H, s, C_3'- and C_5'-O-CO-CH_3, 2.45 (2H, m, C_2'-H_2), 4.35 (2H, m, C_5'-H_2), 4.45 (1H, m, C_4'-H), 5.30 (1H, m, C_3'-H), 6.25 (1H, dd, J=6 Hz, C_1'-H), 7.20 (1H, d, J=15 Hz, vinylic $C_{(1)}$-H), 7.40 (1H, d, J=15 Hz, vinylic $C_{(2)}$-H), 7.80 (1H, s, C_6-H).

Exact mass calculated for $C_{15}H_{11}N_2O_7$ ($[M - CO_2]^+$) : 338.11258 ; measured (hrms) : 338.1121 (intensity=0.41%).

(E)-5-(2-Iodovinyl)-2'-deoxyuridine-3',5'-diacetate

Potassium acetate (5 mg, 60 μmol) and N-iodosuccinimide (6 mg, 27 μmol) were added to a solution of (*E*)-5-(2-carboxyvinyl)-2'-deoxyuridine-3',5'-diacetate (10 mg, 28 μmol) in DMF (7 mL). The reaction was allowed to proceed at 25° C with stirring for 20 h at which time TLC indicated the reaction was complete. The solvent was removed *in vacuo* and the residue was purified by column chromtography [solvent ; chloroform : acetone (90:10 by volume)] to give the title product as a syrup (5 mg, 41% yield); R*f* 0.79 (solvent 2).

^{1}H NMR (CH_3OH-d_4) δ : 2.15 (6H, s, C_3'- and C_5'-O-CO-CH_3, 2.45 (2H, m, C_2'-H_2), 4.35 (2H, m, C_5'-H_2), 4.45 (1H, m, C_4'-H) 5.30 (1H, m, C_3'-H), 6.25 (1H, dd, J = 6 Hz, C_1'-H), 7.20 (1H, d, J = 15 Hz, vinylic $C_{(1)}$-H), 7.40 (1H, d, J = 15 Hz, vinylic $C_{(2)}$-H), 7.80 (1H, s, C_6-H).

Exact mass calculated for $C_{15}H_{17}N_2O_7I$ (M^+) : 464.00394 ; measured (hrms) : 464.0081 (intensity = 2.27%).

5-Formyl uracil

Silver nitrate (15 mg) and potassium persulfate (2.0 g) were added to a suspension of 5-(hydroxymethyl)uracil (500 mg, 3.5 mmol) in water (30 mL). The reaction mixture was stirred at 30° C for 10 min. Upon cooling the title product crystallized (400 mg, 80% yield); R*f* 0.67 (solvent 4), mp 295-300° C [Lit (198) 300-303° C].

(E)-5-(2-Carboxyvinyl)uracil

Malonic acid (15 mg, 144 μmol) and piperidine (1 drop) were added to a suspension of 5-formyl uracil (20 mg, 143 μmol) in dry pyridine (1 mL). The mixture was heated in an oil bath at 65° C for 4 h. The solvent was removed and the residue was crystallized from aqueous ethanol (50%) to give the title product (6 mg, 23% yield); R*f* 0.46 (solvent 4), mp 281-283 ° C (dec).

(E)-5-(2-Iodovinyl)uracil

Potassium acetate (20 mg, 232 μmol) in ethanol (100 μL), sodium iodide (22 mg, 147 μmol) in ethanol (100 μL) and chloramine-T (33 mg, 147 μmol) were added to a solution of (*E*)-5-(2-carboxyvinyl)uracil (20 mg, 110 μmol) in dry DMF (2 mL). The reaction mixture was stirred at room temperature for 40 min. The solvent was evaporated *in vacuo*. The residue was purified by preparative HPLC to give chromatographically pure title product which did not crystallize (3 mg, 10% yield). R*f* 0.34 (solvent 4).

^{1}H NMR (CH_3OH-d_4) : 7.12 (1H, d, J = 15 Hz, vinylic $C_{(1)}$-H), 7.22 (1H, d, J = 15 Hz, vinylic $C_{(2)}$-H), 7.56 (1H, s, C_6-H). The ^{1}H NMR data were in agreement with those previously reported (197).

C. Radiochemical Synthesis

[^{131}I, ^{125}I, ^{123}I]-(E)-5-(2-Iodovinyl)-2'-deoxyuridine

(a) Chloramine-T method

(i) High specific activity synthesis : A solution of sodium iodide (50 μg, 0.33 μmol) in ethanol (100 μL) and potassium acetate (500 μg) in ethanol (50 μL) were added to a 1 mL reaction vial and the solvent was removed under a stream of nitrogen. [^{131}I, ^{125}I]-Iodide (118.4 MBq) in ethanol (500 μL) was then added and the volume was then reduced to about 20 μL. (*E*)-5-(2-Carboxyvinyl)-2'-deoxyuridine (1 mg, 3.3 μmol) in dry DMF (100 μL) was added to the reaction vial and the reaction mixture was then stirred for 5 min using a magnetic stirrer. The reaction was initiated by addition of chloramine-T (200 μg) in dry DMF (20 μL) and stirring was continued at room temperature for 1 h. The solvent was removed under a stream of nitrogen and the residue purified by preparative HPLC. The radioactive fraction that corresponded to an authentic sample with a retention time of 20 minutes afforded IVdU (88 μg, 69% chemical yield, 80 MBq, 67.2% radiochemical yield, specific activity 344 GBq mmol^{-1}).

^{123}I-IVdU was synthesised by the procedure described above except that the reaction time was reduced to 30 min. The chemical yield was 57.0% and the radiochemical yield after purification was 40.7%.

(ii) "No-carrier added" synthesis : [^{131}I]-IVdU was synthesised as described above in (i) without the addition of cold sodium iodide using Na^{131}I (37 MBq) which has not been isotopically diluted. The reaction was terminated after 30 min. The product was purified by HPLC to give [^{131}I]-IVdU (24 MBq, 65% yield).

(a) Halogen isotope exchange method

A solution of IVdU (70 μg, 0.18 μmol, ^{131}I-Iodide (3.7 MBq) and cuprous chloride (2 μg, 20 nmol) in dry DMF (20 μL) were heated at 70-80° C in a reaction vial. The incorporation of radioactivity into IVdU was monitored by TLRC. The maximum incorporation of radioactivity into IVdU was achieved after 20 h at which time the solvent was removed. The residue was purified by preparative HPLC to yield [^{131}I]-IVdU (38 μg, 54.3% chemical recovery; 1.67 MBq, 45.1% radiochemical yield; specific activity 16.7 GBq mmol^{-1}).

[^{131}I]-(E)-5-(2-Iodovinyl)-2'-deoxyuridine-3',5'-diacetate

[^{131}I]-IVdU-3',5'-diacetate was synthesized by the chloramine-T method as described for the high specific activity synthesis by reaction of (*E*)-5-(2-carboxyvinyl)-2'-deoxyuridine-3',5'-diacetate (500 μg, 1.4 μmol) with [^{131}I]-sodium iodide (5μg, 33 nmol, 14.8 MBq) and chloramine-T (100 μg) in the presence of potassium acetate (250 μg) in DMF (50 μL) for 1 h. The product obtained after purification by column chromatography using a small glass column (0.5 cm id X 10 cm length) [solvent ; chloroform : acetone (90:10 by volume)] co-chromatographed with an authentic sample of (*E*)-5-(2-iodovinyl)-2'-deoxyuridine-3',5'-diacetate on TLRC (7.4 MBq, 50% radiochemical yield, specific activity 54.5 GBq mmol^{-1}).

[^{82}Br]-(E)-5-(2-Bromovinyl)-2'-deoxyuridine (BVdU)

(a) Chloramine-T method

A solution of (*E*)-5-(2-carboxyvinyl)-2'-deoxyuridine (2 mg, 6.1 μmol), potassium acetate (1 mg), [^{82}Br]-ammonium bromide (300 μg, 3.1 μmol, 0.72 MBq) and chloramine-T (2 mg) in dry DMF (200 μL) and ethanol (20 μL) were stirred at room temperature using a magnetic stirrer. The reaction was complete within 10 min as indicated by TLRC. The solvent was evaporated under a slow stream of nitrogen. The residue was purified by preparative HPLC as described previously. The radioactive fraction corresponding to an authentic sample with a retention time of 18.6 min afforded BVdU (727 μg, 72% chemical yield, 0.5 MBq, 69.8% radiochemical yield; specific activity 227 MBq mmol^{-1}).

(b) Direct neutron activation

A sample of BVdU (1 mg) (containing natural abundance bromine) was irradiated in a double plastic vial at a neutron flux of 10^{12} n cm^{-2} s^{-1} for 4 h. The sample was allowed to stand for 24 h (to allow the decay of ^{80}Br, ^{80}Br^{m} and ^{82}Br^{m}) prior to purification by preparative HPLC as described previously. The radioactive fraction having a retention time of 18.6 min showed identical TLRC, HPLC and UV spectral characteristics to that of an authentic sample of BVdU. The specific activity of the product calculated to the end of irradiation was 32 MBq mmol^{-1}. Radiolytic decomposition was estimated to be less than 3%. The radioactivity associated with BVdU was 30% of the overall activity produced.

D. Quantitative Uptake Studies of Radiolabeled Nucleosides in HSV-1-Infected Cells *In Vitro*

Cells

Two 2-5 day old rabbits were sacrificed by cervical dislocation. The kidneys were removed, washed with phosphate buffered saline (PBS) and cut into small pieces. The pieces

were incubated at 37° C in PBS (20 mL) containing Trypsin 1:250 (0.25%). The supernatants were collected from three 20 min sequential incubations and added to Basal Medium Eagle's (BME) or Minimum Esential Medium (MEM) containing foetal calf serum. After a cell count the tissue culture flasks were seeded at a concentration of 5 X 10^4 cells per 25 cm^2 flask. Cells were maintained in 10 mL of BME or MEM supplemented with 10% foetal calf serum, penicillin-G (100 IU mL^{-1}), and streptomycin sulphate (100 μg mL^{-1}), 2 mM glutamine and sodium bicarbonate (2 g L^{-1}). When monolayers became confluent, cells were split twice at a ratio of 1:3.

Viruses

HSV-1 (strain JLJ) isolated from a patient with HSV encephalitis was used as the HSV-1 (TK^+) infecting agent. HSV-1 (strain 2006 which is TK deficient) was used as the HSV-1 (TK^-) infecting agent. All viral titrations were performed by Drs. D. R. Tovell or M. J. Gill (Faculty of Medicine, University of Alberta, Edmonton, Canada).

Radiolabeled nucleosides

[^{131}I]-IVdU samples (specific activity 43.3 GBq $mmol^{-1}$, 370 GBq $mmol^{-1}$ and 80 GBq $mmol^{-1}$) were prepared as described in section C.

[5-^{131}I]-1-(2-deoxy-2-fluoro-β-D-ribofuranosyl)-5-iodouracil (specific activity 20.4 GBq $mmol^{-1}$) and [2-^{14}C]-1-(2-deoxy-2-fluoro-β-D-ribofuranosyl)-5-fluorouracil (specific activity 1.86 GBq $mmol^{-1}$) were synthesised by Mr. T. Iwashina (Faculty of Pharmacy, University of Alberta, Edmonton, Canada).

[2-^{14}C]-1-(2-deoxy-2-fluoro-β-D-ribofuranosyl)-5-chlorouracil (specific activity 1.86 GBq $mmol^{-1}$) was synthesised by Dr. J. R. Mercer (Faculty of Pharmacy, University of Alberta, Edmonton, Canada). [5-^{131}I]-1-(2-deoxy-2-fluoro-β-D-arabinofuranosyl)-5-iodouracil (specific activity 111 GBq $mmol^{-1}$) was synthesised by Dr. H. K. Misra (Faculty of Pharmacy, University of Alberta, Edmonton, Canada).

Quantitation of cellular uptake of radiolabeled nucleosides by primary rabbit kidney (PRK) cells

The rabbit kidney cells were grown to confluency in Falcon 25 cm^2 flasks or 60 mm Petri dishes. The medium was removed and the cell monolayer was infected with a known infecting dose (plaque forming units per ml, PFU/mL) either HSV-1 (TK^+), HSV-1 (TK^-) or mock infection in 0.2 mL of medium. Unless otherwise stated, HSV-1 (TK^+) infections were performed in triplicate and HSV-1 (TK^-) and mock infections were performed in duplicate. After the infection, the flasks were incubated at 37° C for 1 h, at which time 2 mL of medium was added to each flask. After 7 h of post-infection incubation a known quantity of the radiolabeled nucleoside was added to each flask. Unless otherwise stated the flasks were incubated for a further 4 h. The early cytopathic effect was confirmed microscopically before determining the radioactivity in the cells. The supernatant was decanted, and the cells were washed twice with 1 mL PBS. The supernatant along with the washings were counted for radioactivity. Modified RIPA buffer (1 mL) was added to dissolve the cells (199). The flask was left for 5 min and the fluid was removed. The flask was further washed twice with 1 mL of modified RIPA buffer. The solubilized cells and the washings were counted for radioactivity in a gamma counter or a liquid scintillation counter.

E. Tissue Distribution of [^{131}I]-IVdU in a Herpes Simplex Encephalitis Animal Model

Animal model

The herpes encephalitis animal model was developed by Drs. M. J. Gill, D. R. Tovell and D. L. Tyrrell (Faculty of Medicine, University of Alberta, Edmonton, Canada). Rabbits (Dutch) were infected with intracerebral injection of 10^6 PFU of HSV-1 (JLJ). After 4 days the infected rabbits showing symptoms of HSE including convulsions were used for the tissue distribution studies or diagnostic imaging using [^{125}I or ^{123}I]-IVdU. Brain samples of HSV-1-infected rabbits were obtained and the radioactivity was compared with the virus titer.

Quantitative tissue distribution of [^{125}I]-IVdU

Rabbits (infected and uninfected controls) were given a bolus i.v injection of 0.74 MBq of [^{125}I]-IVdU. The animals were sacrificed at 1 or 6 h after the injection . Blood samples were collected by cardiac puncture just before sacrificing the animals. Organ samples (brain, liver, kidney, spleen, lung and muscle) were collected, weighed and the radioactivity quantitated by gamma counting.

F. Pharmacokinetics and Metabolism of [^{131}I]-IVdU in Dogs

Quantitative radio high-pressure liquid chromatography (r-HPLC)

The radioactive components of the plasma were separated, identified and quantitated by the following method. The plasma samples were mixed with an equivalent volume of methanol and chilled in ice (0-4° C) for 5 min. The supernatant was subsequently evaporated at room temperature under a stream of nitrogen and the residue dissolved in aqueous methanol (30% by volume). Two reference compounds [(*E*)-5-(2-iodovinyl)-2'-deoxyuridine and (*E*)-5-(2-iodovinyl)uracil] were added and the methanolic solution was filtered through a Millex®-HV$_4$ filter (Waters Scientific, LTD., 3688, Nashua Drive, Mississauaga, Ont. L4V 1M3, Canada) and injected onto the r-HPLC system (Waters Scientific, LTD., column: Waters radial pak C_{18}, 1.8 mm cartridge). The mobile phase was either A: a mixture of aqueous 0.01 M KH_2PO_4 (polar eluent) and methanol (non-polar eluent) B: a mixture of paired ion chromatography (PIC) solution [(aqueous 0.01 M KH_2PO_4 containing 1 vial of low UV PIC A reagent® (Waters Scientific, LTD.) in a 2L volume] and methanol (9:1 by volume). The plasma components were eluted by gradient elution with mobile phase A, increasing from 30% to 70% of the non-polar eluant over 15 min (Waters curve profile 7), followed by an additional elution for 5 min at 70% non-polar eluant. The identities of the radioactive components were confirmed by co-elution with authentic reference compounds, as evidenced by the simultaneous detection of radioactivity (by NaI-Tl γ-ray detector) and UV absorbance (at

298 nm). The fractions corresponding to the radioactive peaks were quantitated by gamma counting (Tracor Gamma 2200). A typical radiochromatogram (Fig.14) showed four radioactive peaks: A, B, C, and D. Peaks C and D were identified as [^{131}I]-(*E*)-5-(2-iodovinyl)uracil (IVU) and [^{131}I]-IVdU respectively. The identification of peak A was achieved by paired ion chromatography. The radioactive fraction A, on rechromatography with mobile phase B, co-eluted with the reference sample of inorganic iodide (UV absorption at 214 nm) with a retention time of 6.5 min.

Metabolism of [^{131}I]-IVdU in blood *in vitro*.

Heparinised blood (5 mL) obtained from a dog was incubated at 37° C with ^{131}I-IVdU (1.85 MBq in 100 μL of saline; specific activity: 2035 GBq mmol^{-1}). Blood samples (250 μL each) were periodically withdrawn into precooled Eppendorf® tubes, cooled for 30 sec and centrifuged at 20,000 rpm for 2 min. The supernatant was removed and analysed by quantitative r-HPLC as described above.

Metabolism of [^{131}I]-IVdU in blood *in vivo*.

The *in vivo* metabolism was studied using both low (1665 MBq mmol^{-1}) and high specific activity (37 TBq mmol^{-1}) samples of [^{131}I]-IVdU. Dogs were anaesthetised by i.v administration of sodium pentobarbital (25 mg/kg body wt) and the femoral vein was canulated for blood sampling. [^{131}I]-IVdU (2.5 MBq/kg body wt) in saline was injected via the radial vein and the blood samples were periodically (30 sec, 1, 2, 3, 5, 7, 9, 11, 15, 20, 30, 45 min, 1, 2, 3.5, 4, 6, 8, and 24 h) collected through the femoral canula into precooled tubes and the plasma was separated from cells by centrifugation as described previously. An aliquot of the plasma sample was counted to estimate total radioactivity. Another portion (1 mL) was processed immediately and analysed by r-HPLC as described above. Alternatively some samples (1 mL) at selected time points (3, 11, 30 min and 3.5 h) were dialysed in PBS and the radioactivity remaining in the dialysis bag was estimated by gamma counting.

Urine samples were collected at 2 , 4.5 and 8 h after the injection of [^{131}I]-IVdU, using a catheter. The urinary bladder was rinsed with saline to ensure efficient removal of urinary metabolites. Aliquots of each urine and wash samples were counted for radioactivity. Other aliquots of the urine sample were filtered through a Millex®-HV$_4$ filter and analysed by quantitative r-HPLC.

G. Diagnostic Imaging

Planar imaging

Rabbits (2 infected and 2 uninfected) were anaesthetised by i.v injection of sodium pentobarbital injection (25 mg/Kg body wt). [^{131}I]-IVdU (37 MBq) was administered as an intravenous bolus injection. Diagnostic imaging in the planar mode (static images) was performed at 30 min, 45min, 1 h, and 6 h after injection of [^{131}I]-IVdU using a Searle gamma camera (Pho/Gamma III) interfaced with an ADAC (CAM III) computer. For each static image 200,000 counts were collected.

SPECT

Rabbits (1 infected and 2 uninfected) were anaesthetised as described above. Right common carotid artery was exposed by dissection. [^{123}I]-IVdU (37 MBq) in saline (0.2 mL) was administered carefully as an intracarotid bolus injection. Intracarotid injection was carried out by Dr. D. L. Tyrrell (Faculty of Medicine, University of Alberta, Edmonton, Canada). Diagnostic brain imaging in the tomographic mode was started 20 minutes after the injection using a GE-400 AT gamma camera interfaced with a DEC-11/70 computer (Department of Nuclear Medicine, Cross Cancer Institute, University of Alberta, Edmonton, Canada). The radioactive counts were acquired at different angular orientations in 64 frames, with each frame collecting 50,000 counts. The time required for the aquisition of the data was about 30 min.

III. RESULTS AND DISCUSSION

A. The Problem and the Approach

The objective of this study was to develop a radionuclide brain imaging agent for the diagnosis of HSE. The metabolic transformations of the antiviral nucleosides in HSV-infected cells discussed in chapter I offer a new approach to the development of specific biochemical probes for the non-invasive diagnosis of HSE. The nucleoside phosphates selectively formed in the HSV-infected cells would be expected to have a very low permeability across the plasma membrane. Therefore, these nucleosides may be metabolically trapped in HSV-infected cells. Since such metabolic transformations are limited to the infected cells, the uninfected cells will be free of any selective accumulation of these nucleoside analogs (Fig. 3). Therefore an anti-HSV nucleoside analog labeled with a suitable gamma emitting isotope may be used as a specific probe to non-invasively differentiate a normal from HSV-infected brain with the aid of brain imaging techniques. While this study was in progress, Siato *et al* have reported the successful application of the selective metabolic trapping of radiolabeled nucleosides for quantitative autoradiographic mapping of HSE in a rat model (200-202), supporting the *in vivo* feasibility of such an approach.

Several antiviral nucleosides qualify as potential candidates for the development of radiopharmaceuticals for the diagnosis of HSE. We have chosen (*E*)-5-(2-iodovinyl)-2'-deoxyuridine (IVdU) and (*E*)-5-(2-bromovinyl)-2'-deoxyuridine (BVdU) in our investigations for the following reasons. IVdU and BVdU are among the most selective and potent compounds effective against HSV-1, which is the most common causative agent of adult HSE. Since IVdU and BVdU already contain halogens, labeling these molecules with radiohalogens does not alter their chemical or biological properties. IVdU labeled with ^{131}I may be used for two-dimensional (planar) conventional brain imaging using equipment currently available to many general hospitals. Alternatively, the incorporation of ^{123}I into IVdU would permit its use in tomographic brain imaging using a SPECT system. BVdU offers the

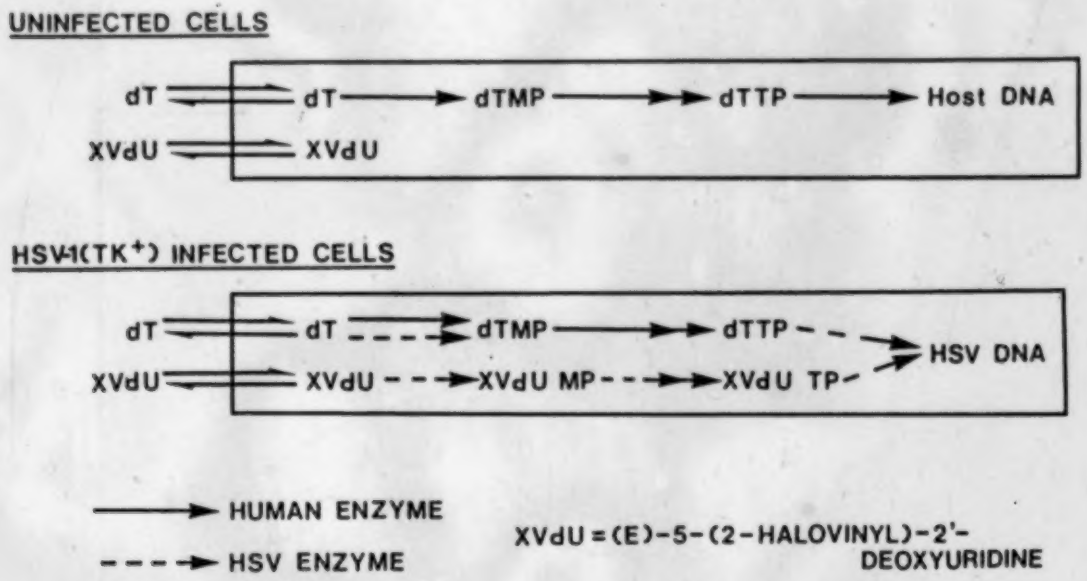

Fig. 3 Selective Metabolic Trapping of (*E*)-5-(2-Halovinyl)-2'-deoxyuridines in Herpes Simplex Virus-Infected Cells.

possibility of introduction of ^{77}Br, a positron emitting radionuclide, and therefore the development of a diagnostic test for HSE, using PET.

B. Chemical Synthesis

The major objectives of the non-radioactive syntheses were twofold :

1. To prepare authentic samples of nucleoside analogs as reference compounds for radiochemical syntheses and metabolic studies.
2. To explore alternate synthetic routes suitable for radiochemical syntheses and to show that the products thus formed are identical to those obtained from previously reported methods.

The syntheses of (*E*)-5-(2-halovinyl)-2'-deoxyuridines (Fig. 4) have been reported (197). The general synthetic route employed for the syntheses of iodo and bromo derivatives is shown in Fig. 5. 5-Chloromercuri-2'-deoxyuridine (**2**) was synthesised from commercially available 2'-deoxyuridine in 84.2% yield by the reaction of 2'-deoxyuridine with mercuric acetate followed by sodium chloride (196). Introduction of the 5-alkenyl group onto 2'-deoxyuridine was achieved by coupling ethyl acrylate with an organopalladium intermediate generated *in situ* from 5-chloromercuri-2'-deoxyuridine (**2**) (203). The use of organometallic intermediates for the syntheses of nucleoside analogs has been reviewed by Bergstrom (204). The reaction of ethyl acrylate with C_5-organopalladium derivatives of 2'-deoxyuridine is stereospecific. The reaction mechanism is likely to be similar to that proposed for the Heck reaction for the arylation of olefins (Fig. 6) (203-206). 5-Chloromercuri-2'-deoxyuridine reacted with dilithium pallladium tetrachloride to form a bond between C_5 of the pyrimidine ring and Pd (**2a**). This is followed by formation of a π complex between ethyl acrylate and Pd to afford an intermediate **2b**. The insertion of the π-bonded olefin into the C_5-Pd bond would then give **2c** which on *cis* elimination of Pd-H leads to the formation of a π complex **2d**. This π complex then undergoes dissociation to give Pd(0) and the nucleoside **3**. Compound **3** was readily hydrolysed to the corresponding carboxylic acid (**4**) by 0.5 N aqueous potassium

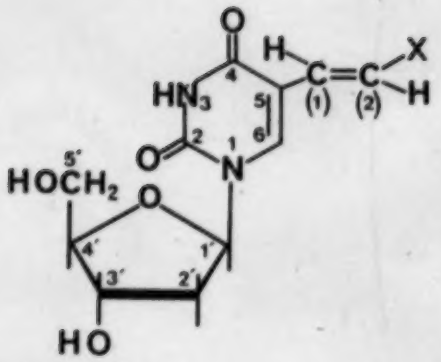

Fig. 4 Chemical Structure for (*E*)-5-(2-Halovinyl)-2'-deoxyuridines.

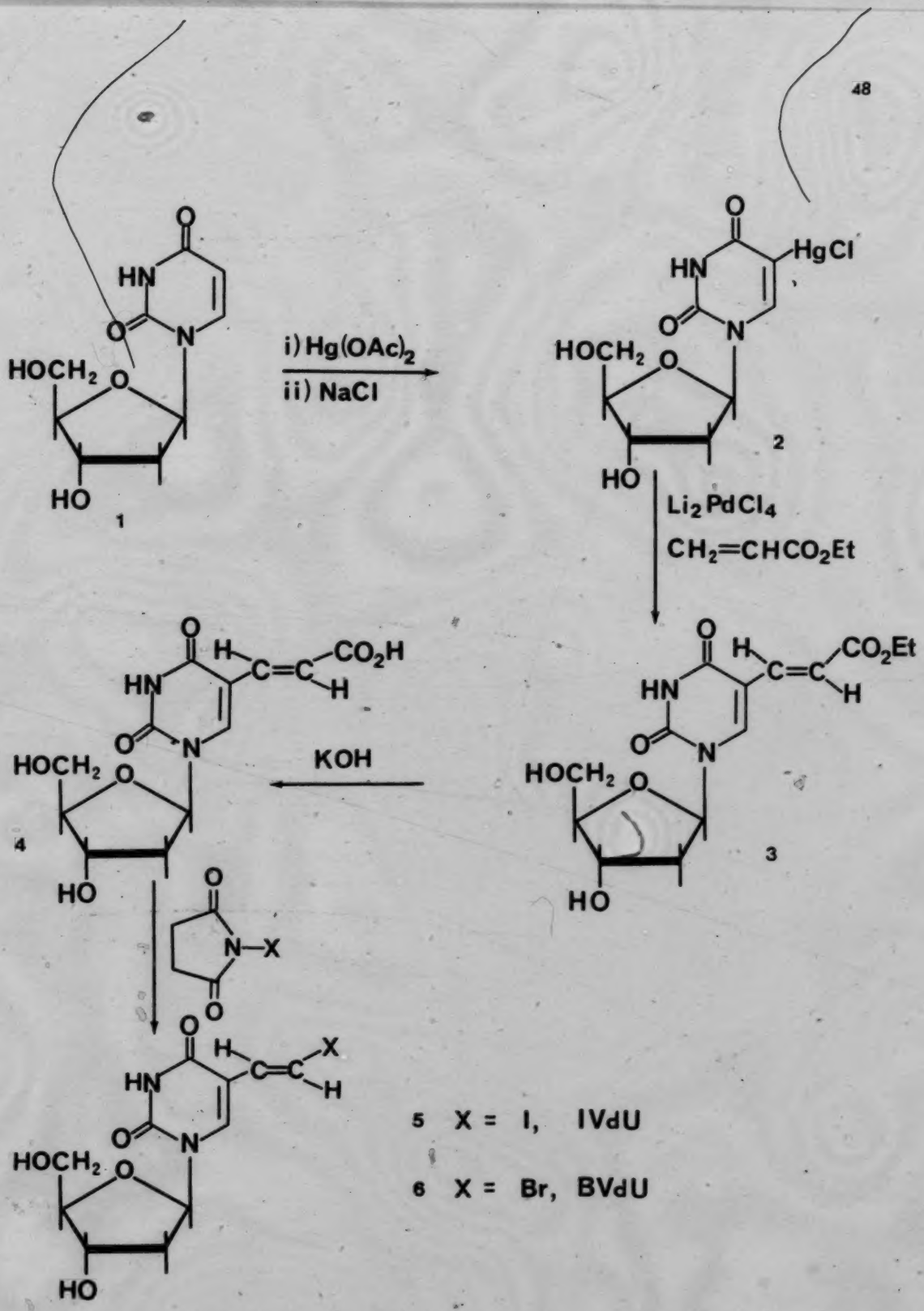

Fig. 5 General Synthetic Route for the Synthesis of IVdU and BVdU.

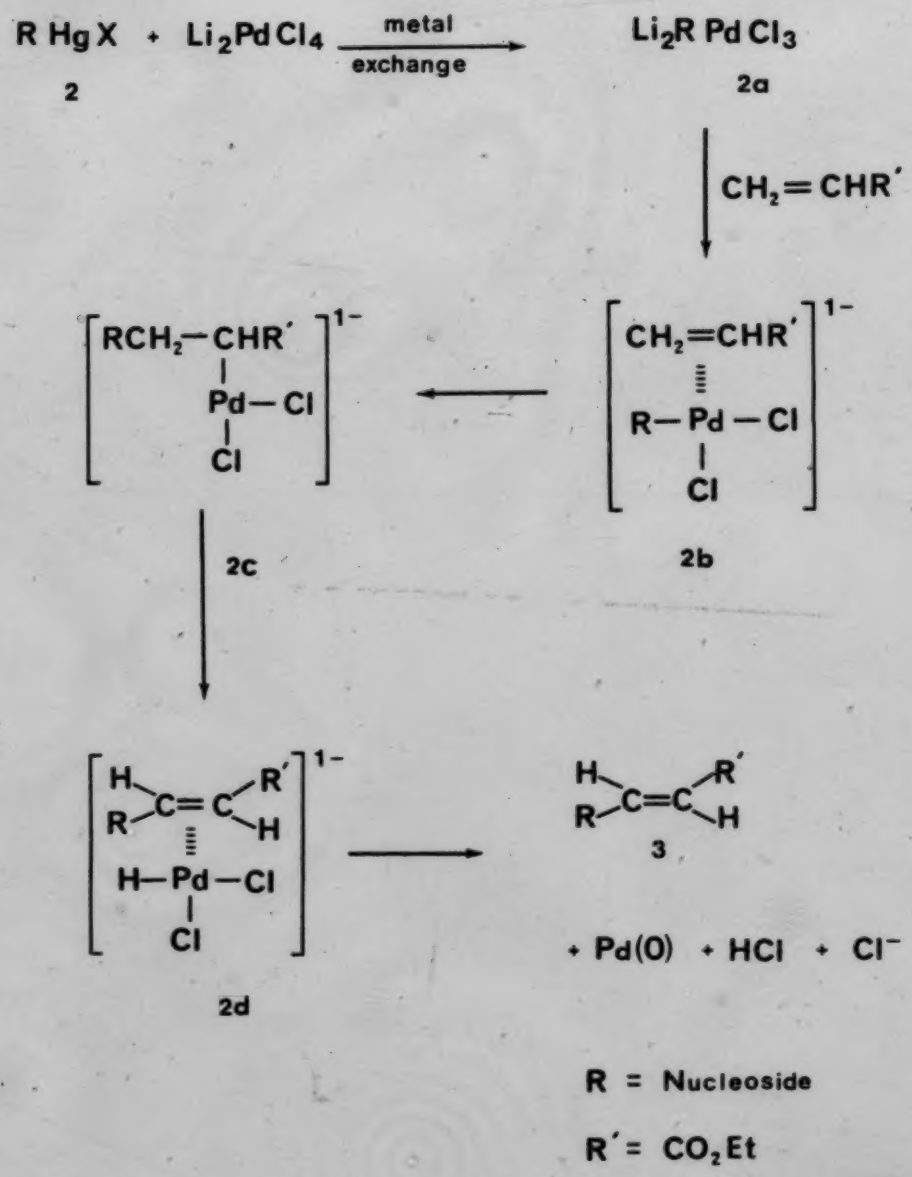

Fig. 6 Reaction Mechanism for Coupling of Dilithium Palladium Tetrachloride with 5-Chloromercuri Nucleosides.

hydroxide (73.7% yield) (197). The carboxylic acid **4** was the key intermediate in several subsequent chemical and radiochemical syntheses. The final step involved the reaction of **4** with N-iodo- or N-bromosuccinimide (NIS or NBS) to give (*E*)-5-(2-iodovinyl)-2'-deoxyuridine (IVdU, **5**, 30.4% yield) or (*E*)-5-(2-bromovinyl)-2'-deoxyuridine (BVdU, **6**, 42% yield). The NBS reaction was performed in aqueous medium, whereas the NIS reaction required dry DMF due to the instability of NIS in water. The halogenation reactions were stereospecific since little or no *Z* isomer was produced. The identities of products were established by R*f* values (TLC and HPLC), UV and ^{1}H NMR spectral data. These data were in agreement with those reported in the literature (197). The vicinal coupling constant (J) of 15 Hz for the vinylic protons confirmed that compounds **5** and **6** were *E* isomers. The *Z* isomer of BVdU has been reported to have a J value of 8 Hz for the vinylic protons (207). The NIS and NBS reactions are not suitable for radiohalogenations employing short-lived isotopes such as ^{123}I, ^{75}Br and ^{82}Br, since these require the radiochemical synthesis of radiohalogenated NIS and NIS as the first step. Therefore, alternate methods using chloramine-T, amenable to a radiochemical synthesis were developed (Fig. 7). IVdU and BVdU obtained in these reactions were identical to the corresponding products formed by the NIS or NBS reaction with respect to R*f* value, UV and ^{1}H NMR spectral characteristics and HPLC retention time. The chemical yields obtained by the chloramine-T method (26.3% for IVdU, 18% for BVdU) were lower than those obtained by the NIS and NBS methods.

(*E*)-5-(2-Iodovinyl)-2'-deoxyuridine-3',5'-diacetate was required as a reference compound for the radiochemical synthesis of [^{131}I]-(*E*)-5-(2-iodovinyl)-2'-deoxyuridine-3',5'-diacetate. The synthetic route employed is shown in Fig. 8. Acetylation of (*E*)-5-(2-carboxyvinyl)-2'-deoxyuridine (**4**) using acetic anhydride in pyridine gave the corresponding diacetyl compound **7** (55.4% yield), which on iodination by the NIS method gave (*E*)-5-(2-iodovinyl)-2'-deoxyuridine-3',5'-diacetate (**8**) (41% yield). The ^{1}H NMR confirmed the presence of the two acetyl groups in this molecule. The vicinal coupling constants (J) of 15 Hz for the vinylic protons confirmed that it is an *E*

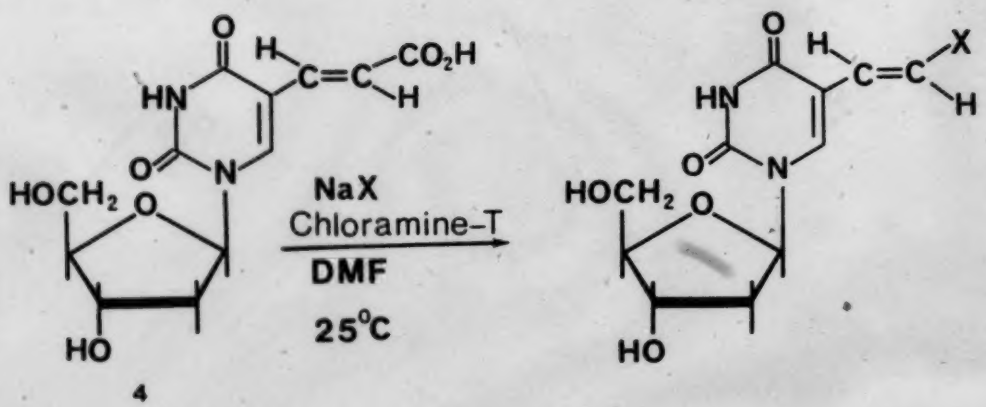

4

5 X = I, IVdU

6 X = Br, BVdU

Fig. 7 Synthesis of IVdU and BVdU Using the Chloramine-T Method.

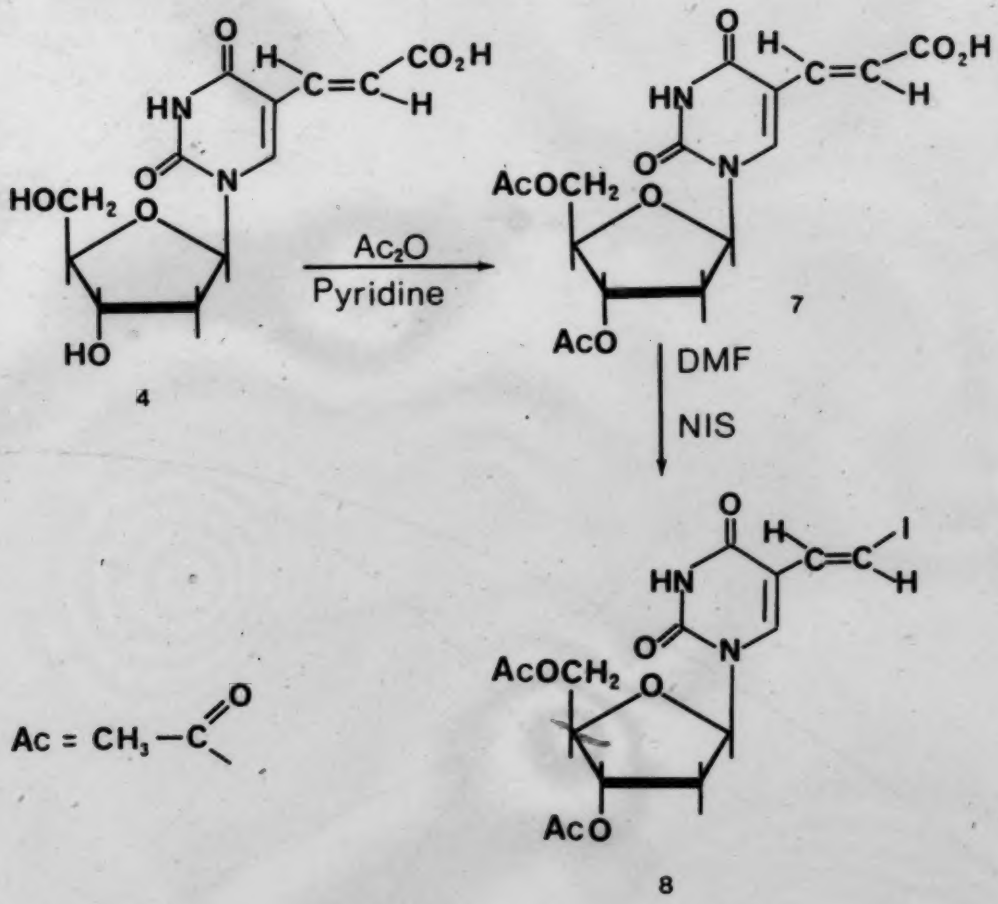

Fig. 8 Synthesis of IVdU-3',5'-diacetate.

isomer. The high resolution mass spectra showed a molecular ion (M^+) at 464.0081 which corresponded to the molecular formula $C_{13}H_{17}N_2O_7I$ (calculated mass : 464.00394)

(*E*)-5-(2-Iodovinyl)uracil was required as one of the reference compounds for metabolic studies of [^{131}I]-IVdU. It was synthesised by a 3 step procedure from commercially available 5-(hydroxymethyl)uracil (Fig. 9). Oxidation of 5-(hydroxymethyl)uracil (**9**) with potassium persulfate and silver nitrate at 30° C gave 5-formyluracil (**10**) (80% yield), which on condensation with malonic acid in the presence of piperidine gave (*E*)-5-(2-carboxyvinyl)uracil (**11**) (23% yield). (*E*)-5-(2-Iodovinyl)uracil (**12**) was obtained by iodination of compound **11** using chloramine-T and sodium iodide (10% yield)

C. Radiochemical Syntheses

The major objective of the radiochemical syntheses was to develop radiochemical routes suitable for the high specific activity syntheses of radiohalogenated IVdU and BVdU labeled with short-lived isotopes such as ^{123}I, ^{77}Br and ^{75}Br. Specific activity is an important factor to be considered in the design of a radiopharmaceutical aimed at a relatively small number of molecular targets (208). A low specific activity sample may quickly saturate the small number of molecular sites and any selective uptake may be left unnoticed due to the small ratio of radiolabeled to unlabeled molecules in the target. The specific activity of radiolabeled IVdU or BVdU used in this study is likely to be a critical factor, since the ratio of the HSV-infected cells to uninfected cells in an infected region of the brain of an HSE patient is likely to be very small.

The techniques for radioiodination and radiobromination of small molecules have been reviewed (209-211). Radioiodination reactions very often require *in situ* generation of an electrophilic species of iodine. Mild oxidising agents such as chloramine-T (212, 213), iodogen (214-216), and lactoperoxidase (213, 217, 218) are commonly used to oxidise radioactive iodide. The electrophilic species is believed to be I^+. A simpler method for radioiodination of small molecules is the halogen-halogen exchange of a radioactive iodine isotope for a

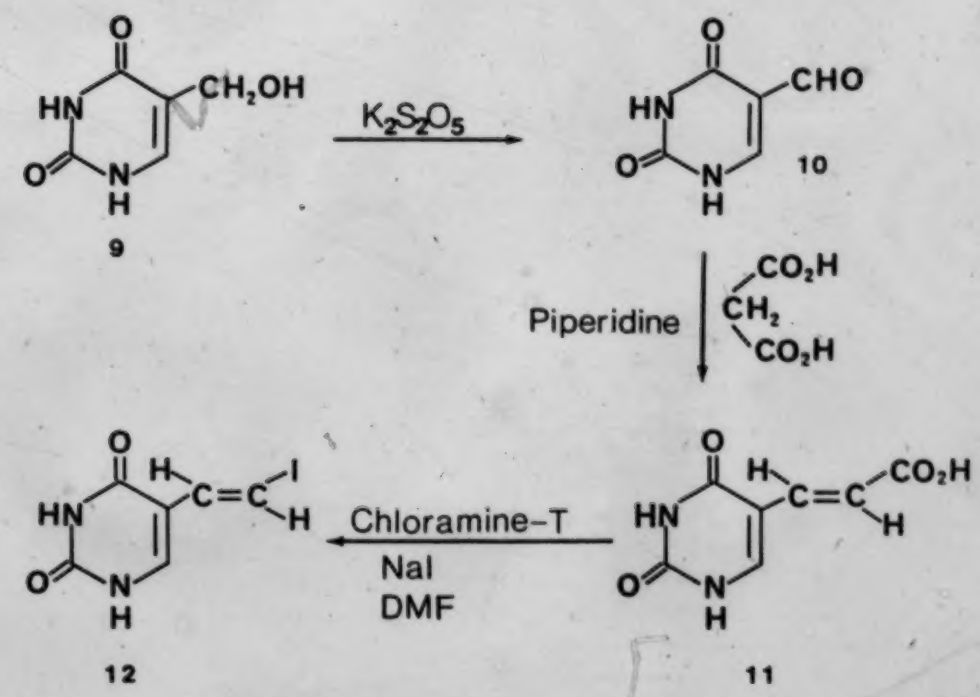

Fig. 9 Synthesis of (*E*)-5-(2-iodovinyl)uracil.

non-radioactive iodine atom (219, 220). This can often be achieved by simply heating the compound with radioactive iodide in a suitable solvent. Copper (I) salts have been reported to catalyze this isotope exchange (221, 222). The major limitation of this method is that it is not useful for the preparation of 'high specific activity' or 'no-carrier-added' ('NCA') syntheses. Electrophilic radiobromination reactions involve generation of an electrophilic species of bromine from bromide using a mild oxidising agent. Chloramine-T and N-chlorosuccinimide have been used for the *in situ* generation of an electrophilic species of bromine (probably BrCl) from bromide (223-225).

The synthetic routes developed for the preparation of radiohalogenated IVdU and BVdU are shown in Fig. 10. These include

1. radioiodination and radiobromination using chloramine-T (routes C and D)
2. halogen isotope exchange reaction for radioiodination (route E) and
3. direct neutron activation of unlabeled BVdU (route F).

The radiochemical yields of radioiodinated IVdU (**5a**) using a variety of reaction conditions is summarised in Table 7. The Chloramine-T reaction used for the 'high specific activity' synthesis of [^{131}I or ^{125}I]-IVdU was complete in less than 1 h and gave 67.2% chemical yield and 69% radiochemical yield. A NCA reaction using ^{131}I, terminated at 30 min, gave [^{131}I]-IVdU without any substantial reduction in radiochemical yield (65%). This method was shown to be suitable for the synthesis of [^{123}I]-IVdU for the imaging studies using single photon emission computed tomography (SPECT). The lower radiochemical yield (40.7%) obtained for the ^{123}I synthesis is due to the short half-life of the isotope (13.26 h). The radiochemical yield corrected for decay is 57% and corresponds closely with that for ^{131}I synthesis. [^{131}I]-(*E*)-5-(2-Iodovinyl)-2'-deoxyuridine-3',5'-diacetate was also synthesised by chloramine-T method. The radiochemical yield was 50%.

The cuprous ion catalysed halogen isotope exchange reaction (route E) required heating for a prolonged time (20 h). The low chemical recovery (54.3%) and radiochemical yield (45.1%) may have been due to thermal decomposition. The stereospecificity of the iodine

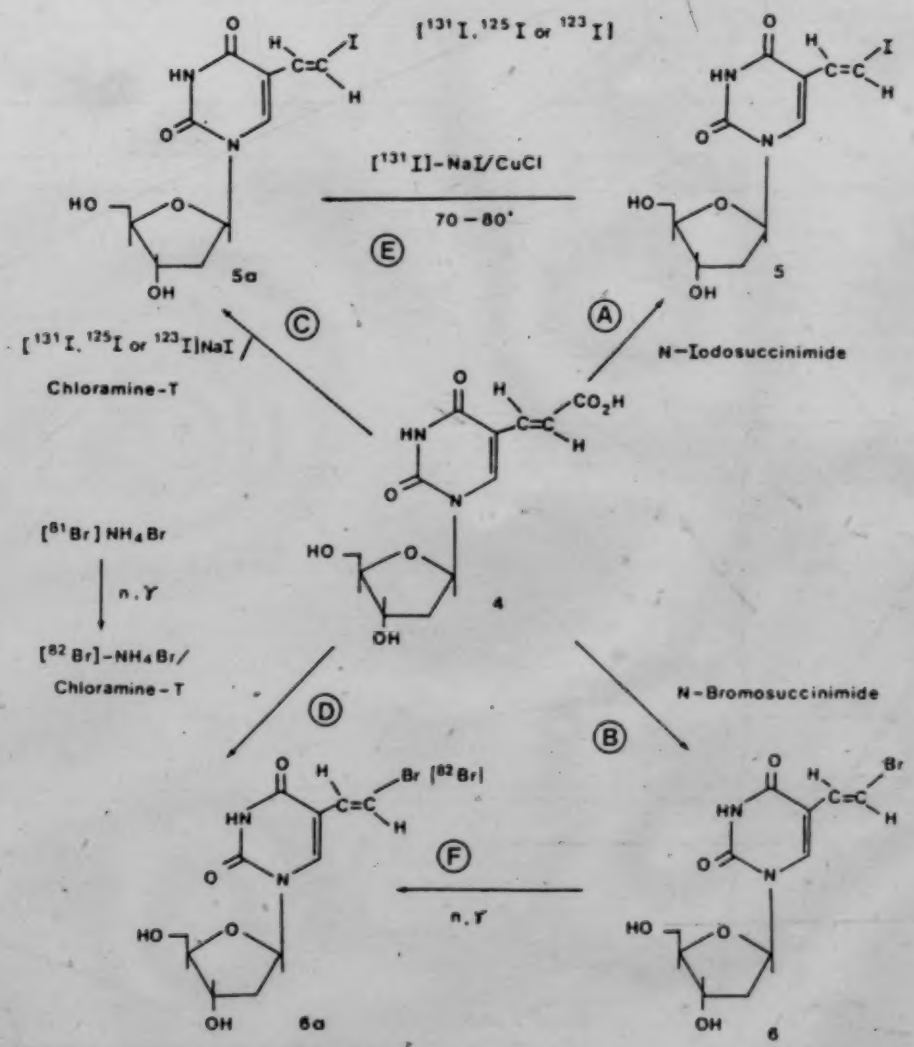

Fig. 10 Synthesis of Radiohalogenated IVdU and BVdU.

Table 7. Radiochemical Synthesis of IVdU

Method	Isotope	Specific Activity (GBq mmol^{-1})	Temperature (°C)	Time [1]	Radiochemical Yield [1] (%)	Chemical Yield Isolated
Chloramine-T	^{131}I,^{125}I	343.5	25	1 h	67.2	69.0
Chloramine-T	^{123}I	370	25	30 min	40.7	57.0
Chloramine-T	^{131}I	"NCA"	25	30 min	65.0	-
Halogen Isotope Exchange	^{131}I	16.7	70-80	20 h	45.1	54.3

[1] Does not include the time required for purification.

[2] Radiochemical yields are those obtained at the end of purification.

exchange is consistent with previous studies involving halogen exchange reactions for other vinyl iodides (226). The exchange reaction is believed to proceed via generation of a small quantity of $Cu^{131}I$, which undergoes ligand exchange with the unlabeled IVdU (5). There is less radiation hazard using this technique since it does not generate a volatile radioiodine species. This exchange reaction is limited to the preparation of low and medium specific activity products.

^{82}Br was used as a model isotope of radiobromine in these studies since it is easily prepared at the University of Alberta SLOWPOKE Reactor Facility. [^{81}Br]-NH_4Br, required for the preparation of [^{82}Br]-NH_4Br was obtained form [^{81}Br]-NaBr by ion exchange using Amberlite CG 120 [NH_4^+] resin. Neutron activation of [^{81}Br]-NH_4Br using the $^{81}Br(n,\gamma)^{82}Br$ nuclear reaction at a flux of 10^{12} n cm^{-2} s^{-1} for 4 h gave [^{82}Br]-NH_4Br with a specific activity of 2.3 MBq mg^{-1}. The theoretical yield calculated was 2.6 MBq mg^{-1} (Appendix). It would be possible to increase the specific activity to 6 MBq mg^{-1} with a subsequent 16 h irradiation at a neutron flux of 0.5 X 10^{13} n cm^{-2} s^{-1}. The SLOWPOKE reactor conditions do not allow irradiations at a higher neutron flux during this second period of 16 h irradiation.

The chemical and radiochemical yields of [^{82}Br]-BVdU obtained by chloramine-T method and by direct neutron activation are shown in Table 8. The reaction of (*E*)-5-(2-carboxyvinyl)-2'-deoxyuridine (**4**) with [^{82}Br]-NH_4Br in the presence of chloramine-T gave [^{82}Br]-BVdU (**6a**) (69.8% radiochemical yield; specific activity 227 MBq $mmol^{-1}$). The short reaction time (10 min) makes this a suitable method for the incorporation the positron emitter ^{75}Br (half-life 95.5 min) into BVdU. The direct neutron activation for the preparation of [^{82}Br]-BVdU was carried out using BVdU which contained natural abundance bromine (^{79}Br and ^{81}Br). A 24 h cool-off time was required to allow decay of ^{80}Br, $^{80}Br^m$ and $^{82}Br^m$ (half-lives of 17.6 min, 4.3 h and 6.05 min respectively) before the irradiated sample was purified. Although radiolytic decomposition was minimal (<3%), only 30% of the overall activity produced was associated with [^{82}Br]-BVdU. This is due to the Szilard-Chalmers cleavage reaction which frequently occurs during neutron activation of organic halides (227).

Table 8. Preparation of [^{77}Br]-BVdU

Method	Specific Activity (MBq mmol^{-1})	Temperature (°C)	Time [1]	Radio-chemical Yield [2] (%)	Chemical Yield Isolated (%)
Chloramine-T	227	25	<10 min	69.8	72.0
Direct Neutron Activation	31.82		4 h	30.0	97.0

[1] Does not include the time required for purification
[2] Radiochemical yields are those obtained at the end of purification.

The neutron capture by bromine nucleus is followed by emission of a γ-ray, which gives recoil energy to the radioactive nucleus. This recoil energy may cause cleavage of the bond between C and radioactive Br. Because of this, the specific activity achieved from an organic bromide by direct neutron activation is much lower than the calculated theoretical yield. The radioactive inorganic bromine formed by Szilard-Chalmers cleavage would be of high specific activity. Therefore, Szilard-Chalmers cleavage of organic bromides could be used for the generation of high specific activity samples of inorganic bromine, which if separated from the organic compounds, could be used for high specific activity radiobrominations. A recent study at the University of Alberta SLOWPOKE Reactor Facility has shown that the inorganic bromine generated by the Szilard-Chalmers cleavage of an organic bromide attained a specific activity of about 500 times greater than that attained for an inorganic bromine sample by direct irradiation under the same irradiation conditions (228). The specific activity of [^{82}Br]-BVdU calculated to the end of irradiation was 32 MBq mmol^{-1}. The theoretical specific activity attainable for [^{82}Br]-BVdU by neutron irradiation of BVdU containing natural abundance bromine at a flux of 1 X 10^{12} n cm^{-2} s^{-1} for 4 h is 130 MBq mmol^{-1} (Appendix). The direct irradiation method is not the method of choice for the preparation of [^{82}Br]-BVdU, since most *in vivo* studies require a much higher specific activity product.

D. Quantitative Uptake Studies of ^{131}I-Labeled (E)-5-(2-Iodovinyl)-2'-deoxyuridine in Herpes Simplex Virus-Infected Cells *In Vitro*

The biochemical rationale for the development of radiolabeled nucleoside analogs as potential diagnostic agents for the diagnosis of herpes simplex encephalitis (HSE) is based on their selective trapping in HSV-infected cells. The metabolic trapping of the radiolabeled nucleoside [^{131}I]-IVdU was evaluated by quantitating its uptake in HSV-1 (TK$^+$)-infected PRK cells *in vitro*. In biological evaluations IVdU was preferred over BVdU, since radioisotopes of iodine are more commonly used in clinical nuclear medicine than radioisotopes of bromine. The uptake of [^{131}I]-IVdU was studied with respect to three variables :

1. duration of exposure of cells to radiolabeled drug
2. concentation of radiolabeled drug and
3. the infecting dose of virus.

HSV-1 (TK^-)- and mock-infected PRK cells were used as controls. The mean and range values of the cellular uptake of IVdU under various conditions are shown in Fig. 11, 12 and 13.

Time-response curve for cellular uptake of [^{131}I]-IVdU

Confluent PRK cells in Falcon 25-cm^2 flasks were either infected with 6 X 10^6 PFU of HSV-1 (TK^+) or mock infected. After 7 h of incubation, 0.629 KBq of [^{131}I]-IVdU was added to each flask to give a final concentration of 2.76 ng ml^{-1}. Quantitation of both the intracellular and extracellular radiolabeled IVdU were determined at 20 s, 30 min, 1 h, 2h, 4 h, and 9 h respectively. Four HSV-1-infected flasks and three mock-infected flasks were used for the quantitation of intracellular and extracellular radioactivity at each time point.

The response for the cellular uptake of IVdU relative to time is shown in Fig. 11. The amount of radiolabeled IVdU in mock-infected cells remained low throughout the period of the study, whereas uptake of IVdU in HSV-infected cells increased with increasing time of exposure to the drug. The concentration of radiolabeled IVdU in the supernatant of HSV-1 (TK^+)-infected cells decreased with time, while that of the mock-infected cells remained high throughout the period of the experiment. The uptake of [^{131}I]-IVdU by the HSV-1 (TK^+)-cells up to 9 h corresponded to 36% of the total activity present. This study demonstrates the selective time dependent uptake of ^{131}I-IVdU by HSV-1-infected cells. A 5-10 fold higher concentration of the isotope could be detected in HSV-infected cells relative to uninfected cells as early as 1 h after the administration of IVdU. This suggests that uptake was rapid enough to permit the development of a radionuclide brain image even using a nucleoside with a relatively fast excretion or metabolism.

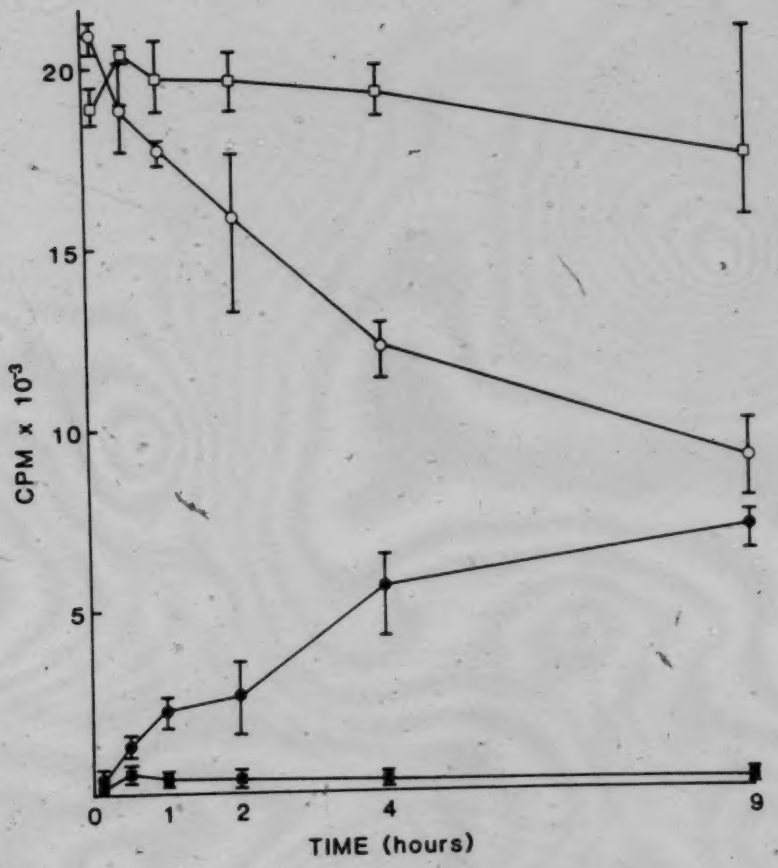

Fig. 11 Time-Response Curve for [^{131}I]-IVdU Uptake in HSV-1 (TK$^-$) (n=3) and Mock-Infected (n=2) PRK cells. • Intracellular Counts in HSV-1 (TK$^-$)-Infected cells ○ Extracellular Counts in Medium Overlay of HSV-1 (TK$^-$)-Infected cells ■ Intracellular Counts in Mock-Infected cells □ Extracellular Counts in Medium Overlay of Mock-Infected cells (Mean and Range).

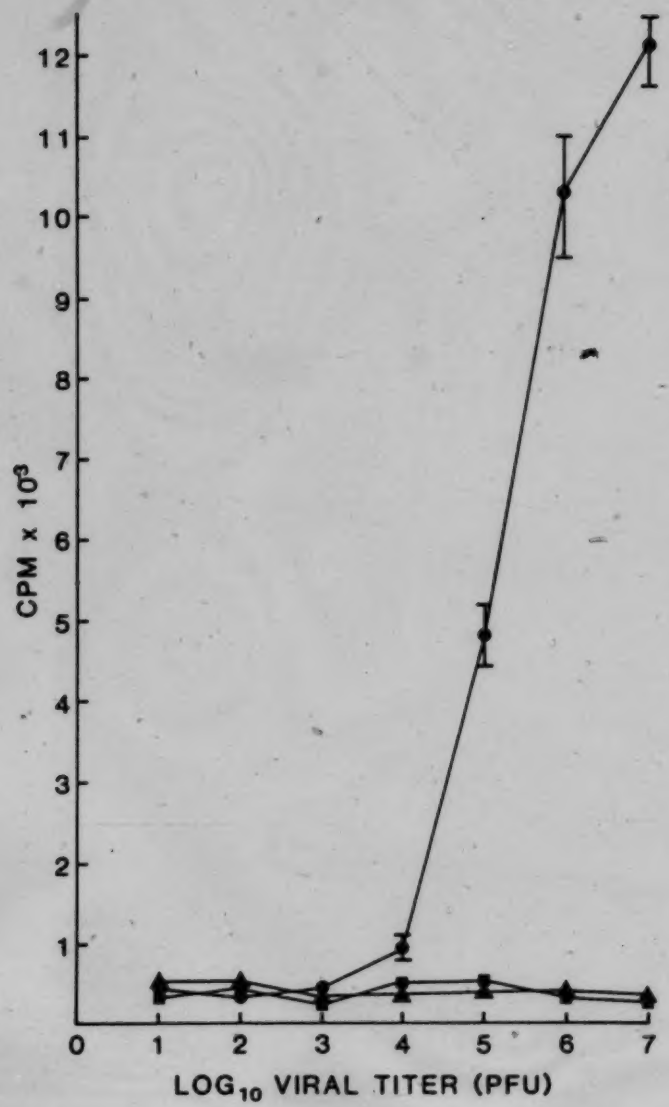

Fig. 12 Effect of Increasing the Titer of the Infecting Dose on the Uptake of [^{131}I]-IVdU in HSV-1 (TK$^-$) (n=3) (●), HSV-1 (TK$^-$) (n=2) (▲), Mock-Infected Cells (n=3) (■) (Mean and Range).

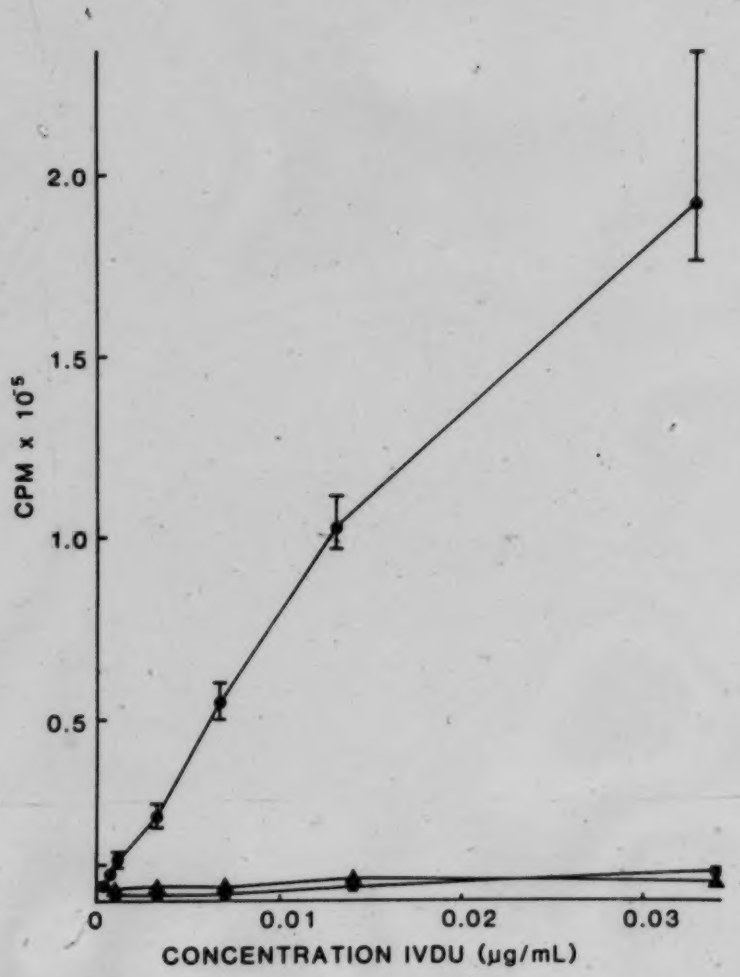

Fig. 13 Effect of Increasing Concentrations of [^{131}I]-IVdU on its Uptake in HSV-1 (TK$^-$) (n=3) (●), HSV-1 (TK$^-$) (n=2) (▲), Mock-Infected Cells (n=2) (■) (Mean and Range).

Effect of increasing infecting dose of virus on [^{131}I]-IVdU uptake

Serial dilutions of stock HSV-1 (TK$^+$) and HSV-1 (TK$^-$) were made to give an infecting dose range of 10^1 to 10^7 PFU per flask. Three flasks were infected with HSV-1 (TK$^+$), two flasks were infected with HSV-1 (TK$^-$), and two flasks were mock infected. After 7 h 0.836 KBq of [^{131}I]-IVdU was added to each flask to give a final concentration of 0.858 ng ml^{-1}. The cells were removed for the quantitation of the radioactivity after 4 h of incubation. The results are shown in Fig. 12. The quantity of [^{131}I]-IVdU taken up by HSV-1 (TK$^+$)-infected cells increased with increasing titer of infecting virus. HSV-1 (TK$^-$)-infected cells showed insignificant uptake even at high doses of infecting virus. The inclusion of HSV-1 (TK$^-$) controls in this study demonstrates that the selective uptake observed was mediated by HSV-encoded TK.

Since this experiment was completed in less than 14 h, it was assumed that the time was inadequate for a second phase of viral infection to occur. As shown in Fig. 12, an infecting dose of 10^4 PFU for a 25-cm^2 flask containing 5 x 10^5 cells is required before significant uptake can be detected. On this basis, in an animal model, at least 1 in 50 cells at any time would have to be infected before selective concentration of ^{131}I-labeled IVdU could concievably be detected by radionuclide brain imaging. The titer of HSV measured in brain biopsy specimens from HSE patients is not well documented. Nahmias *et al* have reported that in 11 out of 18 brain biopsies, the virus concentration was less than 10^4 50% tissue culture infective dose per g brain (79). A number of factors could affect the titer of virus from brain biopsy. The most important factor is probably the proximity of the biopsy to the most active site of infection. Since there is extensive histological destruction of HSV-infected brain tissue, it is likely that the titer of virus at the site of infection will be adequate to allow selective sequesteration of the radiolabeled nucleoside.

Dose-response curve for [^{131}I]-IVdU uptake

Known dilutions of ^{131}I-labeled IVdU (specific activity 80 GBq mmol^{-1}) were made and added to the flasks 7 h after infection with either 6 X 10^6 PFU of HSV-1 (TK$^+$), HSV-1 (TK$^-$), or mock infection. Concentrations were selected to cover a broad range around the dose known to cause a 50% reduction of PFU (ID_{50}). The ID_{50} of IVdU for the JLJ strain used in these experiments was 8 ng per mL. The cells were incubated with [^{131}I]-IVdU for 4 h. The uptake of ^{131}I-labeled IVdU increased proportionately to the amount of the labeled drug in the media (Fig. 13). This relationship was observed only in HSV-1 (TK$^+$)-infected cells and occurred even at concentrations greater than the ID_{50}. [^{131}I]-IVdU was intracellularly trapped even when the nucleoside concentration was sufficient to inhibit virus replication. This suggests that medium specific activity compounds may be satisfactorily used for a radionuclide imaging and that the selective uptake of a nucleoside analog into HSV-infected cells may not be inhibited by the presence of an antiviral drug. A recent study on the effect of ara-AMP and acycloguanosine (ACG) on the *in vitro* uptake of [^{131}I]-IVdU in HSV-1-infected cells have shown that the uptake was virtually not affected by the presence of inhibitory concentrations of ara-AMP and ACG for a period of 24 h (229) This suggests that a diagnostic imaging of HSE using a radiolabeled nucleoside may prove to be successful even during the initial period of therapy by an antiviral nucleoside.

The results of these *in vitro* studies validate the concept of metabolic trapping of radiolabeled nucleoside in HSV-infected tissues as a basis for the development of a radiopharmaceutical for the non-invasive diagnosis of HSE.

E. Tissue Distribution of [^{125}I]-IVdU in a Herpes Simplex Encephalitis Animal Model

The main objective of the preliminary tissue distribution study was to compare the uptake of [^{125}I]-IVdU in HSV-1-infected brain with that in uninfected brain to determine the feasibility of IVdU as a radiopharmaceutical for the *in vivo* detection of HSE. Eight rabbits (4 infected and 4 uninfected) were injected with an i.v dose of [^{125}I]-IVdU. A group of tissues

including blood, brain, liver, kidney, spleen, lung, and muscle were collected at 1 h and 6 h after injection and counted for radioactivity. The brain samples of the infected rabbits were assayed for the viral titer to confirm the presence of HSV infection. A viral titer of about 1 X 10^5 per g brain could be detected. Tissue distribution expressed as % injected dose per g tissue at 1 h and at 6 h are shown in Table 9 and Table 10 respectively. Tissue distribution expressed as a tissue to blood ratio at 1 h and 6 h are shown in Table 11 and 12.

None of the organs examined demonstrated high uptake of radioactivity. The uptake of radioactivity by brain was found to be relatively low at both time points studied. This may be due to a relatively low permeability of the nucleoside across the BBB. IVdU has a log P value of 0.60, whereas the optimal log P range for good permeability accross BBB is 0.9 to 2.5. The mean uptake of the radiotracer in the infected brain was 5.4 to 6.4 times higher than in uninfected brain 1 hour after injection. The difference was smaller (1.5 to 1.9 times greater in the infected brain as compared to the uninfected) 6 h after injection. The reasons for this are not clear. One plausible explanation is that radioactive IVdU, selectively trapped in infected cells may undergo metabolic degradation to radioactive compound(s) having good permeability across plasma membrane, resulting in decreased intracellular radioactivity. The differences in the brain uptake between infected and uninfected animals was highest at 1 h. However, these data need to be viewed with caution since this study does not exclude the possibility that the higher uptake noted in infected brain tissue may in part be due to non-selective accumulation caused by increased BBB permeability in infected animals.The only organs other than brain which showed a pronounced difference in uptake of radioactivity between the infected and uninfected animals were liver and spleen for the organs examined. The reason for this is not clearly understood. Since these rabbits did not have antibodies to HSV, there is a possibility of infection of organs other than brain. However, this could not be confirmed, since organs other than brain were not assayed for the viral titer.

The radioactivity in blood remained higher than that in the target organ brain at 1 and 6 h. A comparison of the blood activity at 1 h and at 6 h (Table 9 and 10) indicated that

Table 9. Tissue distribution of ^{123}I-IVdU (Expressed as % Injected Dose per Gram Tissue) in a Rabbit Model 1 Hour After i.v Injection of 0.74 MBq of ^{123}I-IVdU (mean of two animals with range)

Tissue	Uninfected Rabbit	Infected Rabbit
Blood	0.1756 ±0.0130	0.2045 ±0.0017
Brain	0.0155 † ±0.0039	0.0989 † ±0.0089
Liver	0.1132 ±0.0169	0.2511 ±0.0105
Kidney	0.2512 ±0.0080	0.3261 ±0.1069
Spleen	0.0787 ±0.0065	0.1667 ±0.0257
Lung	0.1185 ±0.0086	0.0764 [1]
Muscle	0.0565 ±0.0047	0.0676 ±0.0413

† $p < 0.025$

[1] Data from a single animal

Table 10. Tissue distribution of ^{125}I-IVdU (Expressed as % Injected Dose per Gram Tissue) in a Rabbit Model 6 Hours After i.v Injection of 0.74 MBq of ^{125}I-IVdU (mean of two animals with range)

Tissue	Uninfected Rabbit	Infected Rabbit
Blood	0.1332 ±0.0057	0.0958 ±0.0058
Brain	0.0057 † ±0.0005	0.0075 † ±0.0015
Liver	0.0673 ±0.0033	0.0420 ±0.0031
Kidney	0.1236 ±0.0068	0.0972 ±0.0183
Spleen	0.0427 [1]	0.0392 ±0.0033
Lung	0.0823 [1]	0.0589 [1]
Muscle	0.0177 ±0.0019	0.0184 ±0.0057

† $p < 0.40$

[1] Data from a single animal

Table 11. Tissue distribution of ^{125}I-IVdU (Expressed as Tissue to Blood Ratio) in a Rabbit Model 1 Hour After i.v Injection of 0.74 MBq of ^{125}I-IVdU (mean of two animals with range)

Tissue	Uninfected Rabbit	Infected Rabbit
Blood	1.0000	1.0000
Brain	0.0906 † ±0.0291	0.4881 † ±0.0477
Liver	0.6553 ±0.1448	1.2386 ±0.0621
Kidney	1.4415 ±0.1518	1.6035 ±0.5140
Spleen	0.4532 ±0.0701	0.8228 ±0.1336
Lung	0.6750 ±0.0006	0.3796 [1]
Muscle	0.3254 ±0.0510	0.3347 ±0.1062

† $p < 0.025$

[1] Data from a single animal

Table 12. Tissue distribution of ^{125}I-IVdU (Expressed as Tissue to Blood Ratio) in Rabbit Model 6 Hours After i.v Injection of 0.74 MBq of ^{125}I-IVdU (mean of two animals with range)

Tissue	Uninfected Rabbit	Infected Rabbit
Blood	1.0000	1.0000
Brain	0.0426 † ±0.0020	0.0798 † ±0.0209
Liver	0.5053 ±0.0032	0.4369 ±0.0054
Kidney	0.9272 ±0.0114	0.9700 ±0.1325
Spleen	0.3346 [1]	0.4089 ±0.0092
Lung	0.6456 [1]	0.5793 [1]
Muscle	0.1316 ±0.0084	0.1892 ±0.0417

† $p < 0.40$

[1] Data from a single animal

clearance of radioactivity from blood during this period was slow. Intact nucleosides usually have fast blood clearance characteristics due to their high water solubility. Lee *et al* have recently reported the tissue distribution of [2-^{14}C]-5-ethyl-2'-deoxyuridine in tumor bearing mice (230). The biological half-life of [2-^{14}C]-5-ethyl-2'-deoxyuridine in blood in the second phase of a bifunctional clearance curve was estimated to be 33 min. The slow blood clearance of radioactivity for [^{125}I]-IVdU in this preliminary study may be largely due to radioactive metabolites of [^{125}I]-IVdU. The high background radioactivity may present a major problem for diagnostic imaging, since it would obscure any selective uptake in the brain of the infected animal.

Saito *et al* have reported the use of quantitative autoradiography for the *in vivo* evaluation of the feasibility of radiolabeled nucleosides as non-invasive diagnostic agents for HSE (200-202). They have reported regional distribution of [2-^{14}C]-1-(2-deoxy-2-fluoro-β-D-arabinofuranosyl)-5-methyluracil in the infected brain of an HSE rat model using this technique. The HSV-infected regions of the brain (presence of the virus confirmed by detection of viral antigens) showed 2 to 13 times higher uptake of radioactivity relative to the uninfected regions. Quantitative autoradiography offers an advantage over tissue distribution studies using scintillation counting in that it is able to demonstrate the high uptake by a small number of cells. In tissue distribution studies using scintillation counting, high uptake in a small area may be left unnoticed, since it may be masked by the background activity associated with the surrounding cells. Our tissue distribution studies succeeded in showing 5.4 to 6.4 times higher radioactivity in the infected brain as compared to the uninfected brain 1 h after injection. However, quantitative autoradiography could have demonstrated even a higher difference in regional uptake of radioactivity.

Our preliminary tissue distribution studies on [^{131}I]-IVdU indicated that there is a need for a clear understanding of pharmacokinetic and metabolic aspects of radioiodinated IVdU *in vivo*. Therefore the next phase of investigation was directed towards an evaluation of the *in vivo* kinetics of IVdU and its metabolites in a dog model.

F. Pharmacokinetics and Metabolism of [^{131}I]-(E)-5-(2-Iodovinyl)-2'-deoxyuridine in Dogs

The pharmacokinetics and metabolism of a radiopharmaceutical may significantly influence its diagnostic value. Rapid excretion and/or metabolism to inactive compounds are usually undesirable since it would result in decreased bioavailability of the compound for accumulation into target tissue. In addition, radioactive metabolites having a long biological half-life may contribute to high background activity and increase the radiation dose.

The metabolic degradation of deoxythymidine and its 5-substituted analogs via phosphorolytic cleavage of the nucleoside bond by pyrimidine phosphorylases (182) have already been discussed in chapter I. The base formed as result of a phosphorolysis may be further catabolised by a reductive pathway (231). The first step is the reduction of the C_5-C_6 double bond of the ring to give dihydropyrimidines, followed by the oxidative cleavage of the N_3-C_4 bond to give β-uriedo acids, from which β-aminoacids, carbon dioxide and ammonia are formed. The 5'-monophosphates of the pyrimidine nucleosides which have halogens or halogen containing substituents at the 5 position are subject to thymidylate synthetase-catalysed dehalogenation (191) as indicated previously. The present investigation involved identification and quantitation of the major radioactive metabolites of [^{131}I]-IVdU in *in vitro* and *in vivo* biological systems.

Metabolism of [^{131}I]-IVdU in blood *in vitro*

[^{131}I]-IVdU was incubated with heparinised whole blood and the radioactive components present in methanolic extracts of plasma were analysed by quantitative r-HPLC. Control experiments indicated that HPLC samples ready for injection contained greater than 90% of the original activity of the plasma sample prior to extraction with methanol. A typical radiochromatogram (Fig. 14) showed four radioactive peaks : A, B, C and D. Peaks C and D were identified as [^{131}I]-(*E*)-5-(2-iodovinyl)uracil (IVU) and [^{131}I]-IVdU respectively. Peak A was suspected to be radioactive iodide. However, the identity could not be confirmed initially since it eluted very close to the solvent front using the solvent system employed for elution of

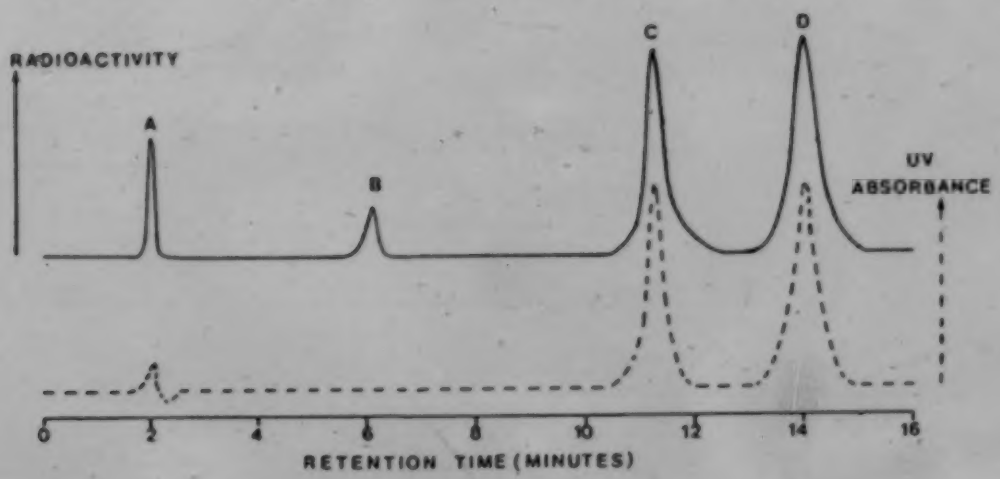

Fig. 14 A Typical Radio High-Pressure Liquid Chromatogram of Plasma Sample Containing [^{131}I]-IVdU and its Metabolites. Peaks A, C, and D are [^{131}I]-I^-, [^{131}I]-IVU, and [^{131}I]-IVdU respectively. Peak B has not been identified.

the other radioactive compounds in plasma. The identity of peak A was subsequently established by rechromatography on r-HPLC using paired ion chromatography (PIC) separation conditions (232). The mobile phase used in PIC may contain a quaternary ammonium compound having hydrophobic groups so that it increases the retention of the anion being analysed on a reverse phase column by formation of an ion pair. Peak A co-chromatographed with a non-radioactive sample of iodide under PIC separation conditions. A peak B, not identified to date, did not correspond to any of the reference compounds used in the experiment.

The kinetics of [^{131}I]-IVdU, [^{131}I]-IVU and [^{131}I]-iodide in blood *in vitro* are shown in Fig. 15. The rapid disappearance of [^{131}I]-IVdU corresponded to an increase in the amount of [^{131}I]-IVU formed (Fig. 15). After a 2 hour incubation, 73% of the radioactivity was associated with [^{131}I]-IVU. Radioactive iodide represented less than 10% of the total radioactivity over a 24 hour period.

The major catabolic pathway for IVdU in blood appears to be phosphorolysis to the corresponding base IVU. Blood platelets are rich in the enzyme deoxythymidine phosphorylase (184) which would be primarily responsible for the observed rapid *in vitro* conversion of IVdU to IVU. These results may be compared with the recently reported data describing the phosphorylase activity of intact blood platelets on several 5-substituted deoxythymidine analogs including BVdU (186). BVdU on incubation with human blood platelets was metabolised (95% in 2 h) to the corresponding base (*E*)-5-(2-bromovinyl)uracil (BVU). This *in vitro* study on BVdU did not include evaluation of possible debromination. The formation of radioactive iodide from ([^{131}I]-IVdU or [^{131}I]-IVU) remained low (<10% of the radioactivity in the plasma) over a period of 24 hours. This observation is consistent with the relatively high chemical stability expected for the vinyl iodides.

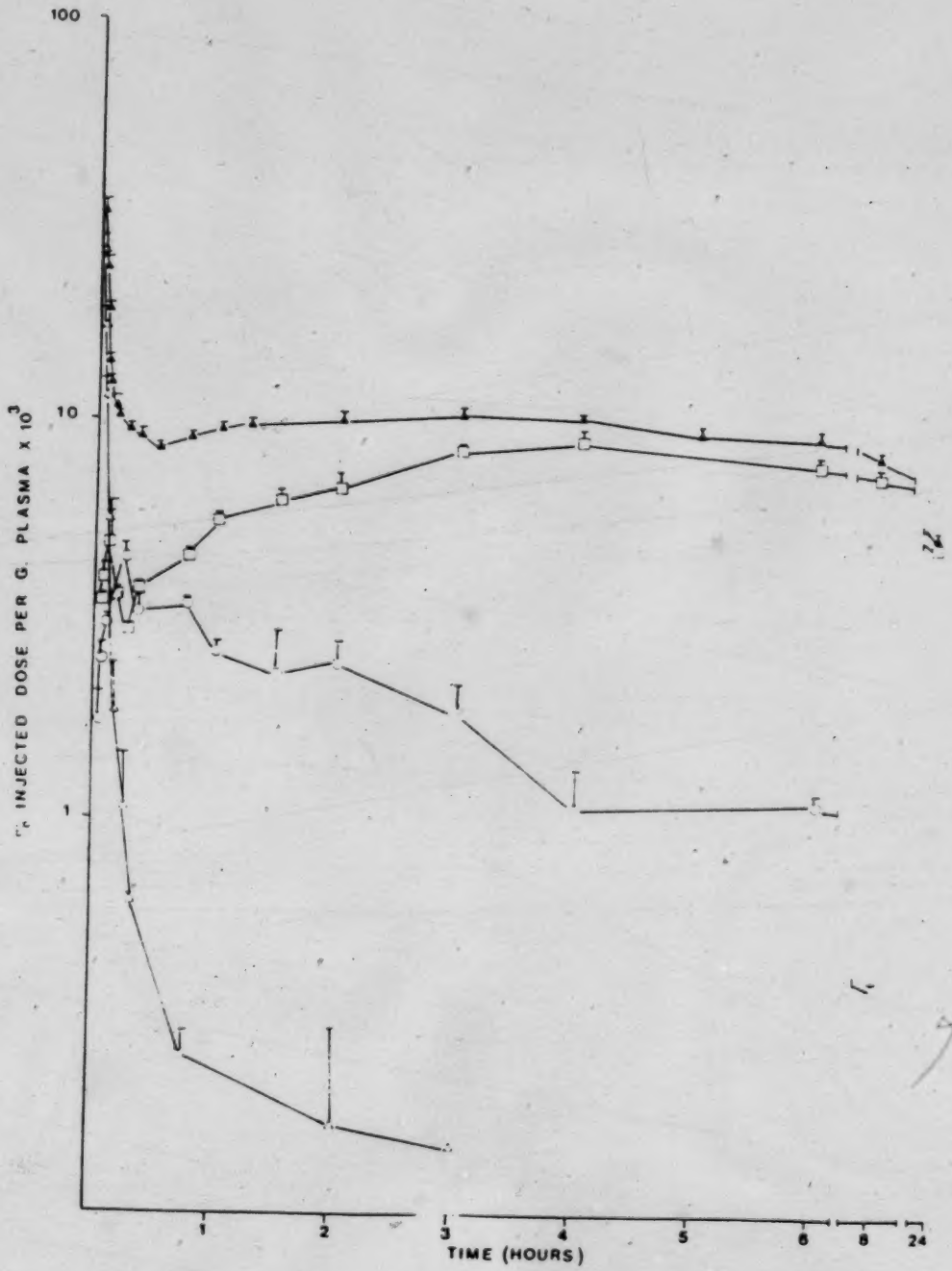

Fig. 16 Metabolites of [^{131}I]-IVdU (specific activity, 1665 MBq /mmol) in Dogs *In Vivo* (n=2). ▲ Total Radioactivity, △ [^{131}I]-IVdU, ○ [^{131}I]-IVU, □ [^{131}I]-I$^-$. (Mean and Range)

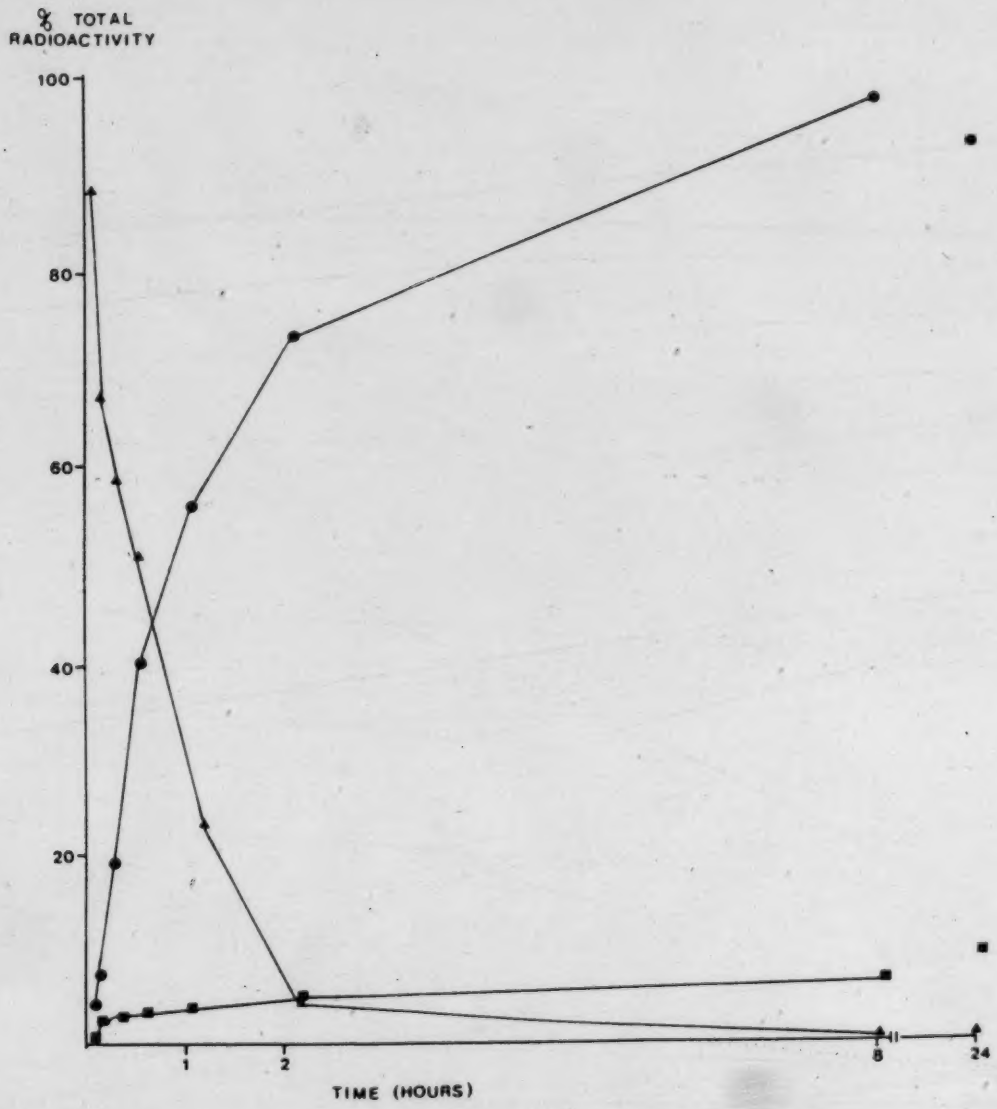

Fig. 15 Metabolites of [^{131}I]-IVdU in Blood *In Vitro*.(n=1) ▲ [^{131}I]-IVdU, ● [^{131}I]-IVU, ■ [^{131}I]-I$^-$

Metabolism of [^{131}I]-IVdU in dog *in vivo*

The *in vivo* pharmacokinetics and metabolism of a radiopharmaceutical may depend on the specific activity of the drug. Therefore, the *in vivo* studies were performed using both low (1665 MBq/mmol) and high specific activity (37 TBq/mmol) [^{131}I]-IVdU compounds.

The kinetics of the total radioactivity and its components in plasma for a 24 hour period after an i.v injection of [^{131}I]-IVdU (low specific activity) are shown in Fig. 16. The plasma clearance curve for total radioactivity showed an initial rapid clearance of the isotope followed by a very slow clearance phase (Fig. 16). An unexpected increase in the total radioactivity in the blood could be noticed during the period of 30 min to 1.5 h. This was reproducible. This may be due to the release of radioactive metabolites of [^{131}I]-IVdU from body compartment(s), which might have selectively accumulated [^{131}I]-IVdU during the first phase of the curve. The clearance profile for intact [^{131}I]-IVdU was characterised by a major rapid clearance phase. The concentration of [^{131}I]-IVdU in plasma 1 hour after injection accounted for less than 2% of the overall radioactivity. The kinetics of the metabolites [^{131}I]-IVU and radioactive inorganic iodide are also shown in Fig. 16. The radioactivity due to the unidentified component B rarely exceeded 10% of the total radioactivity in each plasma sample. Inorganic iodide was the major radioactive component (95%) in the plasma sample collected 24 hours after injection. Similar results were obtained from an experiment using a high specific activity sample of [^{131}I]-IVdU (Fig. 17). The protein binding of radioactive compounds in the plasma was evaluated by equilibrium dialysis. The protein bound form of radioactivity remained less than 2% of the total activity, suggesting that [^{131}I]-IVdU and its radioactive metabolites existed *in vivo* in unbound form.

The urine samples were collected using a catheter at 2, 4.5, and 8 h after the injection of [^{131}I]-IVdU. The total radioactivity in urine at each time point was quantitated and an aliquot from each sample was analysed by quantitative r-HPLC. The total radioactivity recovered from urine for the three periods and the relative proportions of the radioactive components are shown in Table 13. Less than 8 % of the injected radioactive dose was excreted

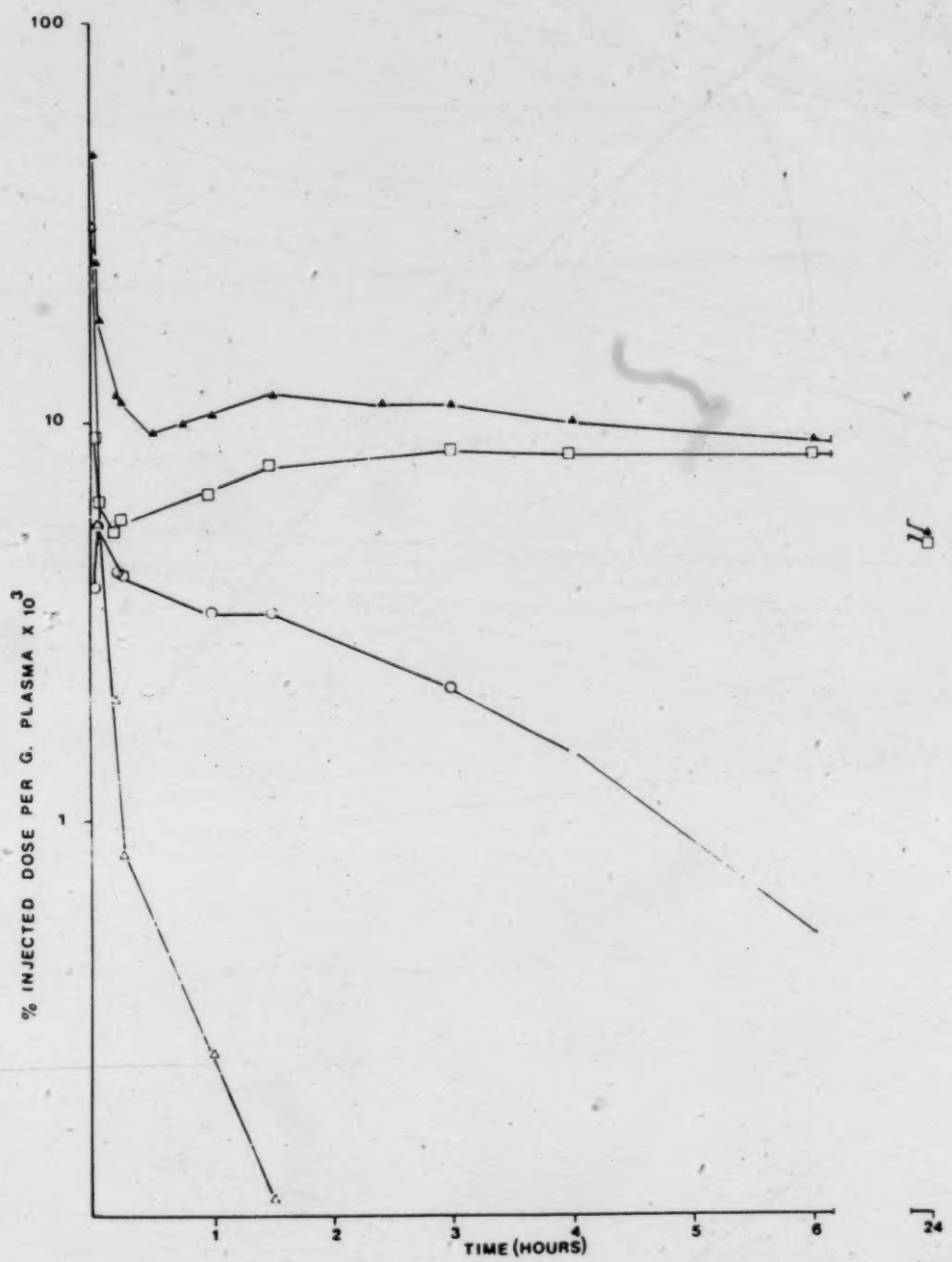

Fig. 17 Metabolites of [^{131}I]-IVdU (specific activity, 37 TBq /mmol) in Dog *In Vivo* (n=1).

▲ Total Radioactivity, △ [^{131}I]-IVdU, ○ [^{131}I]-IVU, □ [^{131}I]-I$^-$.

Table 13. Recovery of the Radioactivity from Urine at Various Times After the i. v. Injection of [^{131}I]-IVdU (mean of two experiments with range)

Time Hours	Radioactivity % Inj. Dose	Radioactive Components (% of the total activity in urine) IVdU	IVU	Iodide	Other
0.0 - 2.0	2.34 ±0.10	43.5 ±4.72	8.50 ±0.11	33.37 ±3.16	13.12 ±0.19
2.0 - 4.5	2.47 ±0.25	5.22 ±3.72	8.86 ±0.80	73.06 ±5.83	13.30 ±1.04
4.5 - 8.0	2.94 ±0.06	1.24 ±0.40	7.34 ±0.18	79.13 ±2.97	12.27 ±2.52

by the kidney during an 8 hour period after intravenous injection.

A comparison of the kinetic data for low and high specific activity samples of [^{131}I]-IVdU (Fig. 16 and 17) suggests a slightly faster rate of clearance of radioactivity from the plasma (in the lower phase of the curve) for the high specific activity compound. The differences in plasma clearance kinetics are of very little importance, considering the 200,000 fold difference in the dose of IVdU administered. The rapid *in vivo* clearance of [^{131}I]-IVdU from plasma corresponds to its distribution in the body, renal excretion and biological transformations to the metabolites [^{131}I]-IVU and radioactive iodide. (Figs.16, 17 and Table 13). The kinetic data correspond to a volume of distribution of about 2 L and a biological half-life of less than 3 minutes. The metabolites, [^{131}I]-IVU and [^{131}I]-iodide, account for most of the radioactivity in the second slow clearance phase. The total radioactivity in the plasma compartment at 1 hour corresponded to about 6.5% of the injected dose, suggesting extensive (possibly nearly uniform) distribution of these metabolites in one or more other body compartments. The increase in free iodide concentration in the plasma even after the virtual disappearance of the intact nucleoside suggests *in vivo* deiodination of the newly formed base [^{131}I]-IVU. The metabolic fate of the radioiodine introduced as [^{131}I]-IVdU *in vivo* is summarised in Fig. 18. The *in vivo* metabolic transformations of [^{131}I]-IVdU are distinctly different from the *in vitro* study since neither [^{131}I]-IVdU nor [^{131}I]-IVU undergo *in vitro* deiodination in blood. The mechanism of the deiodination is not clear. Since IVdU is not phosphorylated to its 5'-monophosphates in uninfected cells, thymidylate synthetase-catalysed dehalogenation of IVdU is unlikely. Such dehalogenations are usually limited to nucleotides (191, 192). Cytochrome P-450-catalysed oxidation of the C-H bond of the carbon atom bearing the halogen is a major route for the metabolism of alkyl halides (233). Metabolic degradations of halogenated alkenes may be mediated by epoxidation (233). It is likely that IVdU and IVU might have undergone dehalogenation by either of the above routes.

The percentage of injected radioactivity recovered from urine (8%) over a period of 8 hours was substantially lower than expected. This data may be compared with the renal

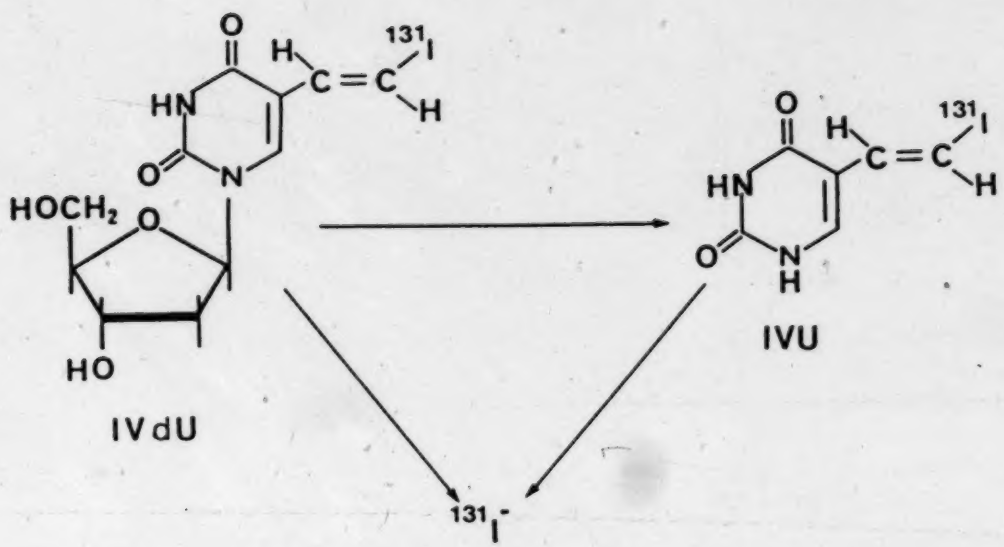

Fig. 18 Schematic Presentation of the Metabolism of [^{131}I]-IVdU in Dogs *in vivo*.

clearance data for [^{131}I]-5-iodo-2'-deoxyuridine in mice where 77.8% of the radioactivity injected was recovered in urine over a period of 8 hours. (234). The renal excretion data for the radioactive components (Table 13) show that the intact nucleoside was the most rapidly excreted major radioactive component. The base (IVU) showed extremely slow renal excretion. Desgranges *et al* recently reported the pharmacokinetics and *in vivo* metabolism of BVdU in mice which demonstrated the persistence of high concentrations of the base (BVU) in plasma over a period of 24 hours (187). This suggests similarities in the excretion behaviour of IVU and BVU. However, the kinetics of the metabolism and excretion of IVdU are more complicated due to deiodination. The possible *in vivo* debromination of BVdU has not been investigated.

The prevention or reversal of undesired *in vivo* metabolic transformations of IVdU would be of great value with respect to its use as a diagnostic agent. Such steps would result in increased bioavailability of the active radiopharmaceutical and faster clearance of the background radioactivity from the blood prior to imaging. The chemical modification of IVdU to develop analogs which are resistant to glycosidic bond cleavage would be one approach. Rosowsky *et al* have recently reported that the 5'-pivaloate of deoxythymidine does not undergo phosphorolytic cleavage by deoxythymidine phosphorylase *in vitro* (235). Deoxythymidine 5'-pivaloate acts as a prodrug of deoxythymidine *in vivo* . Plasma levels of deoxythymidine were significantly higher (about 2.5 times 1 h after a subcutaneous injection) when deoxythymidine was given to mice as the 5'-pivaloate than when it was given as the free nucleoside (236). In view of these results, Lee *et al* have made a preliminary *in vivo* evaluation of the tracer kinetics of [^{131}I]-IVdU-3',5'-diacetate, a prodrug of [^{131}I]-IVdU, in mice (237). The tracer kinetics of [^{131}I]-IVdU-3',5'-diacetate was virtually the same as that for [^{131}I]-IVdU, presumably due to the rapid *in vivo* degradation of the ester to the free nucleoside. This is consistent with the high serum esterase activity reported for mice (238). Studies using [^{131}I]-IVdU-3',5'-diacetate were not continued beyond this point. Another approach to increasing the bioavailability of IVdU would be its regeneration from IVU using

deoxythymidine, in a manner analogous to that reported for BVdU (187). However, preliminary studies in this direction by Lee *et al* showed that tracer kinetics of [^{131}I]-IVdU in mice was virtually unaltered by a subsequent intravenous administration of deoxythymidine (237).

The *in vivo* pharmacokinetic and metabolism studies on [^{131}I]-IVdU suggested that its rapid *in vivo* metabolism may prove to be a limiting factor with respect to its development as a radiopharmaceutical for the diagnosis of HSE.

G. Diagnostic Imaging

The feasibility for *in vivo* use of radiolabeled IVdU as a radiopharmaceutical for HSE was also evaluated by diagnostic imaging in planar and tomographic modes. Rabbits (2 infected and 2 uninfected) were injected i.v with [^{131}I]-IVdU (37 MBq). Planar brain imaging was performed at 30 min, 45 min, 1 h and 6 h after the injection of IVdU. Planar images from an uninfected and an infected rabbit 1 h after injection of [^{131}I]-IVdU are shown in Fig. 19 and 20 respectively. The region of greatest activity in the whole body scintigram was urinary bladder. Uptake in the area corresponding to brain was minimal. None of the images succeeded in differentiating HSV-1-infected from normal brains. This was not surprising in view of the high blood radioactivity observed in the tissue distribution studies, which could obscure any small differences in radiotracer uptake between infected and uninfected brains.

Brain imaging in the tomographic mode (ECT) offers the potential to detect differential uptake in a relatively small region. The radioisotope of iodine most suited for SPECT is ^{123}I. The rapid and efficient methods develped for radioiodination permitted the synthesis of [^{123}I]-IVdU ready for injection (about 37 MBq) in a radiochemical yield of 40%. In view of the rapid *in vivo* metabolism of IVdU, intracarotid injection was chosen as the route of administration of the labeled drug. The injection of drug via common carotid artery would be expected to allow a major portion of the drug to pass through brain at least once before any significant metabolic degradation occurs. The optimum time point for imaging was thought to

Fig. 19 Planar Whole Body Image of an Uninfected Rabbit 1 h After an Intravenous Injection of [^{125}I]-IVdU

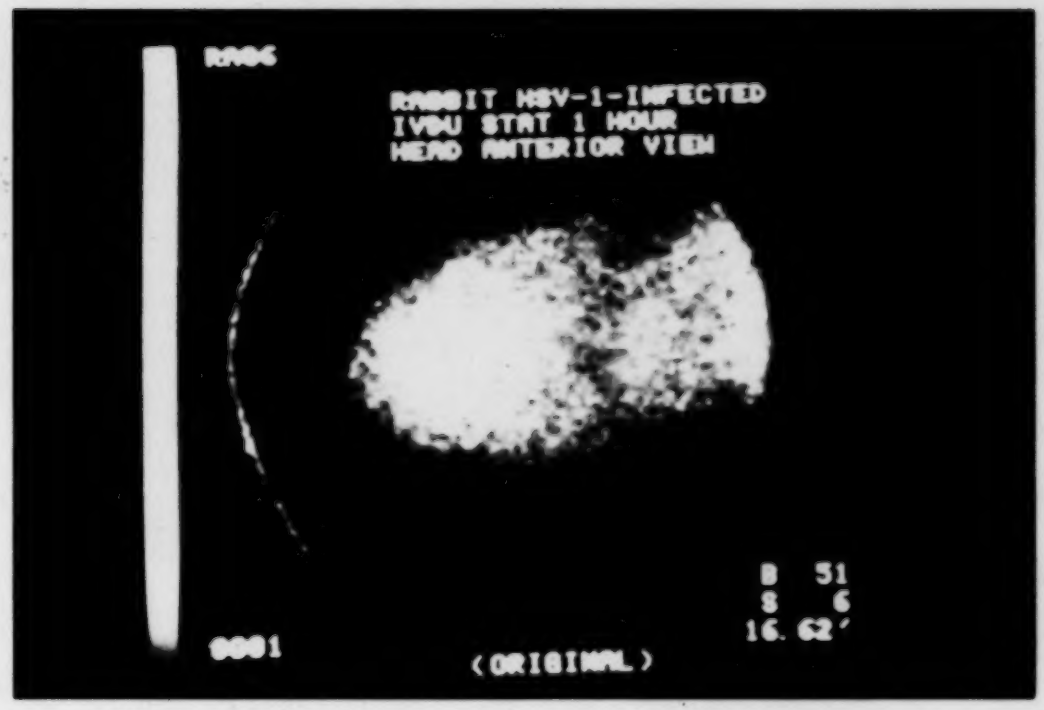

Fig. 20 Planar Image (Head) of an HSV-1-infected Rabbit 1 h After an Intravenous Injection of [^{125}I]-IVdU.

be around 30 min after the injection of [^{123}I]-IVdU for two reasons. First, pharmacokinetic and metabolic studies in dogs suggested that within a period of 2 h after injection of IVdU, blood radioactivity was lowest at 30 min. Second, most of the labeled IVdU was already metabolised at this point. Therefore prolonging the time of imaging beyond this time offers little or no advantage. Brain imaging in the tomographic mode (SPECT) was performed on rabbits (2 normal and 1 infected) over a period of 30 min (20 to 50 min after injection of [^{123}I]-IVdU). The tomographic images clearly showed a 'cold spot' in uninfected animals in the area corresponding to brain (Plate 1). Uptake in the infected rabbit brain was not significantly higher than that of controls (Plate 2). This may be due to several reasons. Two important factors deserve mention. The pharmacokinetic and metabolic studies have indicated that the *in vivo* bioavailability of IVdU is very low with a biological half-life of approximately 3 min in dogs. Any increase in bioavailability of IVdU due to intracarotid administration of the drug is limited to the 'first pass' of the drug through brain. The *in vitro* uptake studies of [^{131}I]-IVdU (section D) have shown that HSV-1-infected cells need to be exposed to radiolabeled nucleoside for a period of 30 min to 1 h before a significantly higher uptake could be detected in infected cells relative to uninfected cells. A second factor is the resolution of the imaging system and its relationship to the size of the animal brain. Although the resolution of SPECT is much higher than that of planar imaging, it is still limited to the order of 1 cm. This presents a problem in brain imaging studies with animals having small brains. It would be more desirable to use a non-human primate such as monkey as the animal model for HSE, since they have brains of larger size.

The tissue distribution, pharmacokinetic and metabolic and brain imaging studies indicate radioiodinated IVdU is not the nucleoside of choice as a radiopharmaceutical for non-invasive diagnosis of HSE. The major limiting factor of this nucleoside appears to be its rapid *in vivo* metabolism. In view of this, the next phase of the investigation was directed towards evaluation of a series of nucleoside analogs with structural features likely to be more resistant to *in vivo* metabolism.

Plate 1.SPECT Images of an Uninfected Rabbit 30 min After an Intracarotid Injection of [^{123}I]-IVdU

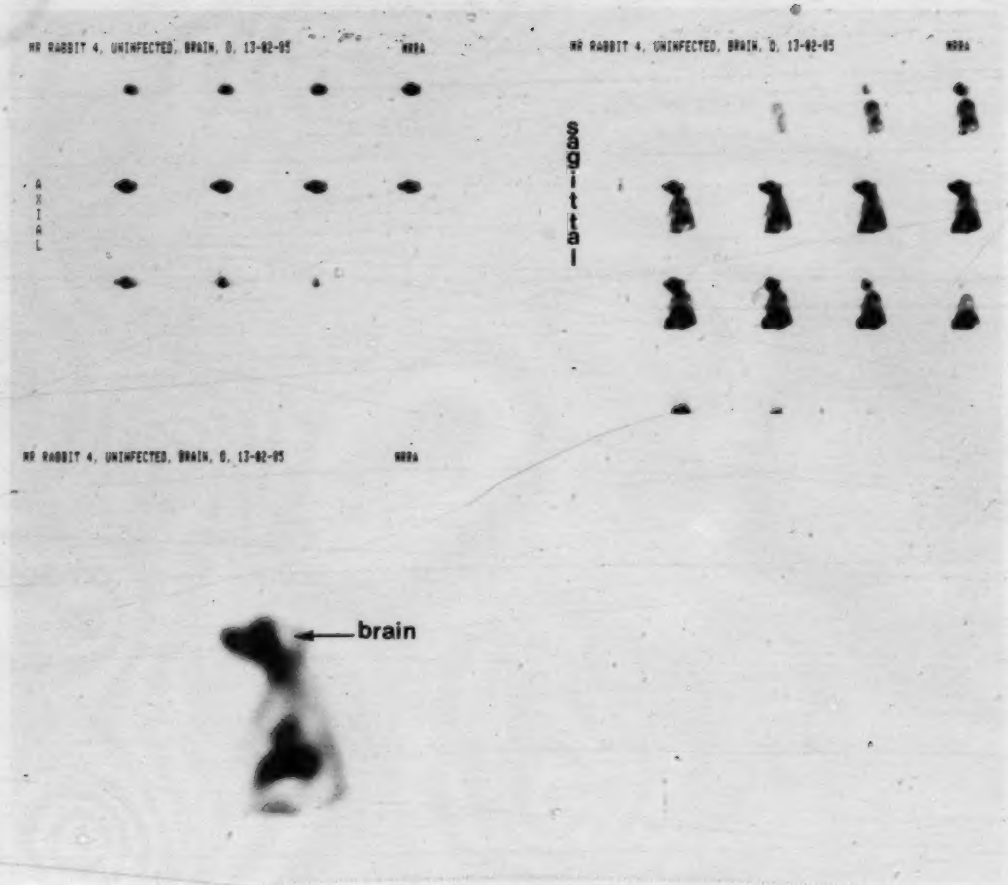
MR RABBIT 4, UNINFECTED, BRAIN, 0, 13-02-95
MRBA
AXIAL
MR RABBIT 4, UNINFECTED, BRAIN, 0, 13-02-95
MRBA
SAGITTAL
MR RABBIT 4, UNINFECTED, BRAIN, 0, 13-02-95
MRBA
brain

Plate 2. SPECT Images of a HSV-1-Infected Rabbit 30 min after an Intracarotid Injection of [^{123}I]-IVdU.

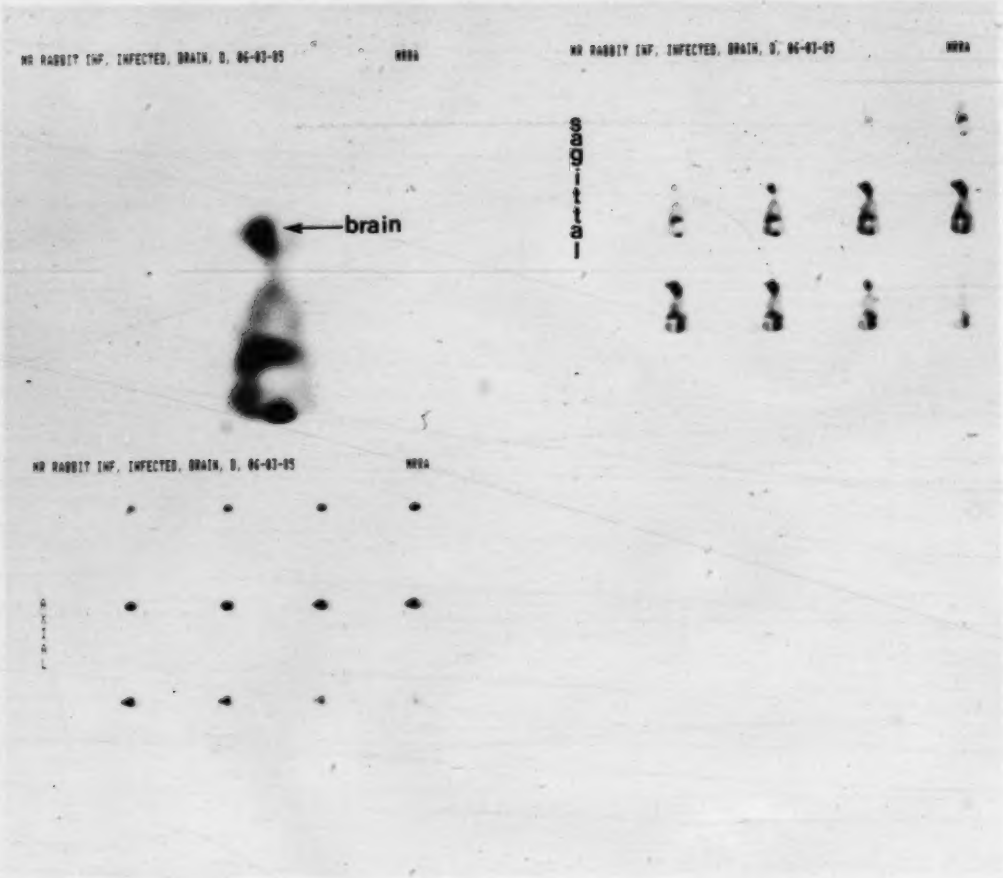
NR RABBIT INF. INFECTED, BRAIN, D, 06-03-05
NRBA
brain
NR RABBIT INF. INFECTED, BRAIN, D, 06-03-05
NRBA
SAGITTAL
NR RABBIT INF. INFECTED, BRAIN, D, 06-03-05
NRBA
AXIAL

H. Quantitative Uptake Studies of Radiolabeled Nucleosides in Herpes Simplex Virus-Infected Cells *In Vitro*

The biochemical aspects of selective antiviral activity for nucleoside analogs has already been discussed in Chapter I. A nucleoside requires the following biochemical characteristics for selective anti-HSV activity:

1. Selective phosphorylation by HSV-encoded TKs to its 5'-monophosphate.
2. Conversion of the nucleoside-5'-monophosphate thus produced to the 5'-diphosphate and then to the 5'-triphosphate by cellular and/or viral kinases.
3. Selective inhibition of HSV-encoded DNA polymerases by the nucleoside-5'-triphosphate.

From these three requirements, only the first characteristic (selective phosphorylation to 5'-monophosphate) is essential for selective metabolic trapping of the nucleoside in HSV-infected cells. Therefore it is plausible that certain nucleosides, which are not potent antiviral agents, may still undergo selective metabolic trapping in HSV-infected cells. This fact is illustrated clearly by the biochemical transformation of BVdU in HSV-2-infected cells *in vivo* (151). BVdU exhibits a 100-1000 times lower activity against HSV-2, relative to HSV-1. However, BVdU is metabolically transformed to BVdU-MP in HSV-1- and HSV-2-infected cells with equal or nearly equal efficiency. The low potency of BVdU against HSV-2 is due to the failure of HSV-2-encoded TK to further phosphorylate BVdU-MP to BVdU-DP as discussed in Chapter I. Thus, antiviral activity is not essential for metabolic trapping of nucleosides in HSV-infected cells. Therefore evaluation of nucleoside analogs as potential radiopharmaceuticals for HSE diagnosis need not be limited to compounds having a potent inhibitory effect on HSV-replication.

The *in vivo* stability of nucleosides is an important factor to be considered in the choice of a radiopharmaceutical for HSE diagnosis. Nucleoside analogs possessing structural features which provide resistance to glycosidic bond cleavage by phosphorylase enzymes offer a distinct advantage in this regard. Deoxythymidine phosphorylase has a high substrate specificity with respect to the 2'-deoxy position (185). Therefore any structural modification at the 2'-position

of a 2'-deoxypyrimidine nucleoside renders it a poor substrate for deoxythymidine phosphorylase. 1-(2-Deoxy-2-fluoro-β-D-arabinofuranosyl)cytosine, 1-(2-deoxy-2-fluoro-β-D-arabinofuranosyl)-5-fluorouracil and 1-(2-deoxy-2-fluoro-β-D-arabinofuranosyl)-5-methyluracil have been shown to have little or no affifnity for the enzymes thymidine phosphorylase and uridine phosphorylase (185). Introduction of a 2'-fluoro substituent (with ribo or arabino configuration) into 2'-deoxyuridine derivatives appears to be a good approach to make them resistant to glycosidic bond cleavage. On this basis, a series of 5-halogenated derivatives of 1-(2-deoxy-2-fluoro-β-D-ribofuranosyl)uracils and 1-(2-deoxy-2-fluoro-β-D-arabinofuranosyl)uracils were selected for preliminary evaluation as potential non-invasive probes for HSE.

The chemical structures for 1-(2-deoxy-2-fluoro-β-D-ribofuranosyl)-5-iodouracil (FIRU, **13**), 1-(2-deoxy-2-fluoro-β-D-ribofuranosyl)-5-bromouracil (FBRU, **14**), 1-(2-deoxy-2-fluoro-β-D-ribofuranosyl)-5-chlorouracil (FCRU, **15**), 1-(2-deoxy-2-fluoro-β-D-ribofuranosyl)-5-fluorouracil (FFRU, **16**), 1-(2-deoxy-2-fluoro-β-D-arabinofuranosyl)-5-iodouracil (FIAU, **17**), 1-(2-deoxy-2-fluoro-β-D-arabinofuranosyl)-5-bromouracil (FBAU, **18**), 1-(2-deoxy-2-fluoro-β-D-arabinofuranosyl)-5-chlorouracil (FCAU, **19**) and 1-(2-deoxy-2-fluoro-β-D-arabinofuranosyl)-5-fluorouracil (FFAU, **20**) are shown in Fig. 21. Compounds **13** to **16** were recently synthesised by Dr. J. R Mercer at the Faculty of Pharmacy, University of Alberta (239). [5-^{131}I]-FIRU, [5-^{77}Br]-FBRU, [2-^{14}C]-FCRU and [2-^{14}C]-FFRU were evaluated as potential diagnostic agents in oncology (239). [2-^{14}C]-FCRU and [2-^{14}C]-FFRU showed selective accumulation in tumor tissue with a tumor to blood ratio of 4.2 and 10.3 at 4 h after injection respectively. Renal excretion studies for [5-^{131}I]-FIRU, [5-^{77}Br]-FBRU, [2-^{14}C]-FCRU and [2-^{14}C]-FFRU in mice indicated that the unmetabolised nucleoside was the major radioactive component present in urine up to 8 h after injection for all four compounds. These results indicated that ribofuranosyl nucleosides **13** to **16** possess high

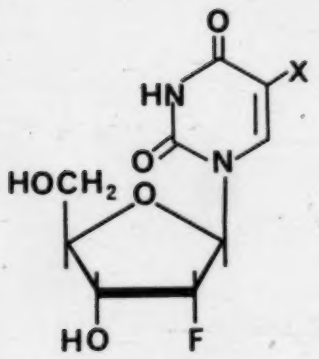

X	Compound	
I	FIRU	13
Br	FBRU	14
Cl	FCRU	15
F	FFRU	16

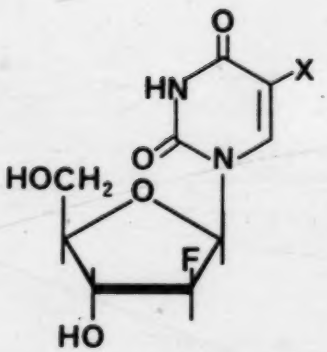

X	Compound	
I	FIAU	17
Br	FBAU	18
Cl	FCAU	19
F	FFAU	20

Fig. 21 Chemical Structures for 1-(2-deoxy-2-fluoro-β-D-ribofuranosyl)-5-halouracils and 1-(2-deoxy-2-fluoro-β-D-arabinofuranosyl)-5-halouracils

in vivo stability (239). The antiviral activity of compounds **13** to **16** has not been reported whereas compounds **17** to **20** have been reported to exhibit pronounced inhibitory activity against HSV-1 (Table 14) (135,240). The biochemical aspects of their (compounds **17** to **20**) antiviral activity have already been discussed in Chapter I. Metabolic studies of the related compounds 1-(2-deoxy-2-fluoro-β-D-arabinofuranosyl)-5-iodocytosine (FIAC) and 1-(2-deoxy-2-fluoro-β-D-arabinofuranosyl)-5-methyluracil (FMAU) have demonstrated resistance to *in vivo* phosphorolytic cleavage (241).

The presence of a halogen atom at the 5-position of the nucleosides **13** to **20** offers the possibility for radiohalogenation. Thus, FFRU and FFAU, if found useful as *in vivo* biochemical probes for HSE, could be labeled with ^{18}F to develop a PET scan for HSE. A radiochemical synthesis of [5-^{18}F]-FFRU has been developed by Dr. J. R. Mercer (239). It is quite likely that this method would also be suitable for the synthesis of [5-^{18}F]-FFAU. FBRU and FBAU, if labeled with ^{75}Br may also hold promise as PET radiopharmaceuticals. Radioiodination reactions suitable for incorporation of ^{123}I into FIRU and FIAU have been developed by Drs. J. R. Mercer (239) and H. K. Misra (242) at the Faculty of Pharmacy, University of Alberta, which offer the possibility for developing SPECT imaging for HSE. At the present time, chlorine isotopes are not used in clinical nuclear medicine. However compounds **15** and **19** may be useful in developing structure activity relationships for the selective uptake of nucleoside analogs by HSV-infected cells.

The selective uptake of compounds **13**, **15**, **16** and **17** has been evaluated in HSV-1-infected cells *in vitro*. Confluent PRK cells in 60 mm-Petri dishes were infected with 6 X 10^6 PFU of HSV-1 (TK^+), HSV-1 (TK^-) or were mock infected. After a 7 h incubation, a known quantity of radiolabeled nucleoside ([5-^{131}I]-FIRU, specific activity 20.4 GBq $mmol^{-1}$, total activity 1.33 KBq ; [2-^{14}C]-FCRU, specific activity 1.86 GBq $mmol^{-1}$, total activity 1.17 KBq ; [2-^{14}C]-FFRU, specific activity 1.86 GBq $mmol^{-1}$, total activity 1.17 KBq ; [5-^{131}I]-FIAU, specific activity 111 GBq $mmol^{-1}$, total activity 1.33 KBq) was added to each Petri dish. The final volume of the media contained in each dish was 2 mL. The Petri dishes

Table 14. *In Vitro* Anti-HSV Activity of Some 5-Halogenated 1-(2-deoxy-2-fluoro-β-D-arabinofuranosyl)uracils (135, 240)

Compound	Anti-HSV-1 Activity ID_{90} (μM) [1]	Cytotoxicity TD_{50} (μM) [2]
FIAU **17**	0.04	0.7
FBAU **18**	0.08	0.7
FCAU **19**	0.2	1.0
FFAU **20**	0.02	0.07

[1] Concentration required to inhibit HSV-1 replication by 90%

[2] Concentration required for 50% inhibition of growth in Vero cells.

were incubated at 37° C until the cells were removed for radioactive counting. Intracellular and extracellular radioactivities were quantitiated at 30 min, 1, 2, 4, 6, 10, and 24 h respectively after addition of the radiolabled nucleoside. Five HSV-1 (TK^+)-infected, four HSV-1 (TK^-)-infected, and four mock-infected dishes were quantitated for the intracellular radioactivity.

The cellular uptake responses for [5-^{131}I]-FIRU, [2-^{14}C]-FCRU, [2-^{14}C]-FFRU and [5-^{131}I]-FIAU are shown in Figs. 22, 23, 24 and 25 respectively. The uptake is presented as a % of the total activity added (mean and range for each time point is shown). The uptake of radiolabeled nucleoside in HSV-1 (TK^+)-infected cells for all four nucleosides increased with increasing time of exposure of cells to the drug for a period of 24 h. Uptake in HSV-1 (TK^-)-infected and mock-infected cells remained low (usually less than 2%) at all times for all four radiolabeled nucleosides evaluated. These results suggest that uptake by HSV-1 (TK^+)-infected cells was selective and mediated by HSV-1-encoded TK. The percent uptake of [5-^{131}I]-FIRU, [2-^{14}C]-FCRU, [2-^{14}C]-FFRU and [5-[^{131}I]]-FIAU in HSV-1 (TK^+)-infected cells for a 4 and 24 h incubation of cells with the nucleoside is shown in Table 15. The nucleoside which demonstrated the highest uptake at the 4 h (27.1%) and 24 h (58.5%)incubation periods was [^{131}I]-FIAU. The rapid and selective uptake of [^{131}I]-FIAU in HSV-1 (TK^+)-infected cells is consistent with the potent anti-HSV activity (ID_{50} 0.1 μM for HSV-1, Table 4) and high affinity of HSV-1-encoded TK (K_i 0.68 μM) reported for FIAU (59). [2-^{14}C]-FFRU showed the lowest percent uptake both at 4 h (7.8%)and 24 h (17.7%).

The uptake studies of radiolabeled nucleosides in HSV-infected cells *in vitro* is intended to be first of several screening tests designed to identify a nucleoside analog having optimal biological characteristics suitable as a radiopharmaceutical for HSE diagnosis. Subsequent screening tests proposed include *in vitro* metabolism by blood platelets, *in vivo* pharmacokinetic and metabolism studies, tissue distribution and quantitative autoradiographic studies in HSV-1-infected animal models and tomographic brain imaging in a non-human primate model such as the monkey. The final stage of these investigations is expected to be the clinical

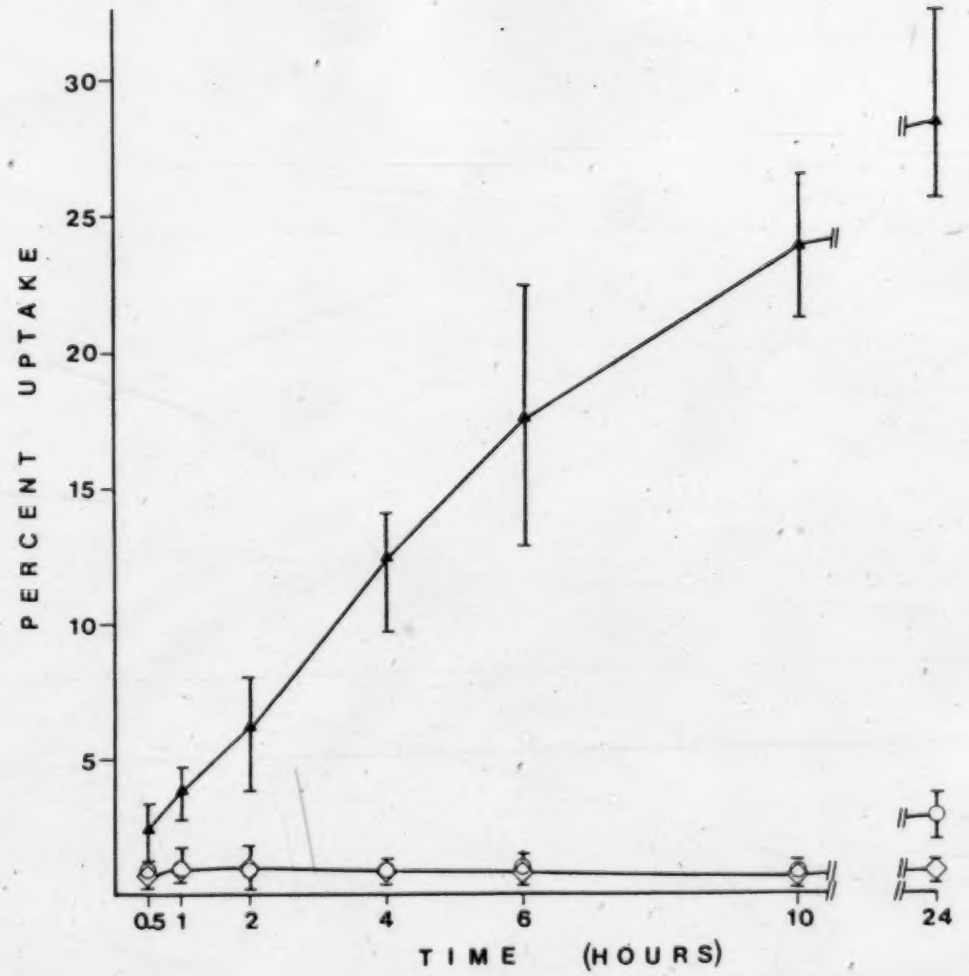

Fig. 22 *In Vitro* Uptake of [5-^{131}I]-FIRU in HSV-1 (TK$^+$) (n=5) (▲), HSV-1 (TK$^-$) (n=4) (○), and Mock-Infected Cells (n=4) (◇) (Mean and Range)

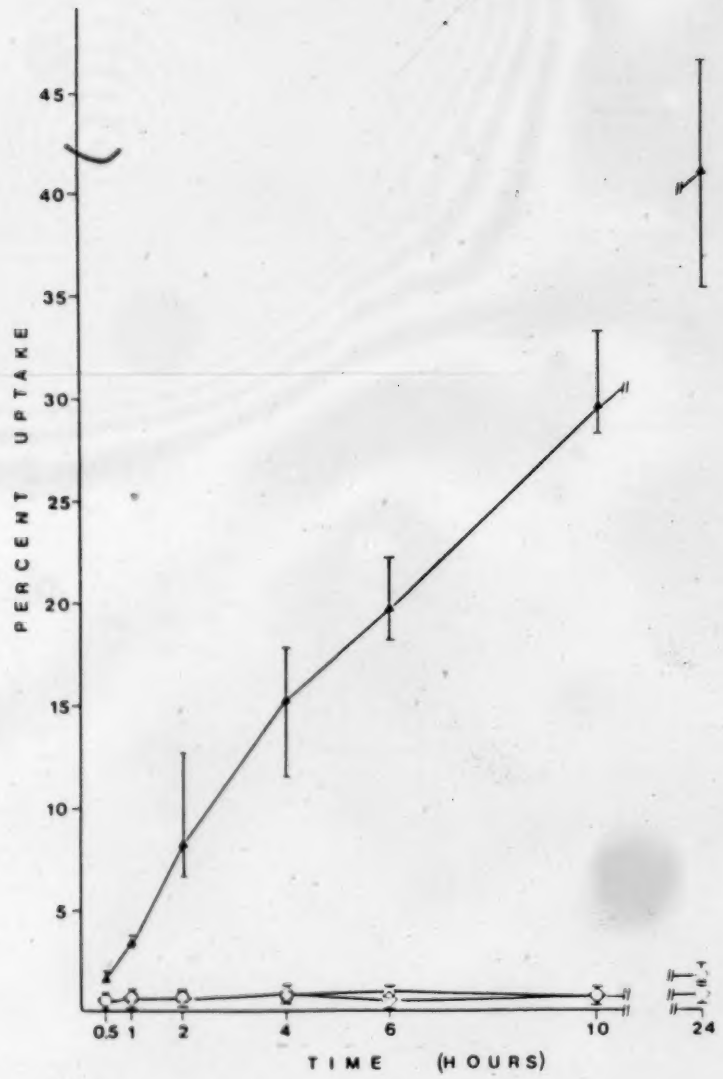

Fig. 23 *In Vitro* Uptake of [2-^{14}C]-FCRU in HSV-1 (TK$^-$) (n=5) (▲), HSV-1 (TK$^-$) (n=4) (○), and Mock-Infected Cells (n=4) (□) (Mean and Range)

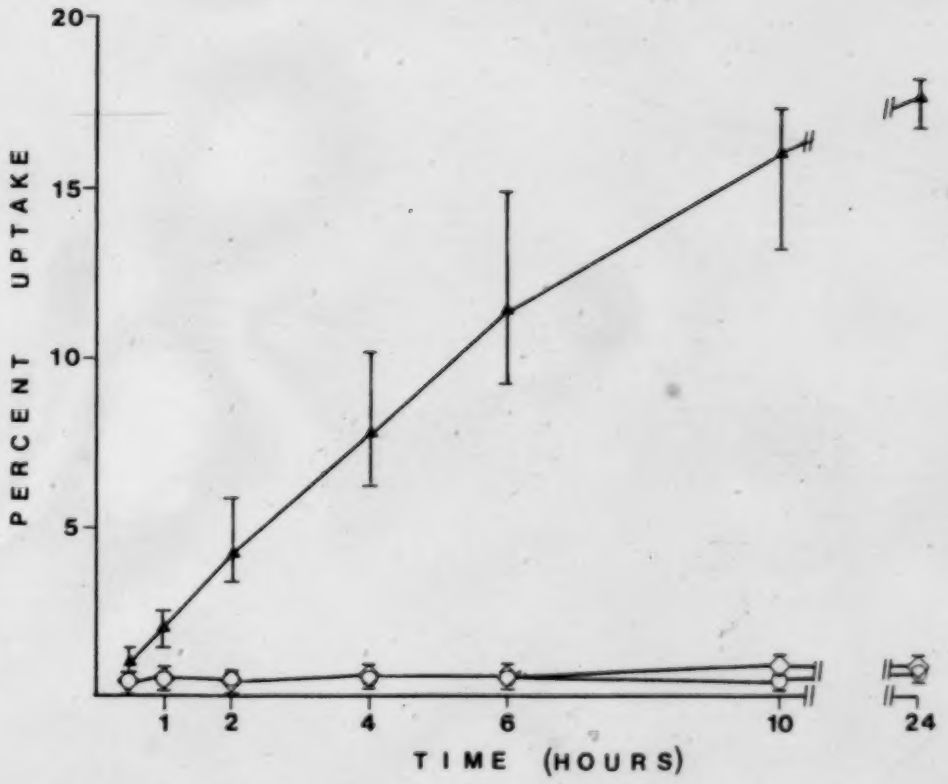

Fig. 24 *In Vitro* Uptake of [2-^{14}C]-FFRU in HSV-1 (TK$^-$) (n=5) (▲), HSV-1 (TK$^-$) (n=4) (○), and Mock-Infected Cells (n=4) (□) (Mean and Range)

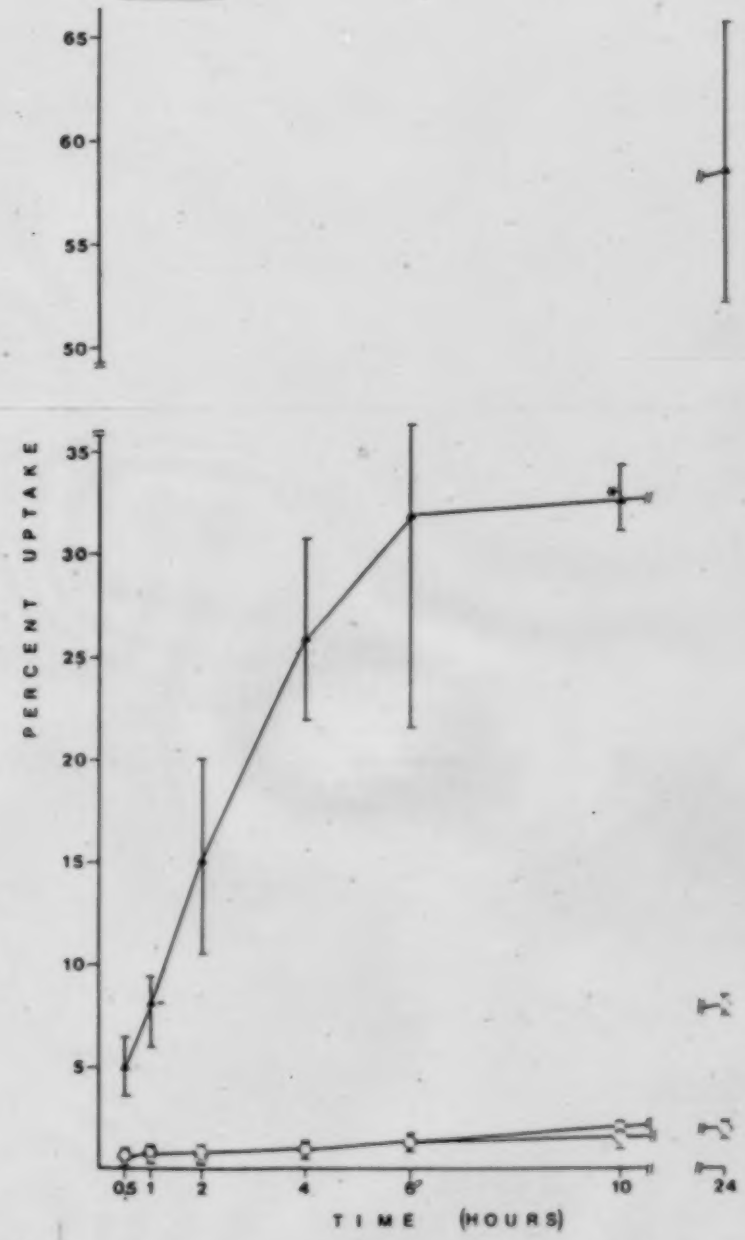

Fig. 25 *In Vitro* Uptake of [5-^{131}I]-FIAU in HSV-1 (TK$^-$) (n=5) (▲), HSV-1 (TK$^-$) (n=4) (○), and Mock-Infected Cells (n=4) (□) (Mean and Range)

• n = 2

Table 15. Percent Uptake of Radiolabeled Nucleoside Analogs in HSV-1 (TK^+)-Infected cells at 4 h and 24 h (Mean and Range, $n=5$)

Compound	Percent Uptake	
	4 h	24 h
[5-^{131}I]-FIRU **13**	12.5 (9.8-14.1)	28.5 (25.6-32.5)
[2-^{14}C]-FCRU **15**	15.3 (11.4-17.9)	41.0 (25.3-46.3)
[2-^{14}C]-FFRU **16**	7.8 (6.2-10.2)	17.7 (16.7-18.1)
[5-^{131}I]-FIAU **17**	27.1 (22.1-31.0)	58.5 (52.1-66.1)

evaluation of the nucleoside(s), showing most favourable characteristics in these screening tests, in HSE patients using tomographic brain imaging.

IV. SUMMARY AND CONCLUSIONS

The aim of this study was to develop radiohalogenated nucleoside analogs as non-invasive diagnostic agents for HSE. Investigations in this direction included chemical and radiochemical syntheses of nucleosides, *in vitro* uptake studies of radiolabeled nucleosides in HSV-infected cells, and *in vivo* evaluation of a radiolabeled nucleoside involving tissue distribution, pharmacokinetic, metabolic and diagnostic imaging studies in animal models.

The objectives of the chemical syntheses were to prepare nucleoside analogs as reference compounds for radiochemical and metabolism studies and to explore synthetic routes suitable for radiochemical syntheses. IVdU and BVdU were synthesised from (*E*)-5-(2-carboxyvinyl)-2'-deoxyuridine using the N-halosuccinimide method in 30.4 and 42% yield respectively. Alternatively, IVdU and BVdU were also prepared by the chloramine-T method (26.3 and 18% respectively), a procedure suitable for radiochemical syntheses. The products obtained using the chloramine-T method were shown to be identical to the corresponding compound obtained employing the N-halosuccinimide method. IVdU-3',5'-diacetate was prepared from (*E*)-5-(2-carboxyvinyl)-2'-deoxyuridine-3',5'-diacetate using the N-iodosuccinimide method in 41.0% yield. (*E*)-5-(2-iodovinyl)uracil (IVU) was prepared from (*E*)-5-(2-carboxyvinyl)uracil employing the chloramine-T method in 10.0% chemical yield. The identity of all compounds described above was established by spectroscopic analysis (^{1}H NMR, UV and MS).

The two reactions investigated for the synthesis of radioiodinated IVdU were the chloramine-T and halogen isotope exchange method. [^{131}I, ^{125}I, and ^{123}I]-IVdU were synthesised by the chloramine-T method (30 min to 1 h reaction time, 40.7 to 67.2% radiochemical yield, 57 to 69.0% chemical yield). The synthesis of [^{131}I]-IVdU using the halogen isotope exchange method required a longer reaction time (20 h) and gave lower yields (45.1% radiochemical yield and 54.3% chemical yield). The halogen isotope exchange method is limited to the preparation of low and medium specific activity compounds and is not suitable

for ^{123}I synthesis. [^{131}I]-IVdU-3',5'-diacetate was synthesised by the chloramine-T method in 50% radiochemical yield. [^{82}Br]-BVdU was synthesised by the chloramine-T method (10 min reaction time, 69.8% radiochemical yield, 72% chemical yield). The chloramine-T method employed for radiobromination is suitable for the synthesis of [^{75}Br]-BVdU. [^{82}Br]-BVdU was also prepared by direct neutron activation of BVdU containing natural abundance bromine (^{79}Br and ^{81}Br) (30.0% radiochemical yield and 97.0% chemical recovery, specific activity 31.82 MBq $mmol^{-1}$). The direct neutron activation of BVdU is limited to the low specific activity synthesis of [^{82}Br]-BVdU.

Quantitative uptake studies of [^{131}I]-IVdU in HSV-infected cells *in vitro* demonstrated selective trapping of [^{131}I]-IVdU in HSV-1 (TK^+)-infected cells. The uptake was dependent on the duration of exposure of cells to [^{131}I]-IVdU, the infecting dose of the virus, and the concentration of [^{131}I]-IVdU in the medium. The observation that the exposure of cells to [^{131}I]-IVdU for 30 min to 1 h was sufficient to differentiate the HSV-1 (TK^+)-infected cells from HSV-1 (TK^-)- and mock-infected cells suggested that a nucleoside analog having a relatively fast excretion or metabolism may be used as a radiopharmaceutical for the diagnosis of HSE. The effect of the virus infecting dose on the uptake of [^{131}I]-IVdU suggested that at least 1 in 50 cells need to be infected with HSV-1 before an infected brain could be differentiated from a normal brain by using a radiolabeled nucleoside. The effect of increasing concentrations of [^{131}I]-IVdU on its uptake suggested that a medium specific activity sample of radiolabeled nucleoside may be satisfactorily used as a radiopharmaceutical for HSE diagnosis.

Tissue distribution studies for [^{125}I]-IVdU in a rabbit model showed 5.4 to 6.4 times higher uptake in HSV-1-infected brain relative to uninfected brain 1 h after i.v. injection of the drug. However, radioactivity in blood was 2 to 10 times higher than that in brain at 1 h. This presents a problem in diagnostic imaging since the high blood activity may obscure any selective uptake in the infected brain.

Pharmacokinetic and metabolic studies for [^{131}I]-IVdU in dogs have shown a very rapid metabolic degradation of [^{131}I]-IVdU. The major catabolic pathway of [^{131}I]-IVdU in blood *in*

vitro was phosphorolysis of the nucleoside to the corresponding base [^{131}I]-IVU (73% of the total radioactivity in blood at 2 h). The major radioactive components resulting from *in vivo* metabolism of [^{131}I]-IVdU were [^{131}I]-IVU and [^{131}I]-iodide. Both [^{131}I]-IVdU and [^{131}I]-IVU appeared to undergo deiodination *in vivo*. The biological half-life of [^{131}I]-IVdU was less than 3 min. [^{131}I]-IVdU-3',5'-diacetate, in preliminary *in vivo* evaluation, did not demonstrate any advantage over [^{131}I]-IVdU with respect to pharmacokinetic characteristics. The renal excretion of the radioactivity was extremely slow (8% of the total radioactivity was recoverd in urine over a period of 8 h). The rapid *in vivo* metabolism of [^{131}I]-IVdU into radioactive components having slow excretion characteristics suggested that radioiodinated IVdU is unlikely to be useful as a brain imaging agent for the diagnosis of HSE.

A series of radiolabeled 1-(2-deoxy-2-fluoro-β-D-ribofuranosyl)-5-halouracils and 1-(2-deoxy-2-fluoro-β-D-arabinofuranosyl)-5-halouracils (halogen = I, Br, Cl, F) have been proposed as potential candidates for preliminary evaluation as radiopharmaceuticals for HSE. Quantitative *in vitro* uptake studies for [5-^{131}I]-1-(2-deoxy-2-fluoro-β-D-ribofuranosyl)-5-iodouracil (FIRU), [2-^{14}C]-1-(2-deoxy-2-fluoro-β-D-ribofuranosyl)-5-chlorouracil (FCRU), [2-^{14}C]-1-(2-deoxy-2-fluoro-β-D-ribofuranosyl)-5-fluorouracil (FFRU), and [5-^{131}I]-1-(2-deoxy-2-fluoro-β-D-arabinofuranosyl)-5-iodouracil (FIAU) have demonstrated selective uptake of all four compounds in HSV-1 (TK$^+$)-infected cells. The highest uptake was shown by [5-^{131}I]-FIAU (27.1% at 4 h and 58.5% at 24 h).

Based on these investigations a general outline may be drawn for the evaluation of radiolabeled nucleoside analogs as non-invasive diagnostic agents for HSE.

1. *In vitro* uptake studies in HSV-infected cells.
2. *In vitro* evaluation of phosphorolysis using whole blood or blood platelets.
3. *In vivo* pharmacokinetic and metabolic studies.
4. Tissue distribution quantitative autoradiographic studies in a HSE animal model such as rabbits or rats

5. Diagnostic imaging in the tomographic mode in an HSE animal model having a large brain (eg: monkey)

These screening procedures would be expected to identify the nuleoside(s) having favourable biological characteristics suitable for a radiopharmaceutical for the diagnosis of HSE.

REFERENCES

1. **Moore, G. E.** 1948. Use of radioactive diiodofluorescein in the diagnosis and localization of brain tumors. *Science* **107**:569-571.

2. **Cassen, B., L. Curtis, and C. Reed.** 1950. A sensitive directional gamma ray detector. *Nucleonics* **6**:78-81

3. **Cassen, B., L. Curtis, C. Reed, and R. Libby.** 1951. Instrumentation for ^{131}I use in medical studies. *Nucleonics* **9**:46-50.

4. **Newell, R. R., W. Saunders, and E. Miller.** 1952. Multichannel collimators for gamma ray scanning with scintillation counters. *Nucleonics* **10**:36-40.

5. **Anger, H. O.** 1958. Scintillation camera. *Rev. Scient. Instrum.* **29**:27-33.

6. **Harper, P. V., R. Beck, D. Charleston, and K. A. Lathrop.** 1964. Optimization of a scanning method using Tc-99m. *Nucleonics* **22**:50-54.

7. **Kuhl, D. E., and R. Q. Edwards.** 1963. Image separation radioisotope scanning. *Radiology* **80**:653-662.

8. **Hounsfield, G. N.** 1973. Computerized transverse axial scanning (tomography). Part 1. Description of system. *Brit. J. Radiol.* **46**:1016-1022

9. **Ambrose, J.** 1973. Computerized transverse axial scanning (tomography): Part 2. Clinical application. *Brit. J. Radiol.* **46**:1023-1047

10. **Ter-Pergossian, M. M.** 1977. Basic principles of computed axial tomography. *Sem. Nucl. Med.* **7**:109-127.

11. **Hendee, W. R.** 1983. The physical principles of computed tomography, p 1-192. Little, Brown and Company, Toronto.

12. **Phelps, M. E.** 1977. What is the purpose of emission computed tomography in nuclear medicine. *J. Nucl. Med.* **18**:399-401.

13. **Shaw Dunn, J., and G. M. Wyburn.** 1972. The anatomy of the blood brain barrier : a review. *Scot. Med. J.* **17**:21-36.

14. **Phelps, M. E.** 1981. Positron computed tomography studies of cerebral glucose metabolism in man : theory and application in nuclear medicine. *Sem. Nucl. Med.* **11**:32-49.

15. **Bidder, T. G.** 1968. Hexose translocation across blood-brain interface : configurational aspects. *J. Neurochem.* **15**:867-874.

16. **Oldendorf, W. H.** 1971. Brain uptake of radiolabeled aminoacids, amines, and hexoses after arterial injection. *Am. J. Physiol.* **221**:1629-1638.

17. **Garnett, E. S., G. Firnau, F. C. Nahmias, S. Sood, and L. Belbeck.** 1980. Blood-brain barrier transport and cerebral utilization of dopa in living monkeys. *Am. J. Physiol.*

238:R318-R327.

18. **Garnett, E. S., G. Firnau, and F. C. Nahmias.** 1983. Dopamine visualised in the basal ganglia of the living man. *Nature* **305**:137-138.

19. **Levin, V. A.,** 1980. Relationship of octanol/water partition coefficient and molecular weight to rat brain capillary permeability. *J. Med. Chem.* **23**:682-684.

20. **Dischino, D., M. J. Welch, M. R. Kilbourn, and M. E. Raichle.** 1983. Relationship between lipophilicity and brain extraction of ^{11}C-labeled radiopharmaceuticals. *J. Nucl. Med.* **24**:1030-1038.

21. **Phelps, M. E., S. C. Huang, E. J. Hoffman, C. Selin, L. Sokoloff, and D. E. Kuhl.** 1979. Tomographic measurement of local cerebral glucose metabolic rate in humans with [^{18}F]-2-fluoro-2-deoxy-D-glucose : validation of method. *Ann. Neurol.* **6**:371-388.

22. **Gallagher, B. M., J. S. Fowler, N. I. Gutterson, R. R. MacGregor, C.-N. Wang, and A. P. Wolf.** 1978. Metabolic trapping as a principle of radiopharmaceutical design : some factors responsible for the biodistribution of [^{18}F]-2-deoxy-2-fluoro-D-glucose. *J. Nucl. Med.* **19**:1154-1161.

23. **Bessell, E. M., A. B. Foster, and J. H. Westwood.** 1972. The use of deoxyfluoro-D-glucopyranoses in a study of yeast hexokinase specificity. *Biochem. J.* **128**:199-204.

24. **Bessell, E. M., and P. Thomas.** 1973. The effect of substitution of C-2 of D-glucose-6-phosphate on the rate of dehydrogenation by glucose phosphate dehydrogenase (from yeast and from rat liver). *Biochem. J.* **131**:83-89.

25. **Bessell, E. M., and P. Thomas.** 1973. The deoxyfluoro-D-glucopyranose-6-phosphates and their effect on yeast glucose phosphate isomerase. *Biochem. J.* **131**:77-82.

26. **Hers, H. G., and C. De Duve.** 1950. Le systeme phosphatasique : repartition de l'activit'e glucose-6-phosphatasique dan les tissus. *Bull. Soc. Chem. Biol.* **32**:20-29.

27. **Raggi, F., D. S. Kronfeld, and M. Kleiber.** 1960. Glucose-6-phosphatase activity in various sheep tissues. *Proc. Soc. Exp. Biol. Med.* **105**:485-486.

28. **Sokoloff, L.** 1981. Localization of functional activity in the central nervous system by measurement of glucose utilization with radioactive deoxyglucose. *J. Cereb. Blood Flow Metabol.* **1**:7-36.

29. **Alavi, A., M. Reivich, J. H. Greenberg, and A. P. Wolf.** 1982. Positron emission tomography of the brain, p. 134-187. *In* P. J. Ell, and B. L. Holman (ed.), Computed Emission Tomography. Oxford University Press, New York.

30. **Comar, D., E. Zarifan, M. Verhas, F. Soussaline, M. Maziere, G. Berger, H. Loo, H. Cuche, C. Kellershohn, and P. Deniker.** 1979. Brain distribution and kinetics of ^{11}C-chlorpromazine in schizophrenics : positron emission tomography studies. *Psychiat. Res.* **1**:23-29.

31. **Comar, D., M. Mazierie, J. M. Godot, G. Berger, F. Soussaline, C. H. Menini, G. Artel, and G. Naguet.** 1979. Visualization of ^{11}C-flunitrazepam displacement in the brain of the live baboon. *Nature* **280**:329-331.

32. **Rosen, B. R., and T. J. Brady.** 1983. Principles of nuclear magnetic resonance for medical application. *Sem. Nucl. Med.* **13**:308-318.

33. **Buonanno, F. S., J. P. Kristler, L. D. De Witt, K. R. Davis, R. De Lapaz, P. F. J. New, C. T. Burt, and T. J. Brady.** 1983. Nuclear magnetic imaging in central nervous system diseases. *Sem. Nucl. Med.* **13**:329-338.

34. **Fenner, F.** 1976. The classification and nomenclature of viruses. Summary of results of meetings of the international committee on taxonomy of viruses in Madrid, September 1975. *Virology* **71**:371-378.

35. **Roizman, B.** 1965. An enquiry into the mechanism of recurrent herpes infections of man. *Perspect. Virol.* **4**:283-301.

36. **Baringer, J. R.** 1975. Herpes virus infections of nervous tissue in animals and man. *Progr. Med. Virol.* **20**:1-26.

37. **Stevens, J. G.** 1975. Latent herpes simplex virus and nervous system. *Curr. Top. Microbiol. Immunol.* **70**:31-50

38. **Klein, R. J.** 1976. Pathogenetic mechanisms of recurrent herpes simplex virus infections. *Arch. Virol.* **51**:1-13.

39. **Klein, R. J.** 1982. The pathogenesis of acute, latent and recurrent herpes simplex virus infections. *Arch. Virol.* **72**:143-168.

40. **Cook, M. J., and J. G. Stevens.** 1973. Pathogenesis of herpetic neuritis and ganglionitis in mice : evidence of intra-axonal transport of infection. *Infect. Immun.* **7**:272-288.

41. **Kristensson, K., B. Ghetti, and H. M. Wisnieski.** 1974. Study on the propagation of herpes simplex virus (type 2) into the brain after intraocular injection. *Brain Res.* **69**:189-201.

42. **Kristensson, K., A. Vahlne, L. A. Persson, and E. Lycke.** 1978. Neural spread of herpes simplex virus type 1 and 2 in mice after corneal or subcutaneous (footpad) inoculation. *J. Neurol. Sci.* **35**:331-340.

43. **Cook, M. L., and J. G. Stevens.** 1976. Latent herpetic infections following experimental viremia. *J. Gen. Virol.* **31**:75-80.

44. **Field, H. J., and T. J. Hill.** 1974. The pathogenesis of pseudorabies in mice following peripheral inoculation. *J. Gen. Virol.* **23**:145-157.

45. **Ritchie, D. A., and M. C. Timburry.** 1980. Herpes viruses and latency : possible relevance of the structure of the viral genome. *FEMS Microbiol. Letters* **9**:67-72.

46. **Wheeler, C. E.** 1975. Pathogenesis of recurrent herpes simplex infections. *J. Invest. Dermatol.* **64**:341-346.

47. **Hill, T. J., and W. A. Blyth.** 1976. An alternate theory of herpes simplex recurrence and a possible role of prostaglandins. *Lancet* **i**:397-398.

48. **Blyth, W. A., T. J. Hill, H. J. Field, and D. A. Harbour.** 1976. Reactivation of herpes simplex infection by ultraviolet light and possible involvement of prostaglandins. *J. Gen.*

Virol. **33**:547-550.

49. **Harbour, D. A., W. A. Blyth, and T. J. Hill.** 1978. Prostaglandins enhance spread of herpes simplex virus in cell cultures. *J. Gen. Virol.* **41**:87-95.

50. **Kit, S., W.-C. Leung, G. N. Jorgensen, D. Trakula, and D. R. Dubbs.** 1975. Viral-induced thymidine kinase isoenzymes. *Progr. Med. Virol.* **21**:13-34.

51. **Kit, S., W.-C. Leung, and D. Trakula.** 1974. Properties of thymidine kinase enzymes isolated from mitochondrial and cytosolic fractions of normal, bromodeoxyuridine-resistant, and virus-infected cells, p. 103-145. *In* M. A. Mehlman, and R. W. Hanson (ed.), Control Processes in Neoplasia. Academic Press Inc., New York.

52. **Kit, S., W.-C. Leung, G. N. Jorgensen, and D. R. Dubbs.** 1974. Distinctive properties of thymidine kinase isoenzymes induced by human and avian herpesviruses. *Int. J. Cancer* **14**:598-610.

53. **Cheng, Y.-C.** 1976. Deoxythymidine kinase induced by Hela TK^- cells by herpes simplex virus type 1 and type 2. Substrate specificity and kinetic behaviour. *Biochim. Biophys. Acta* **452**:370-381.

54. **Lee, L.-S., and Y.-C. Cheng.** 1976. Human deoxythymidine kinase I. Purification and general properties of the cytoplasmic and mitochondrial isoenzymes derived from blast cells of acute myelocytic leukemia. *J. Biol. Chem.* **251**:2600-2604.

55. **Cheng, Y. C., and M. Ostrander.** 1976. Deoxythymidine kinase induced in Hela TK^- cells by herpes simplex virus type I and type II. Purification and characterization. *J. Biol. Chem.* **251**:2605-2610.

56. **Lee, L.-S., and Y.-C. Cheng.** 1976. Human deoxythymidine kinase II : substrate specificity and kinetic behaviour of the cytoplasmic and mitochondrial isoenzymes derived from blast cells of acute myelocytic leukemia. *Biochemistry* **15**:3686-3690.

57. **Thouless, M. E., and P. Wildy.** 1975. Deoxypyrimidine kinases of herpes simplex virus type 1 and 2 : comparison of serological and structural properties. *J. Gen. Virol.* **26**:159-170.

58. **Orgino, T., R. Shiman, and F. Rapp.** 1973. Deoxythymidine kinase from rabbit cells infected with herpes simplex type 1 or type 2. *Intervirology* **1**:80-95.

59. **Cheng, Y.-C., G. Dutschman, J. J. Fox, K. A. Watanabe, and H. Machida.** 1981. Differential activity of potential antiviral nucleoside analogs on herpes simplex virus-induced and human cellular thymidine kinases. *Antimicrob. Agents Chemother.* **20**:420-423.

60. **Cheng, Y.-C., G. Dutschamn, E. De Clercq, A. S. Jones, S. G. Rahim, G. Verhelst, and R. T. Walker.** 1981. Differential affinities of 5-(2-halogenovinyl)-2'-deoxyuridines for deoxythymidine kinases of various origins. *Mol. Pharmacol.* **14**:2159-2169.

61. **De Clercq, E.** 1984. Biochemical aspects of selective antiherpes activity of nucleoside analogues. *Biochem. Pharmacol.* **33**:2159-2169.

62. **Murphree, S., E. C. Moore, and P. T. Beall.** 1968. Regulation by nucleotide of the activity of partially purified ribonucleotide reductase from rat embryos. *Cancer Res.*

28:860-863.

63. **Skoog, L., and B. Nordenkjold.** 1971. Effects of hydroxyurea and 1-β-D-arabinofuranosyl cytosine in deoxyribonucleotide pools in mouse embryo cells. *Eur. J. Biochem.* **19**:81-89.

64. **Averett, D. R., C. Lubbers, G. B. Elion, and T. Spector.** 1983. Ribonucleotide reductase induced by herpes simplex type 1 virus. Characterization of a distinct enzyme. *J. Biol. Chem.* **258**:9831-9838.

65. **Bachetti, S., M. J. Evelegh, B. Muirhead, C. S. Sartori, and H. Huszar.** 1984. Immunological characterization of herpes simplex virus type 1 and 2 polypeptide(s) involved in viral ribonucleotide reductase activity. *J. Virol.* **49**:591-593.

66. **Field, H. J., and P. Wildy.** 1978. The pathogenicity of thymidine kinase-deficient mutants of herpes simplex virus in mice. *J. Hyg.* **81**:267-274.

67. **Tenser, R. B., R. L. Miller, and F. Rapp.** 1979. Trigeminal ganglion infection by thymidine kinase-negative mutants of herpes simplex virus. *Science* **205**:915-917.

68. **Tenser, R. B., S. Ressel, and M. E. Dunstan.** 1981. Herpes simplex virus thymidine kinase expression in trigeminal ganglion infection : correlation of enzyme activity with ganglion virus titer and evidence of *in vivo* complimention. *Virology* **112**:328-341.

69. **Weissbach. A.** 1977. Eucaryotic DNA polymerases. *Ann. Rev. Biochem.* **46**:25-47.

70. **Sarangadharan, M. G., M. Robert-Guroff, and R. C. Gallo.** 1978. DNA polymerases of normal and neoplastic mammalian cells. *Biochim. Biophys. Acta* **516**:419-487.

71. **Weissbach, A., S.-C. L. Hong, J. Aucker, and R. Muller.** 1973. Characterization of herpes simplex virus-induced deoxyribonucleic acid polymerase. *J. Biol. Chem.* **248**:620-627.

72. **Ostrander, M., and Y.-C. Cheng.** 1980. Properties of herpes simplex virus type 1 and type 2 DNA polymerases. *Biochim. Biophys. Acta.* **609**:232-245.

73. **Powell, K. L., and D. J. M. Purifoy.** 1977. Non-structural proteins of herpes simplex virus I. Purification of the induced DNA polymerase. *J. Virol.* **24**:618-626.

74. **Kier, H. M., J. Hay, J. M. Morrison, and J. H. Subaksharpe.** 1966. Altered properties of deoxyribonucleic acid nucleotidyl transferase after infection of mammalian cells with herpes simplex virus. *Nature* **210**:369-371.

75. **Mao, J. C.-H., E. E. Robinshaw, and L. R. Overby.** 1975. Inhibition of DNA polymerase from herpes simplex virus-infected Wi-38 cells by phosphonoacetic acid. *J. virol.* **15**:1281-1283.

76. **Aron, G. M., D. J. M. Purifoy, and P. A. Schaffer.** 1975. DNA synthesis and DNA polymerase activity of herpes simplex virus type 1 temperature sensitive mutants. *J. Virol.* **16**:498-507.

77. **Meyer, Jr. H. M., R. T. Johnson, I. P. Crawford, H. E. Dascomb, and N. G. Rogers.** 1960. Central nervous system syndromes of "viral" aetiology - a study of 713 cases. *Am. J. Med.* **29**:334-347.

78. **Whitley, R. J., S.-J. Soong, C. Linneman, C. Liu, G. Pazin, C. A. Alford, and the**

National Institute of Allergy and Infectious Diseases (NIAID) Collaborative antiviral study group. 1982. Herpes simplex encephalitis : clinical assesment. *J. Am. Med. Assoc.* **15**:317-320.

79. **Nahmias, A. J., R. J. Whitley, A. N. Vinstine, Y. Takei, C. A. Alford, and NIAID Collborative study group.** 1982. Herpes simplex virus encephalitis : laboratory evaluation and their diagnostic significance. *J. Infect. Dis.* **145**:829-836.

80. **Oommen, K. J., P. C. Johnson, and C. J. Ray.** 1982. Herpes simplex type 2 virus encephalitis presenting as psychosis. *Am. J. Med.* 73:445-448.

81. **Whitley, R. J., A. J. Nahmias, S.-J. Soong, G. G. Galasso, C. L. Fleming, and C. A. Alford.** 1980. Vidarabine therapy of neonatal herpes simplex virus infection. *Pediatrics* **66**:495-501.

82. **Whitley, R. J., S.-J. Soong, R. Dolin, G. J. Galasso, L. T. Chien, C. A. Alford, and the Collaborative study group.** 1977. Adenine arabinoside therapy of biopsy-proved herpes simplex encephalitis. *N. Engl. J. Med.* **297**:289-294.

83. **Florman, A. L., A. A. Gershon, P. P. Blackett, and A. J. Nahmias.** 1973. Intrauterine infection with herpes simplex virus. *J. Am. Med. Assoc.* **225**:129-132.

84. **Whitley, R. J., A. D. Lakeman, A. Nahmias, and B. Roizman.** 1982. DNA restriction-enzyme analysis of herpes simplex virus isolates obtained from patients with encephalitis. *N. Engl. J. Med.* **307**:1060-1062.

85. **Buchman, T. G., T. Simpson, C. Nosal, B. Roizman, and A. J. Nahmias.** 1980. The structure of herpes simplex virus DNA and its application to molecular epidemiology. *Ann. N. Y. Acad. Sci.* **354**:279-290.

86. **Hammer, S. M., T. G. Buchman, L. J. D'Angelo, A. W. Karchmer, B. Roizman, and H. S. Hirsch.** 1980. Temporal cluster of herpes simplex encephalitis : investigation by restriction endonuclease cleavage of viral DNA. *J. Infect. Dis.* **141**:436-440.

87. **Pereira, L., E. Cassai, R. W. Honess, B. Roizman, M. Terni, and A. Nahmias.** 1976. Variability in the structural polypeptides of herpes simplex virus type 1 strains : potential application in molecular epidemiology. *Infect. Immun.* **13**:211-220.

88. **Davis, J. E., and R. T. Johnson.** 1978. An explanation for the localization of herpes simplex encephalitis. *Ann. Neurol.* 5:2-5.

89. **Warren, K. G., S. M. Brown, Z. Wroblewska, D. Gilden, H. Koprowski, and J. Subak-Sharpe.** 1978. Isolation of latent herpes simplex virus form superior cervical and vagus ganglions of human beings. *N. Engl. J. Med.* **298**:1068-1069.

90. **Eseri, M. M.** 1982. Herpes simplex encephalitis. An immunohistological study of the distribution of viral antigen within the brain. *J. Neurol. Sci.* **54**:209-226.

91. **Twomey, J. A., C. M. Barker, G. Robinson, and D. A. Howell.** 1979. Olfactory mucosa in herpes simplex encephalitis. *J. Neurol. Neurosurg. Psychiatr.* **42**:983-987.

92. **Dinn, J. J.** 1980. Transolfactory spread of virus in herpes simplex encephalitis. *Brit. Med. J.* **281**:1392.

93. **Sequiera, L. W., J. C. Lennings, L. H. Carrasco, M. A. Lord, A. Curry, and R. N. P. Sutton.** 1979. Detection of herpes simplex virus genome in brain tissue. *Lancet* ii:609-612.

94. **Fraser, N. W., W. C. Lawrence, Z. Wroblewska, D. H. Gilden, and H. Kroprowski.** 1981. Herpes simplex virus type 1 DNA in human brain tissue. *Proc. Natl. Acad. Sci. USA.* 78:6461-6465.

95. **Baringer, J. R.** 1974. Human herpes simplex virus infections. *Adv. Neurol.* 6:41-51.

96. **Drachman, D. A., and R. D. Adams.** 1962. Herpes simplex acute inclusion-body encephalitis. *Arch. Neurol.* 7:45-63.

97. **Bergey, G. K., P. K. Coyle, A. Krumholz, and E. Niedermeyer.** 1982. Herpes simplex encephalitis with occipital localization. *Arch. Neurol.* 39:312-313.

98. **Tucker, B. A., R. C. Dockel, R. J. Whitley, and W. E. Dismukes.** 1978. Herpes simplex viral encephalitis : an atypical presentation. *South. Med. J.* 71:1431-1433.

99. **Dayan, A. D., W. Gooddy, M. J. G. Harrison, and P. Rudge.** 1972. Brain stem encephalitis caused by herpesvirus hominis. *Brit. Med. J.* 4:405-406.

100. **Chore, S. M., and J. D. Cherry.** 1967. Ultrastructre of Cowdry type A inclusions. I. In herpes simplex encephalitis. *Neurology* 17:575-586.

101. **Vanderhaeghen, J. J., O. Prier, and Y. Bossaert.** 1966. Acute necrotizing encephalitis. Observation of herpes-like particle by electron microscopy. *Path. Europ.* 1:29-49.

102. **Upton, A., and J. Gumpert.** 1970. Electroencephalography in diagnosis of herpes simplex encephalitis. *Lancet* i:650-652.

103. **Illis, L. S., and F. M. Taylor.** 1972. The electroencephalogram in herpes simplex encephalitis *Lancet* i:718-721.

104. **Davis, J. M., K. R. Davis, G. M. Kleinman, H. S. Kirchner, and J. M.Taveras.** 1978. Computed tomography of herpes simplex encephalitis with clinico-pathological correlation. *Radiology* 129:409-417.

105. **Greenberg, S. B., L. Taber, E. Septimus, S. Kohl, J. Puck, and N. Byran.** 1981. Computerized tomography in brain biopsy-proven herpes simplex encephalitis. Early normal results. *Arch. Neurol.* 38:58-59.

106. **Karlin, C. A., R. G. Robinson, D. R. Hinthorn, and C. Liu.** 1978. Radionuclide imaging in encephalitis. *Radiology* 126:181-184.

107. **Kim, E. E., F. H. Deland, and J. Montebello.** 1979. Sensitivity of radionuclide brain scan and computed tomography in early detection of viral meningoencephalitis. *Radiology* 132:425-429.

108. **Levine, D. P., C. B. Lauter, and A. M. Lerner.** 1978. Simultaneous serum and CSF antibodies in herpes simplex virus encephalitis. *J. Am. Med. Assoc.*240:356-360.

109. **Coleman, R. M., P. D. Bailey, R. J. Whitley, H. Keyserling, and A. J. Nahmias.** 1983. ELISA for the detection of herpes simplex virus antigens in the cerebrospinal fluid of patients with encephalitis. *J. Virol. Methods* 7:117-125.

110. **Kaufman, H. H., and L. N. Catalano.** 1979. Diagnostic brain biopsy : a series of 50 cases and a review. *Neurosurgery* 4:129-136.

111. **Morawetz, R. B., R. J. Whitley, and D. M. Murphy.** 1983. Experience with brain biopsy for suspected herpes encephalitis. A review of forty consecutive cases. *Neurosurgery* 12:654-657.

112. **Adam, J. H., and G. E. D. Urquhart.** 1977. Early diagnosis of herpes encephalitis. *N. Engl. J. Med.* 297:1288.

113. **York, G. K.** 1980. Herpes simplex encephalitis : biopsy or treatment? *Ann. Int. Med.* 93:506.

114. **Barza, B., and S. G. Pauker.** 1980. The decision to biopsy, treat or wait in suspected herpes encephalitis. *Ann. Int. Med.* 92:641-649.

115. **Caplan, L. R.** 1980. Brain biopsy in herpes simplex encephalitis. *N. Engl. J. Med.* 303:700.

116. **Whitley, R. J., S.-J. Soong, M. S. Hirsch, A. W. Karchmer, R. Dolin., G. Galasso, J. K. Dunnick, C. A. Alford, and NIAID Collabortive Antiviral study group.** 1981. Herpes simplex encephalitis : vidarabine therapy and diagnostic problems. *N. Engl. J. Med.* 304:313-318.

117. **Nadel, A. M.** 1981. Vidarabine therapy for herpes simplex encephalitis. The development of unusual tremor during treatment. *Arch. Neurol.* 38:384-385.

118. **Kern, E. R., J. T. Richards, J. G. Overall, and L. A. Glasgow.** 1981. Alteration of mortality and pathogenesis of three experimental herpesvirus hominis infections of mice with adenine arabinoside-5'-monophosphate, adenine arabinoside and phosphonoacetic acid. *Antimicrob. Agents Chemother.* 13:53-60.

119. **Whitley, R. J.** 1984. Treatment of herpesvirus infections. *N. Engl. J. Med.* 310:654.

120. **Skoldenberg, B., M. Frosgren, K. Alestig, T. Bergstrom, L. Burman, E. Dahlqvist, A. Forkman, A. Fryden, K. Lovgren, K. Norlin, A. Norrby, E. Olding-Stenkvist, G. Steirnstedt, I. Uhnoo, and K. De Vahl.** 1984. Acyclovir versus vidarabine in herpes simplex encephalitis. Randomised multicentre study in consecutive Swedish patients. *Lancet* ii:707-711.

121. **De Clercq, E.** 1983. Pyrimidine nucleoside analogs as antiviral agents, p. 203-231. *In* E. De Clercq and R. T. Walker (ed.), Targets for the design of antiviral agents. Plenum Press., New York.

122. **Drach, J. C.** 1983. Purine nucleoside analogs as antiviral agents, p. 231-258. *In* E. De Clercq and R. T. Walker (ed.), Targets for the design of antiviral agents. Plenum Press., New York.

123. **Schaeffer, H. J., L. Beauchamp, P. de Miranda, G. B. Elion, D. J. Bauer, and P. Collins.** 1978. 9-(2-Hydroxyethoxymethyl)guanine activity against viruses of the herpes group. *Nature* 272:583-585.

124. **Crumpacker, C. S., L. E. Schnipper, J. A. Zaia, and M. J. Levin.** 1979. Growth inhibition of acycloguanosine of herpes viruses isolated from human infections. *Antimicrob. Agents Chemother.* 15:642-645.

125. **Smee, D. S., J. C. Martin, J. P. H. Verheyden, and T. R. Mathews.** 1983. Anti-herpes virus activity of acyclic nucleoside 9-(1,3-dihydroxy- 2-propoxymethyl)guanine. *Antimicrob. Agents Chemother.* **23**:676-682.

126. **Cheng, Y.-C., E.-S. Huang, J.-C. Lin, E.-C. Mar, J. S. Pagano, G. E. Dutschman, and S. P. Grill.** 1983. Unique spectrum of activity of 9-[(1,3-dihydroxy-2-propoxy)methylguanine against herpesviruses *in vitro* and its mode of action against herpes simplex virus type 1. *Proc. Natl. Acad. Sci. USA* **80**:2767-2770.

127. **Field, A. K., M. E. Davies, C. De Witt, H. C. Perry, R. Liou, J. Germershausen, J. D. Karkas, W. T. Ashton, D. B. R. Johnston, and R. L. Tolman.** 1983. 9-[2-Hydroxy-1-(hydroxymethyl)ethoxymethyl]guanine : a selective inhibitor of herpes group virus replication. *Proc. Natl. Acad. Sci. USA* **80**:4139-4143.

128. **De Clercq, E., J. Descamps, G. Verhelst, R. T. Walker, A. S. Jones, P. F. Torrence, and D. Shugar.** 1980. Comparative efficacy of antiherpes drugs against different strains of herpes simplex virus. *J. Infect. Dis.* **141**:563-574.

129. **Smith, K. O., K. S. Galloway, W. I. Kennell, K. K. Ogilvie, and B. K. Radatus.** 1982. A new nucleoside analog, 9-[[2-hydroxy-1-(hydroxymethyl)ethoxy]methyl]guanine, highly active *in vitro* against herpes simplex virus type 1 and 2. *Antimicrob. Agents Chemother.* **22**:55-61.

130. **De Clercq, E., J. Descamps, P. De Somer, and R. T. Walker.** 1979. (*E*)-5-(2-Bromovinyl)-2'-deoxyuridine : a potent and selective anti-herpes agent. *Proc. Natl. Acad. Sci. USA* **76**:2947-2951.

131. **De Clercq, E.** 1982. Comparative efficacy of antiherpes drugs in different cell lines. *Antimicrob. Agents Chemother.* **21**:661-663.

132. **Reefschlager, J., P. Wutzler, K.-D. Thiel, D. Barwolff, P. Langen, M. Sprossig, and H. A. Rosenthal.** 1982. Efficacy of (*E*)-5-(2-bromovinyl)-2'-deoxyuridine against different herpes simplex virus strains in cell culture and experimental herpes encephalitis in mice. *Antiviral Res.* **2**:255-265.

133. **Wingrad, J. R., A. D. Hess, R. K. Stuart, R. Sarl, and W. H. Burns.** 1983. Effect of several antiviral agents on human lymphocyte function and marrow progenitor cell proliferation. *Antimicrob. Agents Chemother.* **23**:593-597.

134. **De Clercq, E., J. Balzarini, J. Descamps, G.-F, Huang, P. F. Torrence, D. E. Bergstrom, A. S. Jones, P. Serafinowski, G. Verhelst, and R. T. Walker.** 1982. Antiviral, antimetabolic, and cytotoxic activities of 5-substituted 2'-deoxycytidine. *Mol. Pharmacol.* **21**:217-223.

135. **Lopez, C., K. A. Watanabe, and J. J. Fox.** 1980. 2'-Fluoro-5-iodo-aracytosine, a potent and selective anti-herpesvirus agent. *Antimicrob. Agents Chemother.* **17**:803-806.

136. **Watanabe, K. A., T.-L. Su, R. S. Klein, C. K. Chu, A. Matsuba, and M. W. Chun.** 1983. Nucleosides 123. Synthesis of antiviral nucleosides : 5-substituted 1-(2-deoxy-2-halogeno-β-D-arabinofuranosyl)cytosine and -uracils. Some structure-activity relationships. *J. Med. Chem.* **26**:152- 156.

137. **Richards, D. M., A. A. Carmine, R. N. Brogden, R. C. Heel, T. M. Speight, and G. S. Avery.** 1983. Acyclovir. A review of its pharmacodynamic properties and therapeutic

efficacy. *Drugs* **26**:378-438.

138. **Jones, B. R., D. J. Coster, P. N. Fison, G. M. Thompson, L. M. Cobo, and M. G. Falcon.** 1979. Efficacy of acycloguanosine (Wellcome 248U) against herpes-simplex corneal ulcers. *Lancet* **i**:243-244.

139. **Corey, L., A. J. Nahmias, M. E. Guinan, J. K. Benedetti, C. W. Critchlow, and K. K. Holmes.** 1982. A trial of topical acyclovir in genital herpes simplex virus infections. *N. Engl. J. Med.* **306**:1313-1319.

140. **Nielsen, A. E., T. Aesen, A. M. Halsos, B. R. Kinge, E. A. L. Tjotta, K. Wikstrom, and A. P. Fiddian.** 1982. Efficacy of oral acyclovir in the treatment of initial and recurrent genital herpes. *Lancet* **ii**:571-573.

141. **Bryson, Y. J., M. Dillon, M. Lovett, G. Acuna, S. Taylor, J. D. Cherry, B. L. Johnson, E. Wiessmeir, W. Growdon, T. Creagh-Kirk, and R. Keeney.** 1983. Treatment of first episodes of genital herpes simplex virus infections with oral acyclovir. *N. Engl. J. Med.* **308**:916-921.

142. **Mitchell, C. D., B. Bean, S. R. Gentry, K. E. Groth, J. R. Boen, and H. H. Balfour Jr.** 1981. Acyclovir therpy for mucocutaneous herpes simplex infections in immunocompromised patients. *Lancet* **i**:1389-1392.

143. **Chou, S., J. G. Gallagher, and T. C. Merigan.** 1981. Controlled clinical trial of intravenous acyclovir in transplant patients with mucocutaneous herpes simples infections. *Lancet* **i**:1392-1394.

144. **Wade, J. C., B. Newton, C. Mclaren, N. Flournoy, R. E. Keeney, and J. D. Meyers.** 1982. Intravenous acyclovir to treat mucocutaneous herpes simplex virus infection after marrow transplantation. *Ann. Int. Med.* **96**:265-269.

145. **Maudgal, P. C., L. Missotten, E. De Clercq, J. Descamps, and E. de Meuter.** 1981. Efficacy of (*E*)-5-(2-bromovinyl)-2'-deoxyuridine in the topical treatment of herpes simplex keratitis. *Albrecht von Graefes Arch. Klin. Opthalmol.* **216**:261-268.

146. **De Clercq, E.** 1983. The chemotherapy of herpesvirus infections with reference to bromovinyldeoxyuridine and other antiviral compounds, p. 295-315. *In* C. H. Stuart-Harris and J. Oxford (ed.), Problems of antiviral therapy. Academic Press. New York.

147. **Young, C. W., R. Schneider, B. Leyland-Jones, D. Armstrong, C. T. C. Tan, C. Lopez, K. A. Watanabe, J. J. Fox, and F. S. Philips.** 1983. Phase I evaluation of 2'-fluoro-5-iodo-1-β-D-arabinofuranosyl cytosine in immunosuppressed patients with herpesvirus infections. *Cancer Res.* **43**:5006-5009.

148. **Elion, G. B., P. A. Furman, J. A. Fyfe, P. de Miranda, L. Beauchamp, and H. J. Schaeffer.** 1977. Selectivity of action of an antiherpetic agent, 9-(2-hydroxyethoxymethyl)guanine. *Proc. Natl. Acad. Sci. USA* **74**:5716-5720.

149. **Furman, P. A., P. de Miranda, M. H. St. Clair, and G. B. Elion.** 1981. Metabolism of acyclovir in virus-infected and uninfected cells. *Antimicrob. Agents Chemother.* **20**:518-524.

150. **Descamps, J., and E. De Clercq.** 1981. Specific phosphorylation of (*E*)-5-(2-iodovinyl)-2'-deoxyuridine by herpes simplex virus-infected cells. *J. Biol. Chem.*

256:5973-5976.

151. **Ayisi, N. K., E. De Clercq, R. A. Wall, H. Hughes, and S. L. Sacks.** 1984. Metabolic fate of (*E*)-5-(2-bromovinyl)-2'-deoxyuridine in herpes simplex virus- and mock-infected cells. *Antimicrob. Agents Chemother.* **26**:762-765.

152. **Kreis, W., L. Damin, J. Colcino, and C. Lopez.** 1982. *In vitro* metabolism of 1-β-D-arabinofuranosylcytosine and 1-β-2'-fluoro-arabino-5-iodocytosine in normal and herpes simplex type 1 virus-infected cells. *Biochem. Pharmacol.* **31**:767-773.

153. **Crumpacker, C. S., P. Chartrand, J. H. Subak-Sharpe, and N. M. Wilkie.** 1980. Resistance of herpes simplex virus to acycloguanosine - genetic and physical analysis. *Virology* **105**:171-184.

154. **Coen, C. M., and P. A. Schaffer.** 1980. Two distinct loci confer resistance to acycloguanosine in herpes simplex virus type 1. *Proc. Natl. Acad. Sci. USA* **77**:2265-2269.

155. **Schnipper, L. E., and C. S. Crumpacker.** 1980. Resistance of herpes simplex virus to acycloguanosine : role of viral thymidine kinase and DNA polymerase loci. *Proc. Natl. Acad. Sci. USA* **77**:2270-2273.

156. **Field, H. J., A. McMillan, and G. Darby.** 1981. The sensitivity of acyclovir-resistant mutants of herpes simplex virus to other antiviral drugs. *J. Infect. Dis.* **143**:281-285.

157. **Darby, G., and H. J. Field.** 1981. Altered substrate specificity of herpes simplex virus thymidine kinase confers acyclovir resistance. *Nature* **289**:81-83.

158. **Larder, B. A., and G. Darby.** 1982. Properties of a novel thymidine kinase induced by an acyclovir-resistant herpes simplex virus type 1 mutant. *J. Virol.* **42**:649-658.

159. **Larder, B. A., Y.-C. Cheng, and G. Darby.** 1983. Characterization of abnormal thymidine kinases induced by drug-resistant strains of herpes simplex virus type 1. *J. Gen. Virol.* **64**:523-532.

160. **Field, H. J., and J. Neden.** 1982. Isolation of bromovinyldeoxyuridine-resistant strains of herpes simplex virus and successful chemotherapy of mice treated with one such strain using acyclovir. *Antiviral Res.* **2**:243-254.

161. **Chen, M. S., and W. H. Prusoff.** 1978. Association of thymidylate kinase activity with pyrimidine deoxyribonucleoside kinase induced by herpes simplex virus. *J. Biol. Chem.* **253**:1325-1327.

162. **Chen, M. S., W. P. Summers, J. Walker, W. C. Summers, and W. H. Prusoff.** 1979. Characterization of pyrimidine deoxyribonucleoside kinase (thymidine kinase) and thymidylate kinase as a multifunctional enzyme in cells transformed by herpes simplex virus type 1 and in cells infected with mutant strains of herpes simplex virus. *J. Virol.* **30**:942-945.

163. **Fyfe, J. A.** 1982. Differential phosphorylation of (*E*)-5-(2-bromovinyl)-2'-deoxyuridine monophosphate by thymidylate kinases from herpes simplex virus type 1 and 2 and varicella zoster virus. *Mol. Pharmacol.* **21**:432-437.

164. **Fyfe, J. A., S. A. McKee, and P. M. Keller.** 1983. Altered thymidine-thymidylate kinases from strains of herpes simplex virus with modified drug sensitivities to acyclovir and

(*E*)-5-(2-bromovinyl)-2'-deoxyuridine. *Mol. Pharmacol.* **24**:316-323.

165. **Miller, W. H., and R. L. Miller.** 1980. Phosphorylation of acyclovir (acycloguanosine) monophosphate by GMP kinase. *J. Biol. Chem.* **255**:7204-7207.

166. **Miller, W. H., and R. L. Miller.** 1982. Phosphorylation of acyclovir diphosphate by cellular enzymes. *Biochem. Pharmacol.* **31**:3879-3884.

167. **Furman, P. A., M. H. St. Clair, J. A. Fyfe, J. L. Rideout, P. M. Keller, and G. B. Elion.** 1979. Inhibition of herpes simplex virus-induced DNA polymerase activity and viral DNA replication by 9-(2-hydroxyethoxymethyl)guanine and its triphosphate. *J. Virol.* **32**:72-77.

168. **Allaudeen, H. S., J. W. Kozarich, J. R. Berlino, and E. De Clercq.** 1981. On the mechanism of selective inhibition of herpes virus replication by (*E*)-5-(2-bromovinyl)-2'-deoxyuridine *Proc. Natl. Acad. Sci. USA* **78**:2698-2702.

169. **Derse, D., Y.-C. Cheng, P. A. Furman, M. H. St. Clair, and G. B. Elion.** 1981. Inhibition of purified human and herpes simplex virus-induced DNA polymerase by 9-(2-hydroxyethoxymethyl)guanine triphosphate. Effects on primer-template function. *J. Biol. Chem.* **256**:11447-11451.

170. **Allaudeen, H. S., J. Descamps, R. K. Sehgal, and J. J. Fox.** 1982. Selective inhibition of DNA replication in herpes simplex virus-infected cells by 1-(2'-deoxy-2'-fluoro-β-D-arabinofuranosyl)-5-iodocytosine. *J. Biol. Chem.* **257**:11879-11882.

171. **Furman, P. A., M. H. St. Clair, and P. Spector.** 1984. Acyclovir triphosphate is a suicide inactivator of herpes simplex virus DNA polymerase *J. Biol. Chem.* **259**:9575-9579.

172. **Ruth, J. L., and Y.-C. Cheng.** 1981. Nucleoside analogs with clinical potential in antiviral chemotherapy. The effect of several thymidine and 2'-deoxyuridine analog 5'-triphosphates on purified human (α, β) and herpes simplex virus (types 1, 2) DNA polymerases. *Mol. Pharmacol.* **20**:415-422.

173. **Sagi, J., A. Szabolcs, A. Szemzo, and L. Otvos.** 1981. (*E*)-5-(2-Bromovinyl)-2'-deoxyuridine 5'-triphosphate as a DNA polymerase substrate. *Nucleic Acids Res.* **9**:6985-6994.

174. **Allauden, H. S., M. S. Chen, J. J. Lee, E. De Clercq, and W. H. Prusoff.** 1982. Incorporation of (*E*)-5-(2-halovinyl)-2'-deoxyuridines into deoxyribonucleic acids of herpes simplex virus type 1-infected cells. *J. Biol. Chem.* **257**:603-606.

175. **Mancini, W. R., E. De Clercq, and W. H. Prusoff.** 1983. The relationship between incorporation of (*E*)-5-(2-bromovinyl)-2'-deoxyuridine into herpes simplex virus type 1 DNA with virus infectivity and DNA integrity. *J. Biol. Chem.* **258**:792-795.

176. **Furman, P. A., P. V. McGuirt, P. M. Keller, J. A. Fyfe, and G. B. Elion.** 1980. Inhibition by acyclovir of cell growth and DNA synthesis of cells biochemically transformed with herpesvirus genetic information. *Virology* **102**:420-430.

177. **Sagai, J., A. Czuppon, M. Katzar, A. Szabolcs, A. Szemzo, and L. Otvos.** 1982. Modified polynucleotides VI. Properties of synthetic DNA containing the antiherpetic agent (*E*)-5-(2-bromovinyl)-2'-deoxyuridine. *Nucleic Acids Res.* **10**:6051-6066.

178. **Goz, B.** 1978. The effects of incorporation of 5-halogenated deoxyuridine into the DNA of eukaryotic cells. *Ann. Rev. Pharmacol.* **29**:249-272.

179. **De Clercq, E., H. Heremans, J. Descamps, G. Verhelst, M. De Ley, and A. Billiau.** 1981. Effects of (*E*)-5-(2-bromovinyl)-2'-deoxyuridine and other selective antiherpes compounds on the induction of retrovirus particles in mouse BALB/3T3 cells. *Mol. Pharmacol.* **19**:122-129.

180. **Cassiman, J. J., E. De Clercq, A. S. Jones, R. T. Walker, and H. Van Den Berghe.** 1981. Sister chromatid exchange induced by antiherpes drugs. *Brit. Med. J.* **283**:817-818.

181. **Crumpacker, C. S., L. E. Schnipper, P. N. Kowalsky, and D. M. Shannon.** 1982. Resistance of herpes simplex virus to adenine arabinoside and (*E*)-5-(2-bromovinyl)-2'-deoxyuridine : a physical analysis. *J. Infect. Dis.* **146**:167-172.

182. **Zimmerman, M., and J. Siedenberg.** 1964. Deoxyribosyl transfer I. Thymidine phosphorylase and nucleoside 2-deoxyribosyl transferase in normal and malignant tissues *J. Biol. Chem.* **239**:2618-2621.

183. **Krenitsky, T. A., M. Barklay, and J. A. Jacquez.** 1964. Specificity of mouse uridine phosphorylase. *J. Biol. Chem.* **239**:805-812.

184. **Desgranges, C., G. Razaka, M. Rabaud, and H. Bricaud.** 1981. Catabolism of thymidine in human blood platelets. Purification and properties of thymidine phosphorylase . *Biochim. Biophys. Acta* **654**:211-218.

185. **Niedzwicki, J. G., M. H. El Kouni, S. Hsi Chu, and S. Cha.** 1983. Structure-activity relationship of ligands of the pyrimidine nucleoside phosphorylase. *Biochem. Pharmacol.* **32**:399-415.

186. **Desgranges, C., G. Razaka, M. Rabaud, H. Bricaud, J. Balzarini, and E. De Clercq.** 1983. Phosphorolysis of (*E*)-5-(2-bromovinyl)-2'-deoxyuridine (BVDU) and other 5-substituted 2'-deoxyuridines by purified human thymidine phosphorylase and intact blood platelets. *Biochem. Pharmacol.* **32**:3583-3590.

187. **Desgranges, C., G. Razaka, F. Drouillet, H. Bricaud, P. Herdewijn, and E. De Clercq.** 1984. Regeneration of the antiviral drug (*E*)-5-(2-bromovinyl)-2'-deoxyuridine. *Nucleic Acids Res.* **12**:2081-2090.

188. **Desgranges, C., G. Razaka, H. Bricaud, and E. De Clercq.** 1985. Inhibition and reversal of the degradation of the antiviral drug (*E*)-5-(2-bromovinyl)-2'-deoxyuridine *in vivo*. *Biochem. Pharmacol.* **34**:405-406.

189. **Friedkin, M.** 1973. Thymidylate synthetase. *Adv. Enzymol.* **38**:235-292.

190. **Barr, P. J., N. J. Oppenheimer, and D. V. Santi.** 1983. Thymidylate synthetase catalysed conversions of (*E*)-5-(2-bromovinyl)-2'-deoxyuridylate. *J. Biol. Chem.* **258**:13627-13631.

191. **Garret, C., Y. Wataya, and D. V. Santi.** 1979. Thymidylate synthetase. Catalysis of dehalogenation of 5-bromo- and 5-iodo-2'-deoxyuridylate. *Biochemistry* **18**:2798-2804.

192. **Chou, T.-C., A. Fienberg, A. J. Grant, P. Vidal, U. Reichaman, K. A. Watanabe, J. J. Fox, and F. S. Philips.** 1981. Pharmacological disposition and metabolic fate of 2'-fluoro-5-iodo-1-β-D-arabinofuranosylcytosine in mice and rats. *Cancer Res.*

41:3336-3342.

193. **North, T. W., and C. K. Mathews.** 1983. Tetrahydrouridine specifically facilitates deoxycytidine incorporation into herpes simplex virus DNA. *J. Virol.* **37**:987-993.

194. **Fox, L., M. J. Dobersen, and S. Greer.** 1983. Incorporation of 5-substituted analogs of deoxycytidine into DNA of herpes simplex-infected or transformed cells without deamination to thymidine analogs. *Antimicrob. Agents Chemother.* **23**:465-476.

195. **de Miranda, P., S. S. Good, H. C. Krasny, J. D. Connor, O. L. Laskin, and P. S. Lietman.** 1982. Metabolic fate of radioactive acyclovir in humans. Acyclovir symposium. *Am. J. Med.* **73**:215-220.

196. **Bergstrom, D. E., and J. L. Ruth.** 1977. Preparation of C-5 mercurated pyrimidine nucleosides. *J. Carbohydr. Nucleosides Nucleotides* **4**:257-269.

197. **Jones, A. S., G. Verhelst, and R. T. Walker.** 1979. The synthesis of the potent anti-herpes virus agent (*E*)-5-(2-bromovinyl)-2'-deoxyuridine and related compounds. *Tetrahedron Lett.* **45**:4415-4418.

198. **Brossmer, R., und D. Ziegler.** 1966. Zur darstellung heterocyclischer aldehyde (1,2). *Tetrahedron Lett.* **43**:5253-5256.

199. **Lamb, R. A., P. R. Etkind, and P. W. Choppin.** 1978. Evidence for a ninth influenza viral polypeptide. *Virology* **91**:60-78.

200. **Saito, Y., R. W. Price, D. A. Rottenberg, J. J. Fox, T. L. Su, K. A. Watanabe, and F. S. Philips.** 1982. Quantitative autoradiographic mapping of herpes simplex virus encephalitis with a radiolabeled antiviral drug. *Science* **217**:1151-1153.

201. **Price, R. W., Y. Siato, and J. J. Fox.** 1983. Prospects for the use of radiolabelled antiviral drugs in the diagnosis of herpes simplex encephalitis. *Biochem. Pharmacol.* **32**:2455-2461.

202. **Saito, Y., R. Rubenstein, R. W. Price, J. J. Fox, and K. A. Watanabe.** 1983. Diagnostic imaging of herpes simplex encephalitis using a radiolabeled antiviral drug: autoradiographic assessment in an animal model. *Ann. Neurol.* **15**:548-558.

203. **Bergstrom, D. E., and M. K. Ogawa.** 1978. C-5 Substituted pyrimidine nucleosides. 2. Synthesis via olefin coupling to organopalladium intermediates derived from uridine and 2'-deoxyuridine. *J. Am. Chem. Soc.* **100**:8106-8112.

204. **Bergstrom, D. E.** 1982. Organometallic intermediates in the synthesis of nucleoside analogs. *Nucleosides Nucleotides* **1**:1-34

205. **Heck, R. F.** 1968. Arylation, methylation, and carboxyalkylation of olefins by group VIII metal derivatives. *J. Am. Chem. Soc.* **90**:5518-5526.

206. **Heck, R. F.** 1969. The mechanism of arylation and carboxymethylation of olefins with organopalladium compounds. *J. Am. Chem. Soc.* **91**:6707-6714.

207. **Jones, A. S., S. G. Rahim, and R. T. Walker.** 1981. Synthesis and antiviral properties of (*Z*)-5-(2-bromovinyl)-2'-deoxyuridine. *J. Med. Chem.* **24**:759-760.

208. **Frost, J. J.** 1982. Pharmacokinetic aspects of the in vivo, noninvasive study of

neuroreceptors in man. p. 25-39. *In* W. C. Eckleman (ed.), Receptor binding radiotracers, vol II. CRC press Inc., Florida.

209. **Seevers, R. H., and R. E. Counsell.** 1982. Radioiodination techniques for small organic molecules. *Chem. Rev.* **82**:575-590.

210. **Dewanjee, M. K., and S. A. Rao.** 1983. Principles of radioiodination and iodine-labeled tracers in biomedical investigations, p. 1-94. *In* G. V. S. Rayadu (ed.), Radiotracers for Medical Applications. CRC Press, Inc., Florida.

211. **Stocklin, G.** 1978. Bromine-77 and iodine 123 radiopharmaceuticals. *Int. J. Appl. Radiat. Isot.* **28**:131-147.

212. **Hunter, W. M., and F. C. Greenwood.** 1962. Preparation of iodine-131 labelled human growth hormone of high specific activity. *Nature* **194**:495-496.

213. **Hadi, U. A. M., D. Malcom-Lawes, and G. Oldham.** 1978. The labelling of small molecules with radioiodine. *Int. J. Appl. Radiat. Isot.* **29**:621-623.

214. **Salacinski, P. R. P., J. E. C. Sykes, V. V. Clement-Jones, and P. J. Lowry.** 1981. Iodination of proteins, glycoproteins, and peptides using a solid-phase oxidising agent 1,3,4,6-tetrachloro-3α,6α-diphenyl glycoluril (iodogen). *Anal. Biochem.* **117**:136-146.

215. **Bakker, C. N. M., F. M. Kaspersen, A. Van Langevelde, and E. J. K. Pauwels.** 1981. The synthesis of ^{131}I-iodo-2-thiouracil with iodo-gen. *Int. J. Appl. Radiat. Isot.* **31**:513-515.

216. **Bakker, C. N. M., and F. M. Kaspersen.** 1981. The electrophilic iodination with ^{131}I of N_1-substituted uracils using chloramine-T as oxidant. *Int. J. Appl. Radiat. Isot.* **32**:176-178.

217. **Marchalonis, J. J.** 1968. An enzymatic method for the trace iodination of immunoglobulins and other proteins. *Biochem. J.* **113**:299-305.

218. **Bakker C. N. M., and F. M. Kaspersen.** 1979. Iodination reactions with lactoperoxidase immmobilized on phenoxyacetyl cellulose. *Int. J. Appl. Radiat. Isot.* **30**:320.

219. **Bovinglon, C. H., D. F. Maundrell, and B. Dacre.** 1971. Aromatic nucleophilic exchange reactions. Part 1. Heterogeneous catalysis. *J. Chem. Soc. B.* 767-770.

220. **Spevacek, V.** 1973. Exchange of halogen bonded on aromatic core. Heterogeneous catalysis - I. Reaction mechanism of iodine exchange in o-iodobenzoic acid. *Tetrahedron* **29**:2285-2291.

221. **Stanko, V. I., and N. G. Iroshnikova.** 1979. Kinetics of isotope exchange reactions of iodine in some meta and para derivatives of iodobenzene. *J. Gen. Chem. USSR* **49**:1823-1827.

222. **Tarle, M., R. Padovan, and S. Spavenli.** 1978. Radioiodination of iodinated estradiol-17-diphosphates. *J. Labelled Comp. Radiopharm.* **15**:7-21.

223. **Petzold, G., and H. H. Coenen** 1981. Chloramine-T for "no-carrier-added" labelling of aromatic biomolecules with bromine-75, 77. *J. Labelled Comp. Radiopharm.* **18**:1319-1336.

224. **Wilbur, D. S., K. W. Anderson, W. E. Stone, and H. A. O'Brien.** 1982. Radiohalogenation

of non-activated compounds via aryltrimethylsilyl intermediates. *J. Labelled Comp. Radiopharm.* **19**:1171-1181.

225. **Wilbur, D. S., and K. W. Anderson.** 1982. Bromine chloride from N-chlorosuccinimide oxidation of bromide ion. Electrophilic addition reactions in protic and aprotic solvents. *J. Org. Chem.* **47**:358-359.

226. **Flanagan, R. J., B. C. Lentle, D. G. McGowan, and L. I. Wiebe.** 1981. α-Halostilbenes related to diethylstilbestrol. *J. Radioanal. Chem.* **65**:81-94.

227. **Harbottle, G., and N. Sutin.** 1959. The Szilard-Chalmers reaction in solids. *Adv. Inorg. Chem. Radiochem.* **1**:267-314

228. **Ford, P., R. J. Flanagan, L. I. Wiebe, I. Koslowsky, and P. Eu.** Unpublished results.

229. **Yacyshyn, H., D. R. Tovell, J. Samuel, E. E. Knaus, L. I. Wiebe, and D. L. Tyrrell.** Manuscript in preparation.

230. **Lee, Y. W., J. B. Giziewicz, E. E. Knaus, and L. I. Wiebe.** 1984. Tumor uptake of radiolabelled pyrimidine bases and pyrimidine nucleosides in animal models: VII. [2-^{14}C]-5-ethyl-1-(2'-deoxy-β-D-ribofuranosyl)uracil. *Int. J. Radiat. Isot.* **35**:1063-1066.

231. **Wasternak, C.** 1981. Degradation of pyrimidines and pyrimidine analogs - pathways and mutual influences. *Pharmac. Ther.* **8**:629-651.

232. **Haddad, P. R., and A. L. Heckenberg.** 1981. Determination of inorganic anions by high-performance liquid chromatography. *J. Chromatogr.* **300**:357-394.

233. **Anders, M. W.** 1982. Aliphatic halogenated hydrocarbons. p. 29-49. *In* Jakoby, W. B., Bend, J. R., and Caldwell, J. (ed.), Metabolic basis of detoxification. Metabolism of functional groups. Academic Press, New York.

234. **Prusoff, W. H., J. J. Jaffe, and H. Gunther.** 1960. Studies in the mouse of the pharmacology of 5-iododeoxyuridine, an analog of thymidine. *Biochem. Pharmacol.* **3**:110-121.

235. **Rosowsky, A., J. E. Wright, G. Steele, and D. W. Kufe.** 1981. Thymidine 5'-O-pivaloate: evidence for prodrug action in rat and rhesus monkey *Cancer Treat. Rep.* **65**:93-99.

236. **Ensminger, W. D., and A. Rosowsky.** 1979. Thymidine 5'-O-pivaloate. A prodrug derivative of thymidine with potential application in high-dose methotrexate therapy. *Biochem. Pharmacol.* **28**:1541-1545.

237. **Lee, Y. W., J. Samuel, E. E. Knaus, and L. I. Wiebe.** Unpublished results.

238. **Sinkula, A. A., and C. Lewis.** 1973. Chemical modifications of Lincomycin : synthesis and bioactivity of selected 2,7-dialkyl carbonate esters. *J. Pharm. Sci.* **62**:1757-1760.

239. **Mercer, J. R.** 1985. Synthesis and evaluation of radiolabeled 5-halo-1-(2'-fluoro-2'-deoxy-β-D-ribofuranosyl)uracil analogs as non-invasive tumor diagnostic radiopharmaceuticals. Ph.D Thesis, University of Alberta, Edmonton, Canada.

240. **Fox, J. J., C. Lopez, and K. A. Watanabe.** 1981. Pyrimidine nucleosides: chemistry, antiviral and potential anticancer activities, p. 27-40. *In* F. G. De las Heras and S. Vega

(ed.), Medicinal Chemistry Advances. Pergamon Press, Oxford.

241. **Philips, F. S., A. Feinberg, T.-C. Chou, P. M. Vidal, T. L. Su, K. A. Watanabe, and J. J. Fox.** 1983. Distribution, metabolism, and excretion of 1-(2-fluoro-2-deoxy-β-D-arabinofuranosyl)thymine and 1-(2-deoxy-2-fluoro-β-D-arabinofuranosyl)-5-iodocytosine. *Cancer Res.* 43:3619-3627.

242. **Misra, H. K., E. E. Knaus, and L. I. Wiebe.** Manuscript in preparation.

APPENDIX

A. Yield Calculation for the $^{81}Br(n,\gamma)^{82}Br$ Nuclear Reaction

The formula for the yield calcualtion for a nuclear reaction is given by the equation

$$A = N_1 \, \emptyset \, \eth \, [1 - \exp(\lambda t)]\dagger$$

where A = the radioactivity in Bq, N_1 = the number of nuclei in the target $\emptyset$ = the flux of bombarding particle (n per cm^2 per s) $\eth$ = cross section in cm^2 and $[1-\exp(\lambda t)]$ is correction term for the decay of the produced radionuclide during the production reaction.

The value of N_1 is determined by the formula

$$N_1 = W \, \Theta \, N(A) / MW$$

where W = the weight of the target in g, Θ = the isotopic abunadance of the target nuclei in the target material, and N(A) = Avagadro's constant (6.02×10^{23} per mol) and MW = molecular weight.

For 1 mg of NH_4Br (97.8% ^{81}Br enriched)

$$N_1 = 0.001 \times 0.978 \times 6.02 \times 10^{23} / 99 = 5.947 \times 10^{18}$$

All bromine irradiations were carried out at a neutron flux of 1×10^{12} n cm^{-2} s^{-1} for 4 h. The cross section for conversion of ^{81}Br to ^{82}Br (including ^{82}Br generated from ^{82}Br) is estimated to be 5.8×10^{-24} cm^2 † Therefore theoretical yield of ^{82}Br obtained from 1 mg of NH_4Br by $^{81}Br(n,\gamma)^{82}Br$ reaction is

$$A = 5.947 \times 10^{18} \times 10^{12} \times 5.8 \times 10^{-24} [1-\exp(0.784)] = 2.6 \times 10^{6} \text{ Bq}$$

Direct neutron activation of BVdU was carried out using a natural abundance bromine (Θ for ^{81}Br=0.4931) containing sample at a neutron flux of 1×10^{12} n cm^{-2} s^{-1} for 4 h. Theoretical yield for 1 mmol may be calculated using the formulae given above.

$$A = 6.02 \times 10^{20} \times 0.4931 \times 5.8 \times 10^{-24} [1-\exp(0.784)] = 1.3 \times 10^{9} \text{ Bq}$$

† Data taken from C. M. Lederer, and V. S. Shirley (ed.), Table of isotopes, 7th edition. Wiley Interscience, New York.